Technical Report GL-97-20
December 1997

US Army Corps of Engineers
Waterways Experiment Station

Analysis of Korean F-16 Aircraft Operating on AM-2 Landing Mat

by Carroll J. Smith, Carlos R. Gonzalez, Donald M. Smith

Prepared for Samsun Industrial Company Ltd.

The contents of this report are not to be used for advertising, publication, or promotional purposes. Citation of trade names does not constitute an official endorsement or approval of the use of such commercial products.

The findings of this report are not to be construed as an official Department of the Army position, unless so designated by other authorized documents.

PRINTED ON RECYCLED PAPER

Technical Report GL-97-20
December 1997

Analysis of Korean F-16 Aircraft Operating on AM-2 Landing Mat

by Carroll J. Smith, Carlos R. Gonzalez, Donald M. Smith

U.S. Army Corps of Engineers
Waterways Experiment Station
3909 Halls Ferry Road
Vicksburg, MS 39180-6199

Final report

Approved for public release; distribution is unlimited

Prepared for Samsun Industrial Co. Ltd.
24 Youido-Dong, Youngdungpo-Ku
Seoul 150-010
KOREA

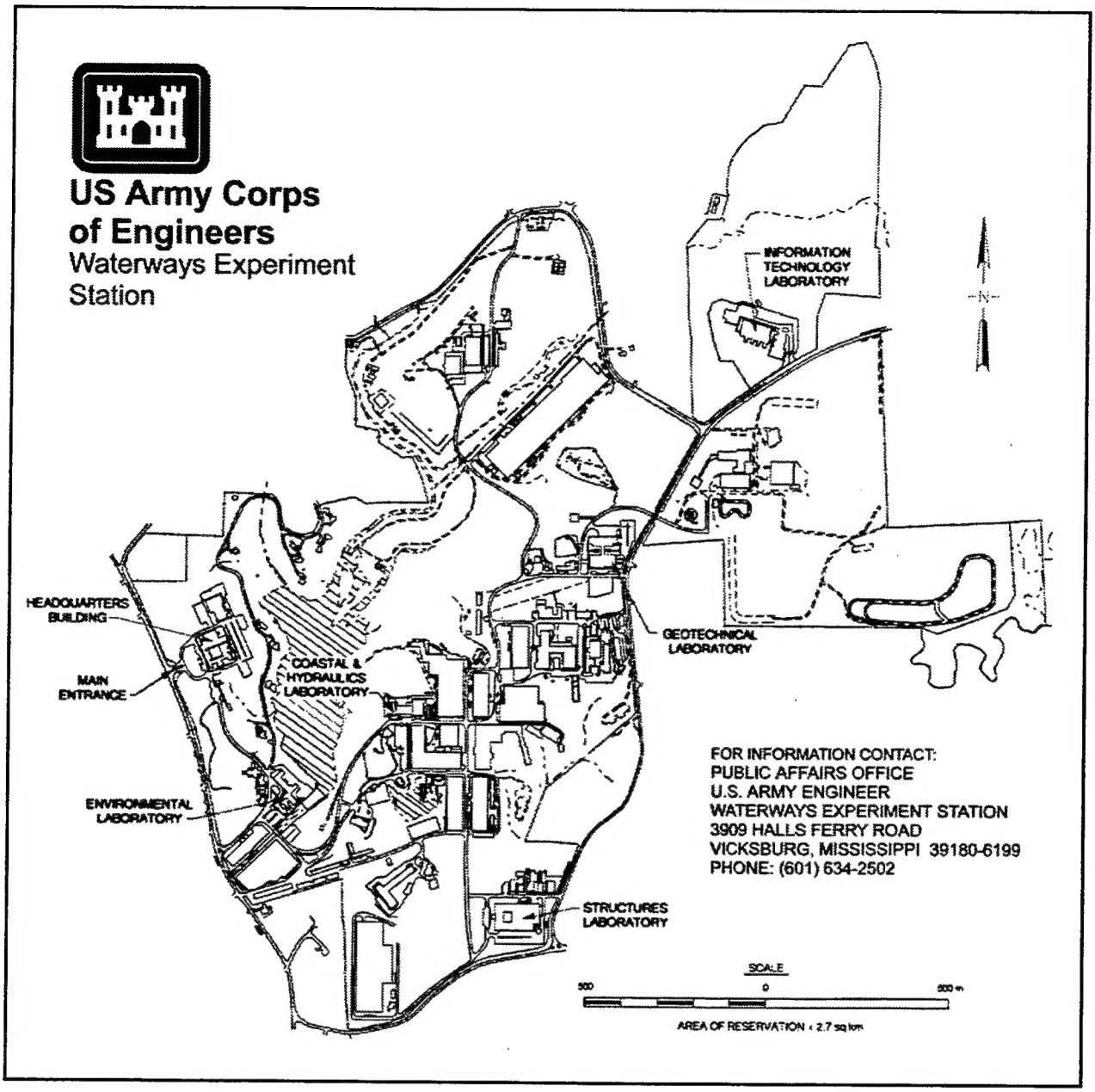

Waterways Experiment Station Cataloging-in-Publication Data

Smith, Carroll J.

Analysis of Korean F-16 aircraft operating on AM-2 landing mat / by Carroll J. Smith, Carlos R. Gonzalez, Donald M. Smith ; prepared for Samsun Industrial Co. Ltd.

129 p. : ill. ; 28 cm. — (Technical report ; GL-97-20)

Includes bibliographic references.

1. F-16 (Jet fighter plane) 2. Landing mats — Testing. 3. Numerical analysis — Computer programs. I. Gonzalez, Carlos R. II. Smith, Donald M. III. United States. Army. Corps of Engineers. IV. U.S. Army Engineer Waterways Experiment Station. V. Geotechnical Laboratory (U.S. Army Engineer Waterways Experiment Station) VI. Samsun Industrial Co. Ltd. (Korea) VII. Title. VIII. Series: Technical report (U.S. Army Engineer Waterways Experiment Station) ; GL-97-20.

TA7 W34 no.GL-97-20

Contents

List of Figures

List of Tables

Preface

The study reported herein was sponsored by the Samsun Industrial Company Ltd., Seoul, Korea, under a Cooperative Research and Development Agreement (CRDA 9709-E-C105). The work involved the conduct of research and development investigations in support of the development of aluminum landing mats for aircraft applications in South Korea.

The study was conducted at the U.S. Army Engineer Waterways Experiment Station (WES) from September through November 1997 by the Airfields and Pavements Division (APD), Geotechnical Laboratory (GL). Personnel of the APD involved in this study were Messrs. D. M. Smith, C. R. Gonzalez, and C. J. Smith. Ms. August W. Giffin, APD Contract Technician, was involved in various computer input and figure preparation.

The work was conducted under the supervision of Dr. Albert J. Bush III, Chief, Technology Applications Branch, and Mr. Timothy W. Vollor, Chief, Materials Analysis Branch, APD; Dr. David W. Pittman, Chief, APD; and Dr. William F. Marcuson III, Director, GL.

At the time of publication of this report, Director of WES was Dr. Robert W. Whalin and Commander was COL Robin R. Cababa, EN.

Conversion Factors, Non-SI to SI Units of Measurement

Non-Si units of measurement used in this report can be converted to SI units as follows:

MULTIPLY	BY	TO GET
LENGTH		
inches (in.)	25.4	millimeters (mm)
inches (in.)	0.0254	meters (m)
feet (ft)	0.305	meters (m)
yards (yd)	0.915	meters (m)
miles (mi)	1.609	kilometers (km)
AREA		
square inches ($in.^2$)	645.2	square millimeters (mm^2)
square inches ($in.^2$)	0.0006452	square meters (m^2)
square feet (ft^2)	0.093	square meters (m^2)
square yards (yd^2)	0.8361	square meters (m^2)
square miles (mi^2)	2.59	square kilometers (km^2)
acres	0.004046	square kilometers (km^2)
VOLUME		
cubic inches (in^3)	16487.0	cubic millimeters (mm^3)
cubic feet (ft^3)	0.028	cubic meters (m^3)
cubic yards (yd^3)	0.7646	cubic meters (m^3)
MASS		
pounds	0.454	kilograms (kg)
FORCE		
pounds (lbf)	4.448	newtons (N)
kips (1000 lbf)	4.448	kilonewton (kN)
STRESS		
pounds/square inch (psi)	6.895	kilopascals (kPa)
DENSITY		
pounds/cubic foot (pounds mass)	16.052	kilograms/cubic meter (kg/m^3)

1 Introduction

Background

The U.S. Army Engineer Waterways Experiment Station (WES) entered into a Cooperative Research and Development Agreement (CRDA) with the Samsun Industrial Company Ltd., Seoul, Korea, to provide joint research and development investigations in support of the development and deployment of aluminum landing mats for aircraft applications in South Korea.

A representative of Samsun contacted WES in June 1997 to discuss the application of AM-2 landing mats as runway repairs for fighter aircraft operations. Samsun fabricates and supplies the South Korean Air Force with AM-2 landing mats and associated repair kits. A meeting between WES and Samsun representatives was held at WES on 30 July 1997 to further discuss the possibility of WES conducting a study to characterize the response of F-16 aircraft (Figure 1) on standard and modified AM-2 repair mat configurations (Figures 2 and 3).

Figure 1. F-16 fighter aircraft

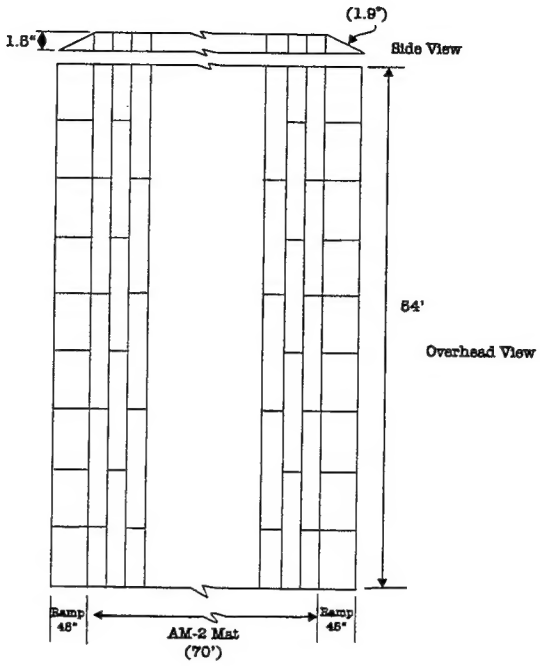

Figure 2. Standard AM-2 repair configuration with 45-in. ramps and 1.9-deg approach angle

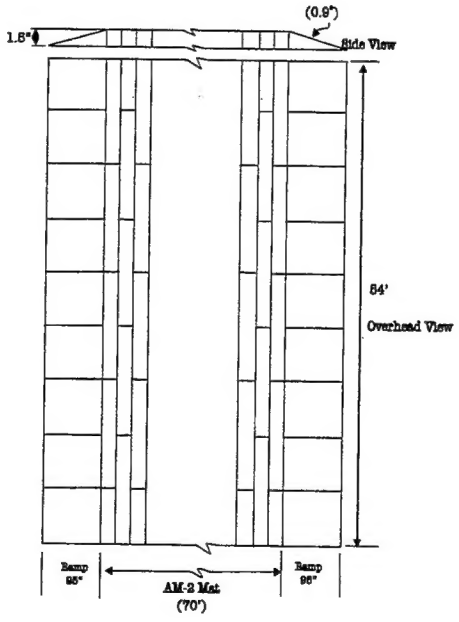

Figure 3. Modified AM-2 repair configuration with 95-in. ramps and 0.9-deg approach angle

As a result of this meeting the WES initiated a Cooperative Research and Development Agreement between the U.S. Army Engineer Waterways Experiment Station and Samsun Industrial Company Ltd., that received final approval on 10 September 1997.

Problem Statement

Aluminum AM-2 landing mats are used to rapidly repair bomb craters and other structural pavement damage along runways and other airfield facilities. These rapid repairs result in a patch that is 1.5 in. above the permanent pavement surface. The takeoff, landing, and taxi operations of F-16 fighter aircraft across a patch or multiple patches raised concerns about the potential for structural damage to the aircraft or reduced operational aircraft stability.

History and Scenario

Airfield landing mats were originally developed to meet the requirements of World War II aircraft, and development was continued to meet military needs during the Korean conflict and Vietnam. These development studies have resulted in four types of mats being available for use by military troops. These mats include the Army's M8A1, XM18, and M19 along with the Air Force and Navy AM-2 mat. A fifth mat, the truss web, has been developed and type-classified; however, there has been no procurement of the mat to date. Studies have been conducted by the U.S. Air Force (USAF) using the AM-2 mat to rapidly repair permanent runways. Repair kits have been developed and consist of AM-2 mat, ramps, and an anchorage system (Barber, Green, and Hammitt 1979).

In a war, airbases will be prime targets of attack. Threat analysts suggest that very extensive damage to runways, taxiways, choke points and other facilities will occur. Hundreds of craters can be expected during an attack. In order to launch and recover aircraft in retaliation, rapid runway repair emplacement personnel must construct a Minimum Operating Strip (MOS). One method to repair and construct a MOS is to use aluminum AM-2 mats.

The repaired surface will result in a runway that is rougher than the undamaged surface and higher than normal loads will be induced into operating aircraft. The question arises as to how much surface roughness can a given aircraft tolerate. In order to answer this question, the USAF project HAVE BOUNCE was begun in the 1970's.

The objective of project HAVE BOUNCE was to determine the ground roughness capability of most aircraft in the USAF inventory and to establish "smoothness" repair requirements based on those aircraft capabilities. The approach for attaining these objectives was through computer simulation, flight testing, and development of repair criteria (Gerardi 1981).

Objective

The objective of this study was to analyze the aircraft-surface interaction and response of F-16 aircraft traversing a 1.5-in.-thick AM-2 landing mat pavement repair. The goal was to identify the potential for structural damage to the aircraft and reduced operational stability of the aircraft.

Scope

The analysis was performed using USAF approved Vehicle-Surface Interaction Software. The software numerically simulates the dynamic response of an F-16 aircraft as it traverses over various configurations of AM-2 landing mats with ramps and compares critical response parameters to aircraft design and operation criteria (Figure 4). Single and multiple patches with ascending and descending ramps of 1.9- and 0.9-deg slopes were investigated. The major phases of this work included the following:

a. *Phase I: Software Integration and Aircraft Criteria.* The F-16 simulation software was obtained, installed, and verified on WES hardware. The F-16 aircraft design and operating criteria were obtained to compare with results of the numerical simulations.

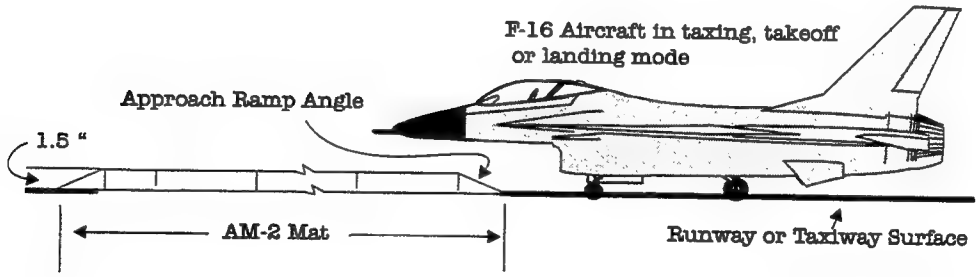

Figure 4. Configuration of F-16 simulation identifying appropriate parameters

b. *Phase II: Symmetric Aircraft Simulations on Singular Patch.* Operations of the F-16 (a tricycle gear aircraft) were numerically simulated and the response calculations were compared to the applicable criteria. The aircraft response parameters evaluated during the numerical simulations included: (1) vertical load on the nose gear, (2) vertical load on the main gears, and (3) minimum fuel tank ground clearance. The

aircraft was modeled with all three F-16 wheels or gears moving along the pavement profile containing a single repair with 1.9-deg ramps (Figure 5). At the request of Samsun, the results of this phase were forwarded to the Partner on 26 September 1997.

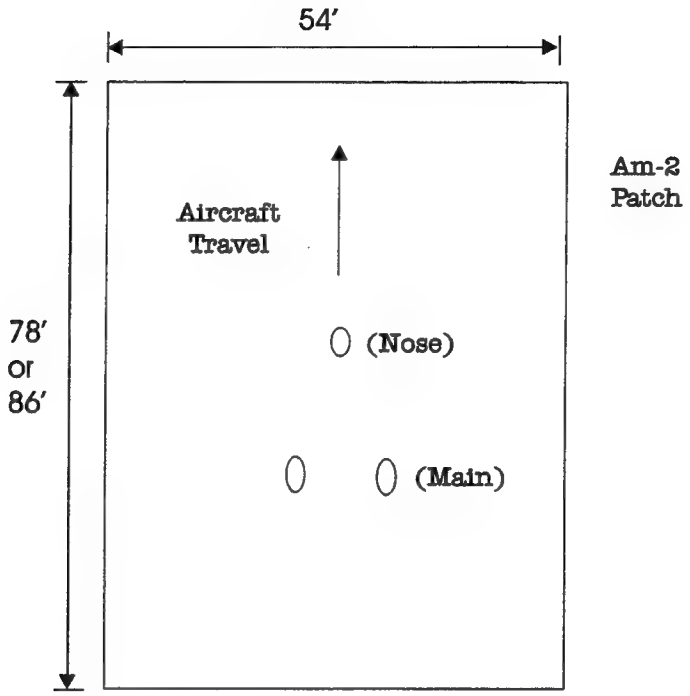

Figure 5. Symmetric, Load case 1 (nose gear and both main gears on patch)

c. *Phase III: Nonsymmetric Aircraft Simulations on Singular and Multiple Repair Patches*. Additional operations of the F-16 were numerically simulated and the response calculations were compared to the applicable criteria. The aircraft was modeled with various combinations of the three wheels or gears moving along the pavement profile (Figures 6 and 7) containing both single and multiple patches as required in the Technical Orders Manual (TO) for F-16 aircraft. Repairs with 1.9- and 0.9-deg ramps were investigated.

d. *Phase IV. Final Documentation of Results*. The results of the analysis were transmitted to the Partner in a draft report on 17 November 1997.

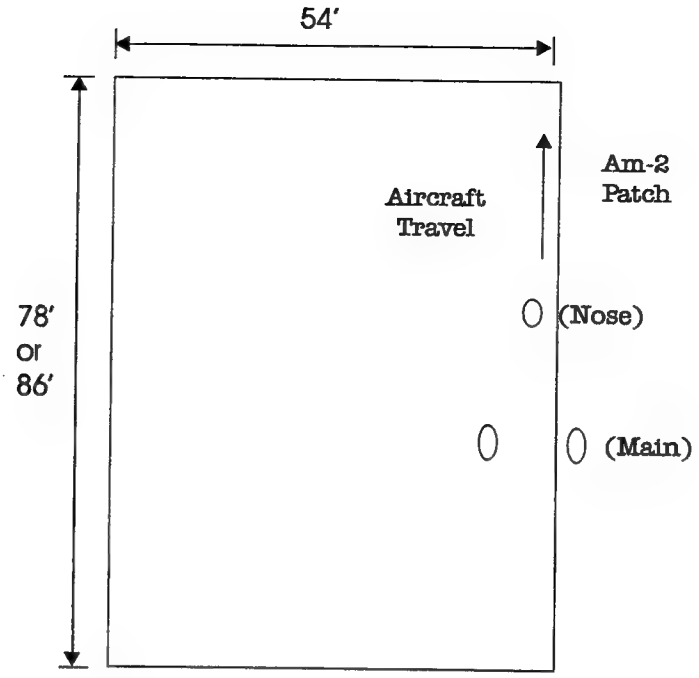

Figure 6. Nonsymmetric, Load case 2 (nose gear and one main gear on patch)

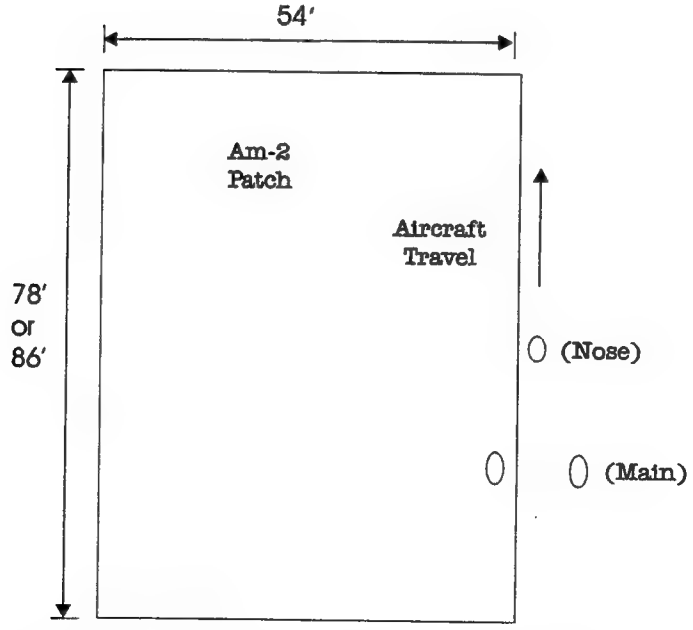

Figure 7. Nonsymmetric, Load case 3 (one main gear on patch)

2 Analysis

Pavement and Landing Mat Properties and Conditions

Runway repair kits were developed by the USAF to provide expedient bomb damage repair for theater air bases. The standard kit consists of AM-2 landing mat, ascending and descending ramps, anchorage, and other materials necessary for repair emplacement. A standard size AM-2 patch (with ramps) measures 54 ft wide by 78 ft long by 1.5 in. high. The leading and trailing edges of the patch consist of ramps which are approximately 45 in. long. The ramps provide a gradual slope (1.9 deg from horizontal) up to the 1.5-in.-thick AM-2 patch (Figure 2).

Ramps which are approximately 95 in. long are being considered by the Korean Air Force for use with the standard size AM-2 patch. The ramps provide a very gradual slope (0.9 deg from horizontal) up to the 1.5 in.-thick AM-2 patch (Figure 3). These modified ramps have not been field evaluated; however, a design drawing for fabrication is available. An AM-2 patch (with modified ramps) measures 54 ft wide by 86 ft long by 1.5 in. high.

Reviewed technical literature indicates that the inclusion of multiple repairs in numerical simulations cause aircraft gear load response increases as compared to single repair simulations (Sanders and Plews 1983). Therefore, double patch simulations with both 1.9- and 0.9-deg ramps were included in the investigation. Field validation evaluations conducted by the USAF used a 70-ft distance between patches; therefore, this same distance was used in the WES simulations.

The double patch simulations (70 ft between patches) presented herein represent a small fraction of the thousands of simulations which are required to develop roughness criteria. Roughness criteria for the F-16 are presented in ESL-TR-81-17 and repair quality criteria guidance with charts to determine allowable runway roughness are presented in TO 35E2-4-1.

The analysis investigated F-16 operations on the standard and modified AM-2 patch(es) (Figures 2 and 3). The longitudinal surface profile of the single and double mat patches for 1.9- and 0.9-deg ramps is shown in Figures 8 and 9, respectively.

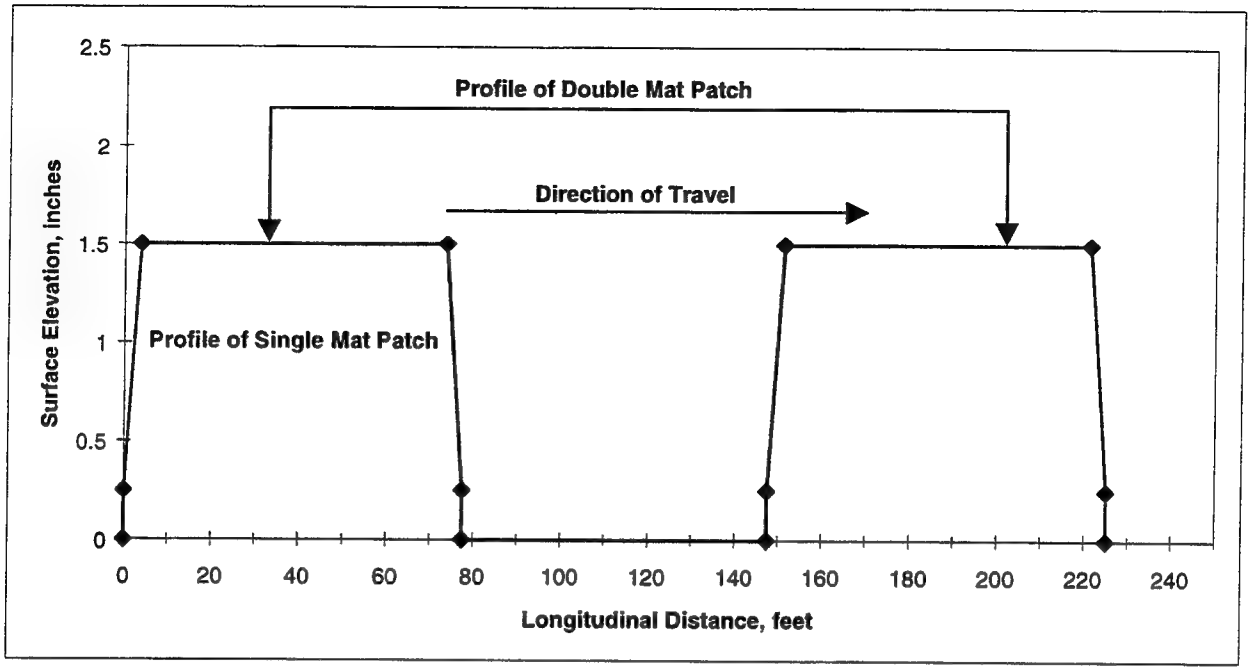

Figure 8. Longitudinal surface profile of single and double mat patches for 1.9-deg ramps

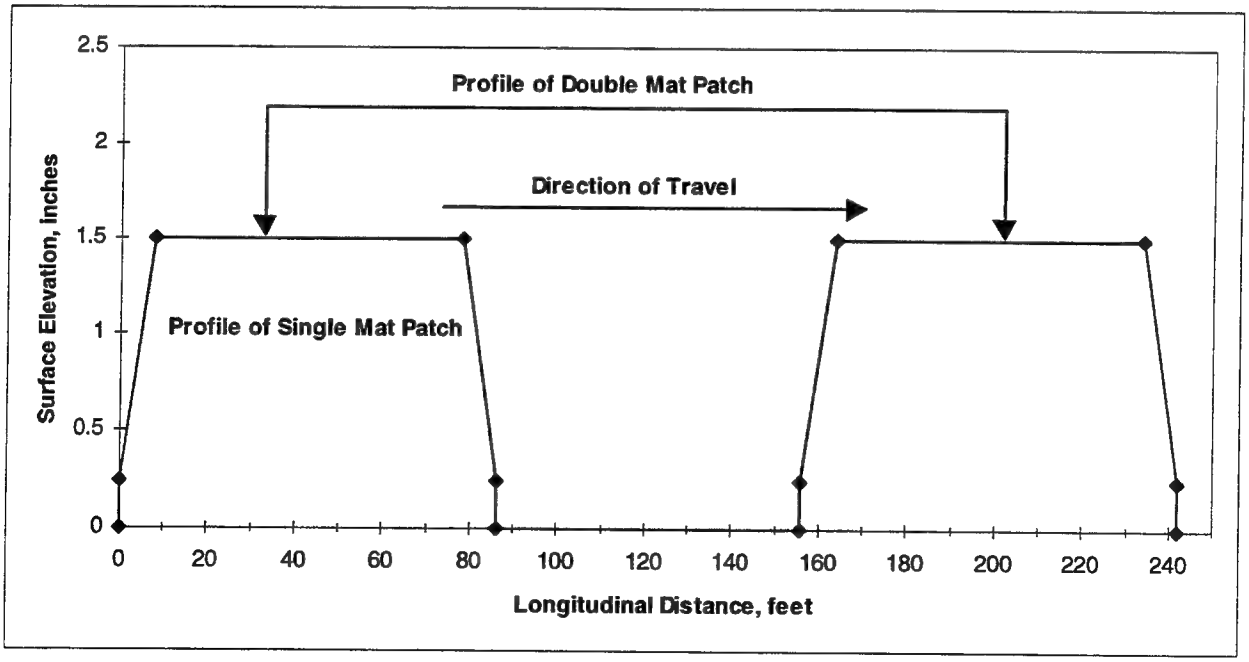

Figure 9. Longitudinal surface profile of single and double mat patches for 0.9-deg ramps

Aircraft Response and Design Criteria

The USAF and other Department of Defense contractors provided unclassified reports and technical literature on aircraft design and operation criteria. This information was used to identify critical aircraft response parameters for comparison with computed numerical simulation responses. A number of parameters were identified in the various references obtained from the USAF. However, for this work the applicable criteria are given in Table 1.

Table 1
Critical Response Parameters

Parameter	Design Limit	Remarks
Nose gear load	18,800 lb*	Explicit design load limit
Main gear load	30,400 lb*	Explicit design load limit
Ground clearance	--	Practical limit
Maximum landing speed at 34,684 lb	150 knots	Estimated value
Maximum landing speed at 20,246 lb	116 knots	Typical mission value
Maximum takeoff speed at 34,684 lb	153 knots	Typical mission value
Maximum takeoff speed at 20,246 lb	120 knots	Estimated value

*(Sander and Plews 1983).

Numerical Simulation Software

The Rapid Runway Repair (RRR) software for conducting vehicle-surface interaction analyses was used to compute these results. This USAF approved software incorporates a mathematical model in which the F-16 landing gear, propulsion system, aerodynamics, and control surfaces are directly modeled. The F-16 is represented as a rigid body with four degrees of freedom system (vertical translation, pitch, longitudinal translation, and roll) and a number of body flexibility modes which vary with aircraft configuration. The response of the aircraft in terms of forces, accelerations, and displacements of critical structural components is computed from the impulse forces generated by a runway repair profile. The software consists of a processing interface, data input files, and a library of executable aircraft models. The software is written in FORTRAN and runs in a PC-Based Windows 95 environments.

Results of Numerical Simulations

The RRR software was used to complete this project. Eight basic simulation runs were conducted using the parameters shown in Table 2. The F-16 loads were derived from guidance for typical maximum and minimum operating weights from General Dynamics reports 16PR4391 and 16PR2429. The accelerating and decelerating condition represents a takeoff and landing; respectively. A total of 24 simulation runs was necessary to complete the work for the three load cases shown in Figures 5-7. A matrix of simulations for the standard AM-2 patch(es) with 1.9-deg ramps is shown in Table 3. The same matrix was used for 24 additional runs for the modified AM-2 patch(es) with 0.9-deg ramps.

Table 2
Description of Simulation Runs

Simulation ID	Patch Configuration	Gross Weight of F-16, lbs	Accelerating (A) or Decelerating (D)
1	Single	34,684	D
2	Single	20,246	D
3	Single	34,684	A
4	Single	20,246	A
5	Double	34,684	D
6	Double	20,246	D
7	Double	34,684	A
8	Double	20,684	A

The critical calculated response values for the 1.9- and 0.9-deg ramps are summarized in Tables 4 and 5, respectively. A graphic presentation of the calculated maximum gear forces as a function of each simulated approach ground speed for the 1.9-deg ramps is shown in Appendix A. Graphic presentations for the 0.9-deg ramps are shown in Appendix B. The calculated minimum tank clearance for both the 1.9- and 0.9-deg ramps as shown in Tables 4 and 5 are not critical responses; therefore, graphic presentations are not included.

The nose gear force of 19,558 and 19,685 lb for run simulation 5 and 13; respectively, shown in Table 4 exceeds the design limit of 18,800 lb for the F-16. These forces were calculated for a double patch, landing operation, heavy aircraft condition, and 1.9-deg ramps. The calculated force of 19,685 lb for a double patch (run 13) is 38 percent greater than the calculated force for a single patch (run 9). The force of 17,277 lb for 0.9-deg ramp simulated run 13 (Table 5) is 12 percent less than the force for 1.9-deg ramp simulated run 13 (Table 4). However, the nose gear force of 17,277 lb is only 1,523 lb less than the nose gear design load limit. The main gear design load limit (30,400 lb) was not exceeded by simulations for the 1.9- and 0.9-deg ramps.

Table 3
Matrix of Aircraft Simulations Performed

Simulation	Load Case[1,2,3]	Light (L)[4] or Heavy (H)[5] Weight	Acceleration (A) or Deceleration (D) Condition	Patch
1	1	H	D	Single
2	1	L	D	Single
3	1	H	A	Single
4	1	L	A	Single
5	1	H	D	Double
6	1	L	D	Double
7	1	H	A	Double
8	1	L	A	Double
9	2	H	D	Single
10	2	L	D	Single
11	2	H	A	Single
12	2	L	A	Single
13	2	H	D	Double
14	2	L	D	Double
15	2	H	A	Double
16	2	L	A	Double
17	3	H	D	Single
18	3	L	D	Single
19	3	H	A	Single
20	3	L	A	Single
21	3	H	D	Double
22	3	L	D	Double
23	3	H	A	Double
24	3	L	A	Double

[1] Load Case 1 = Nose gear and both main gears on patch.
[2] Load Case 2 = Nose gear and one main gear on patch.
[3] Load Case 3 = One main gear on patch.
[4] Light weight = 20,246 lb.
[5] Heavy weight = 34,684 lb.

Table 4
Critical Calculated Response Values for 1.9-Deg Ramps

Simulation ID	Run Configuration[1]	Maximum Nose Gear Force, lb	Maximum Main Gear Force, lb	Minimum Tank Clearance, in.
1	SHD	14,931	21,297	3.88
2	SLD	9,287	18,929	4.96
3	SHA	11,311	21,438	3.84
4	SLA	6,780	18,613	5.87
5	DHD	19,558	24,860	2.98
6	DLD	12,327	20,585	4.40
7	DHA	13,719	25,752	3.50
8	DLA	8,374	20,156	5.62
9	SHD	14,255	21,253	4.03
10	SLD	8,224	18,707	4.87
11	SHA	11,311	21,414	4.48
12	SLA	6,780	18,527	5.87
13	DHD	19,685	26,310	3.37
14	DLD	10,845	18,707	4.77
15	DHA	12,203	26,114	4.35
16	DLA	7,669	18,950	5.85
17	SHD	12,583	21,607	3.59
18	SLD	7,203	19,081	4.32
19	SHA	7,842	21,715	4.21
20	SLA	3,767	18,931	5.59
21	DHD	12,583	25,687	3.32
22	DLD	4,193	19,168	5.59
23	DHA	8,112	26,844	3.69
24	DLA	4,193	19,168	5.59
Limiting Value		18,800	30,400	--

[1] Field 1: S = single patch, D = double patch.
Field 2: H = heavy weight, L = light weight.
Field 3: D = decelerating (landing), A = accelerating (takeoff).

Table 5
Critical Calculated Response Values for 0.9-Deg Ramps

Simulation ID	Run Configuration[1]	Maximum Nose Gear Force, lb	Maximum Main Gear Force, lb	Minimum Tank Clearance, in.
1	SHD	14,872	18,364	3.70
2	SLD	9,621	17,693	4.57
3	SHA	11,026	18,847	3.82
4	SLA	5,771	16,477	6.14
5	DHD	16,753	20,446	3.26
6	DLD	9,621	17,693	4.57
7	DHA	11,026	21,705	3.56
8	DLA	6,642	17,080	5.80
9	SHD	14,179	18,240	4.19
10	SLD	7,905	15,936	4.94
11	SHA	9,412	19,230	4.50
12	SLA	5,771	16,310	6.05
13	DHD	17,277	21,603	3.48
14	DLD	9,137	16,841	4.88
15	DHA	10,897	22,072	4.23
16	DLA	5,882	16,586	6.03
17	SHD	12,583	18,465	3.68
18	SLD	7,203	16,305	4.53
19	SHA	7,753	19,612	4.27
20	SLA	3,940	16,507	5.73
21	DHD	12,583	20,776	3.40
22	DLD	7,203	16,305	4.53
23	DHA	7,819	22,265	3.70
24	DLA	4,260	17,383	5.73
Limiting Value		18,800	30,400	--

[1] Field 1: S = single patch, D = double patch.
Field 2: H = heavy weight, L = light weight.
Field 3: D = decelerating (landing), A = accelerating (takeoff).

Maximum gear forces are presented as a percent of the gear design load limit in Figures 10-12. This summary shows the nose gear design load limit is exceeded in runs 5 and 13 for the 1.9-deg ramps. The maximum nose gear response over a double patch with the F-16 landing at 140 knots is shown in Figure 13. This comparison of the aircraft response over 1.9- and 0.9-deg ramps shows that the nose gear design load limit is exceeded for the 1.9-deg ramps.

Information gleaned from AFMAN 10-219 (Volume 4) states that AM-2 matting should be primarily relegated to secondary use (taxiway repairs). This manual states that "folded fiberglass mats should be considered the primary foreign object damage cover for use on all MOS repairs. AM-2 mats will be used only on taxiways unless FFMs are not available. If AM-2 matting is to be used on a MOS, extensive spacing between patches is required and transitional ramps a must."

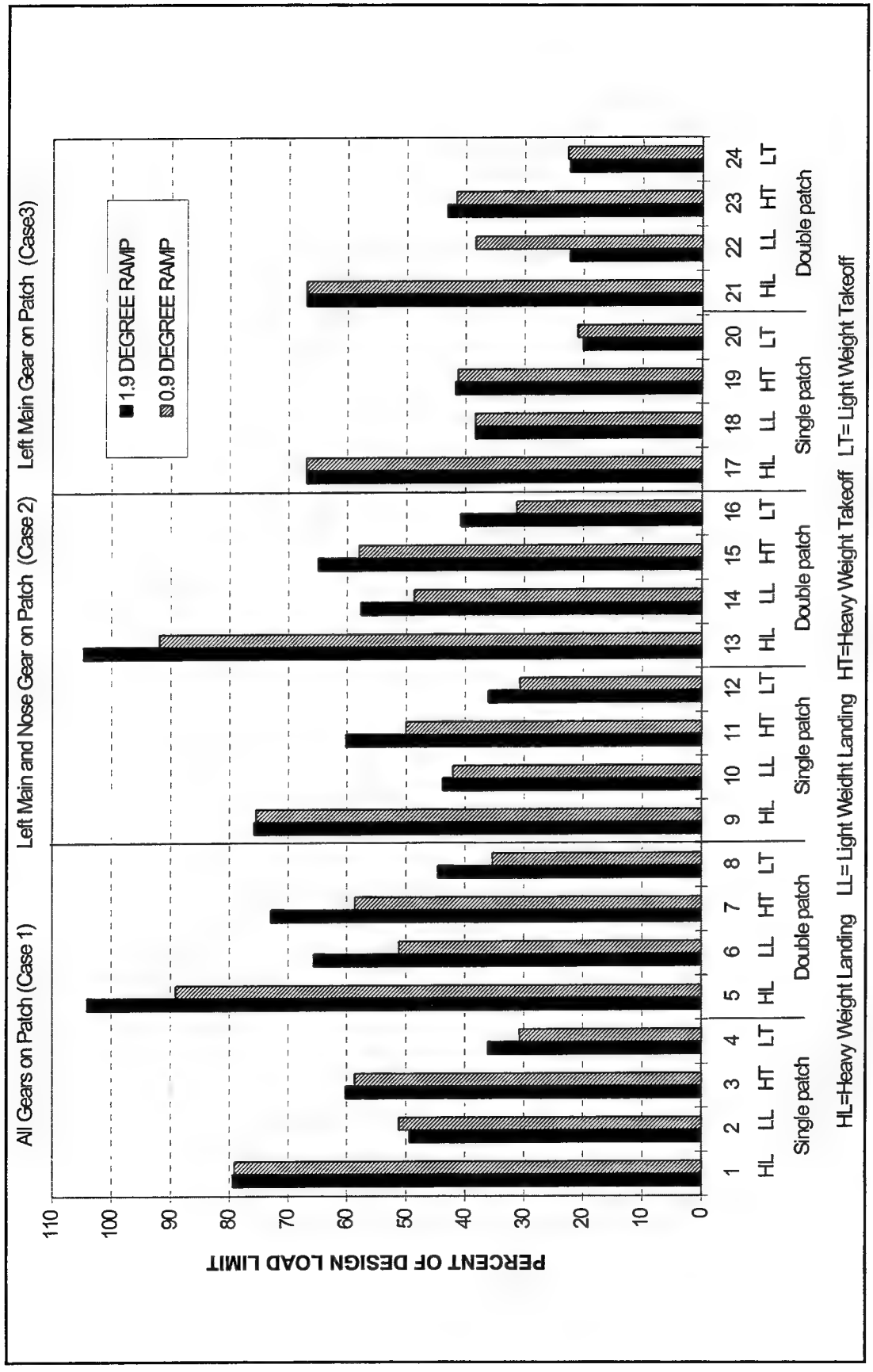

Figure 10. Maximum nose gear forces as percent of design load limit

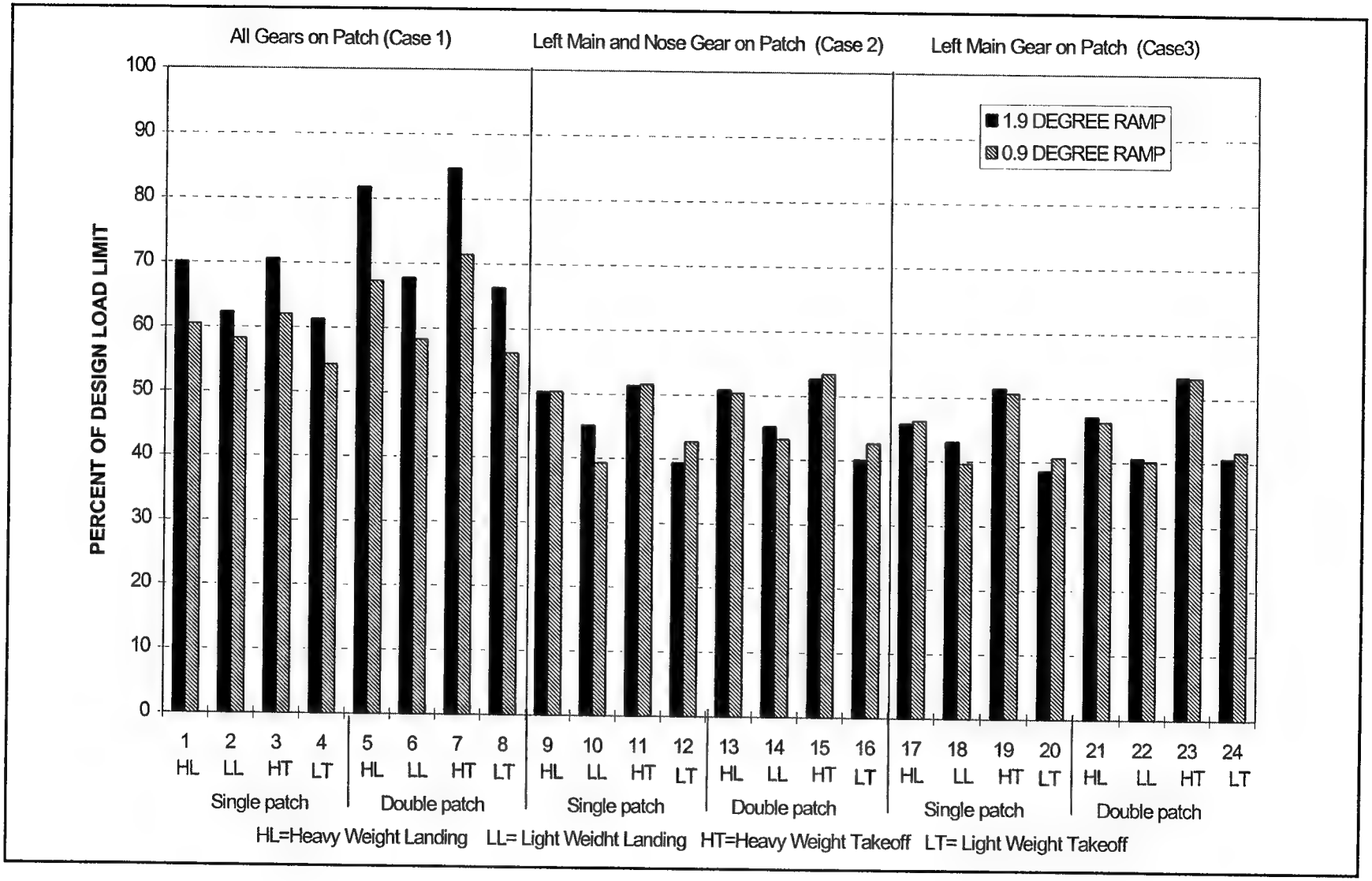

Figure 11. Maximum right main gear forces as percent of design load limit

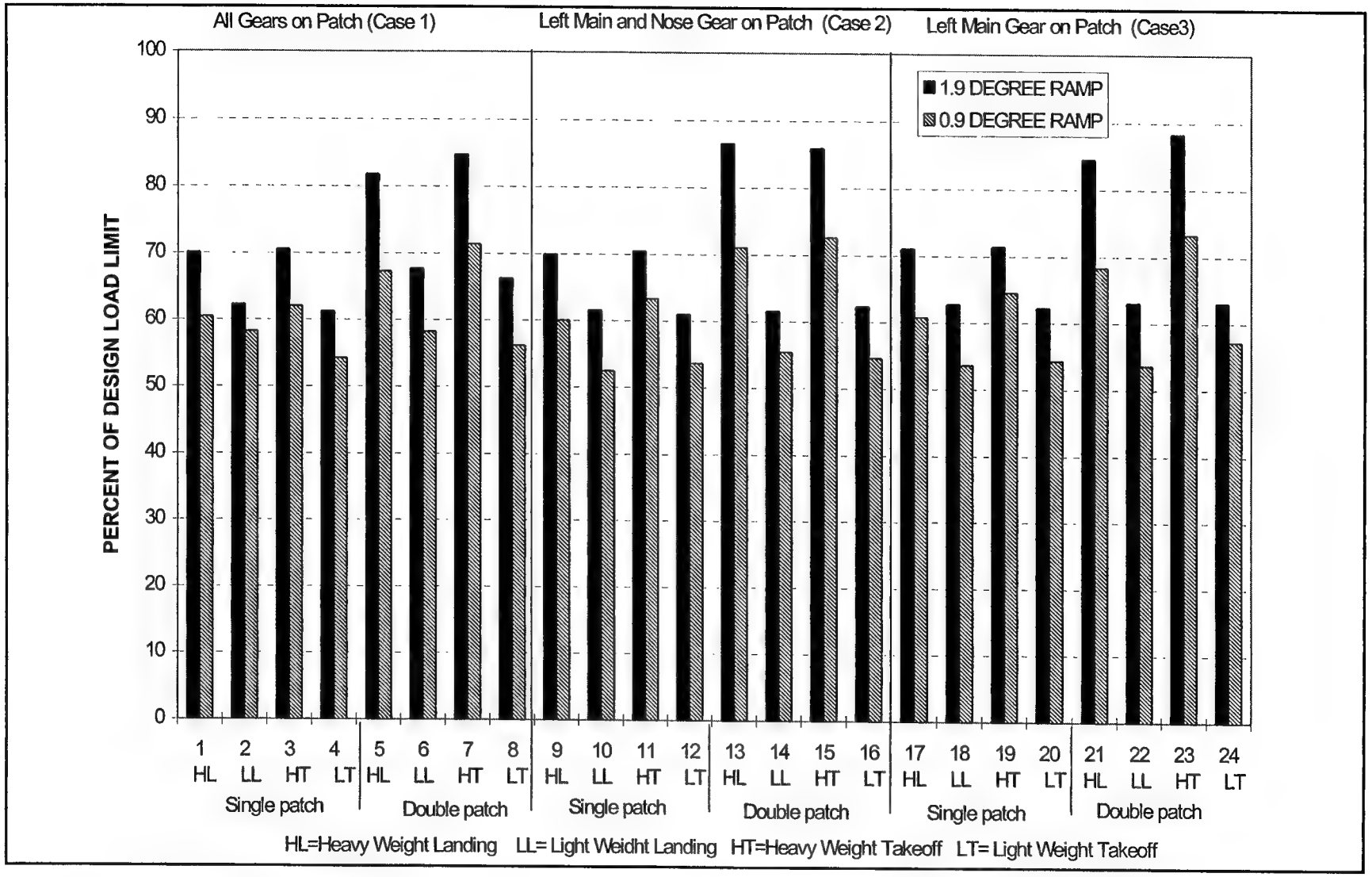

Figure 12. Maximum left main gear forces as percent of design load limit

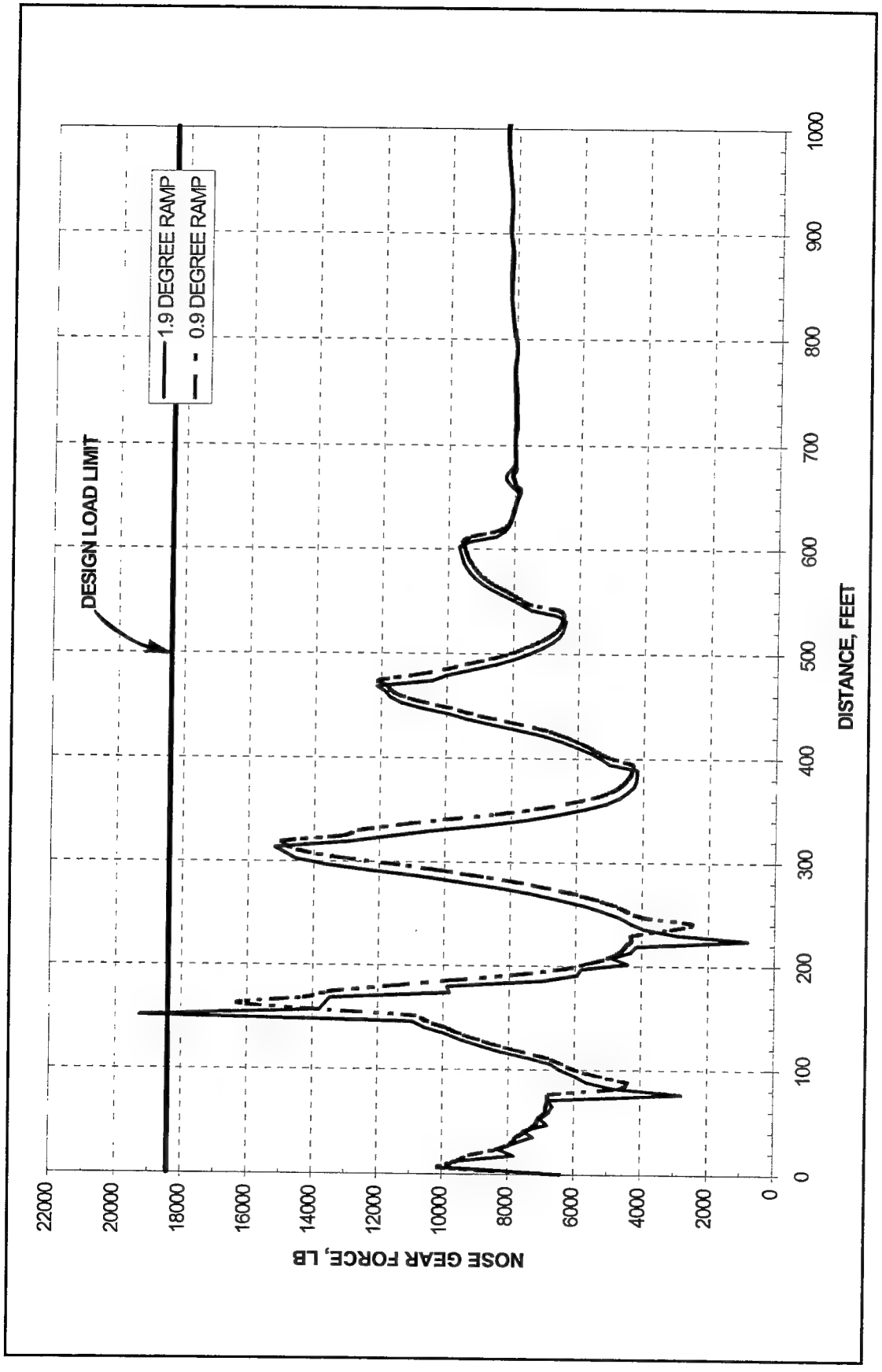

Figure 13. Nose gear vertical forces at 140 knots approach speed on double patches

3 Summary and Conclusions

Summary

Simulations indicate that the critical F-16 aircraft nose gear design load limit (18,800 lb) was exceeded with calculated response nose gear forces of 19,558 and 19,685 lb. These forces occurred in the symmetric case (nose gear and two main gears on patch) and nonsymmetric case (nose gear and one main gear on patch). The forces were calculated for a double AM-2 patch, landing operation, heavy aircraft condition, and 1.9-deg ramps.

The main gear design load limit was not exceeded in the simulations performed for the 1.9- and 0.9-deg ramps. Results indicate that a majority of the nose and main gear calculated response forces are reduced by using the 0.9-deg ramps.

Simulations on the 0.9-deg ramps indicate that the critical F-16 aircraft nose gear design limit was not exceeded with calculated response nose gear forces for either a single or double AM-2 patch condition. Maximum calculated response nose gear forces of 16,753 and 17,277 lb occurred in the symmetric case (nose gear and two main gears on patch) and nonsymmetric case (nose gear and one main gear on patch); respectively. These forces were calculated for a double AM-2 patch, landing operation, and heavy aircraft condition.

Conclusions

Based on the information presented in this study, the following conclusions are warranted:

a. Simulations indicate that the calculated response nose gear force exceeded the F-16 aircraft nose gear design load limit with simulation parameters as follows: symmetric load case, double AM-2 patch, landing operation, heavy aircraft condition, and 1.9-deg ramps.

b. Simulations indicate that the calculated response nose gear force exceeded the F-16 aircraft nose gear design load limit with simulation parameters as follows: nonsymmetric load case (nose gear and one

main gear on patch), double AM-2 patch, landing operation, heavy aircraft condition, and 1.9-deg ramps.

c. Simulations indicate that the main gear design load limit should not be exceeded with either the 1.9- or 0.9-deg ramps.

d. Simulations indicate that the nose gear design load limit should not be exceeded with the 0.9-deg ramps.

e. Simulation results indicate that a majority of the nose and main gear calculated response forces are reduced by using the 0.9-deg ramps.

f. Typically, greater gear forces are generated during landings as compared to takeoffs with the same aircraft weight.

g. Greater gear forces are generated with the double AM-2 patches as compared to the single patch condition.

h. The AFMAN 10-219 (Volume 4) states that AM-2 matting should primarily be used to repair taxiways.

i. Technical order manual (TO 35E2-4-1) provides guidance for AM-2 mat patch spacing and roughness criteria for 1.9-deg ramps. Roughness criteria have not been developed for the 0.9-deg ramps.

j. Proper AM-2 mat patch spacing with 1.9-deg ramps is important for safe F-16 operations on repaired runways.

References

Freck, S. G. (1987). "Development of surface roughness criteria for damaged and damage-repaired surfaces," ESL-TR-81-17 (Addendum VI), Engineering and Services Laboratory, Tyndall AFB, FL.

General Dynamics. (1986). "F-16 air combat fighter program - contract support for HAVE BOUNCE Program," Final Report I, 16PR4391, Fort Worth, TX.

General Dynamics. (1982). "F-16 air combat fighter program - contractor support for HAVE BOUNCE Program," Interim Report - Tasks I and II, 16PR2429, Forth Worth, TX.

Gerardi, T. G. (1981). "Aircraft response to operations on rapidly repaired battle damaged runways and taxiways," The Shock and Vibration Bulletin, Bulletin 51 (Part 3), 205-211.

Headquarters, Department of the Air Force. (1997). "Rapid runway repair operations," AFMAN 10-219 (Volume 4), Tyndall AFB, FL.

Headquarters, Department of the Air Force. (1990). "Repair quality criteria system for rapid runway repair," TO 35E2-4-1, Eglin, AFB, FL.

Office, Chief of Engineers, U.S. Army. (1979). "Airfield damage repair," Field Reference Document, Washington, DC.

Sanders, LT K. W. and Plews, L. D. (1983). "F-16 HAVE BOUNCE aircraft tests," AFFTC-TR-83-56, Air Force Flight Test Center, Edwards AFB, CA.

Appendix A
Relationships of Maximum Calculated Gear Forces Versus Approach Ground Speed for 1.9-Deg Ramps

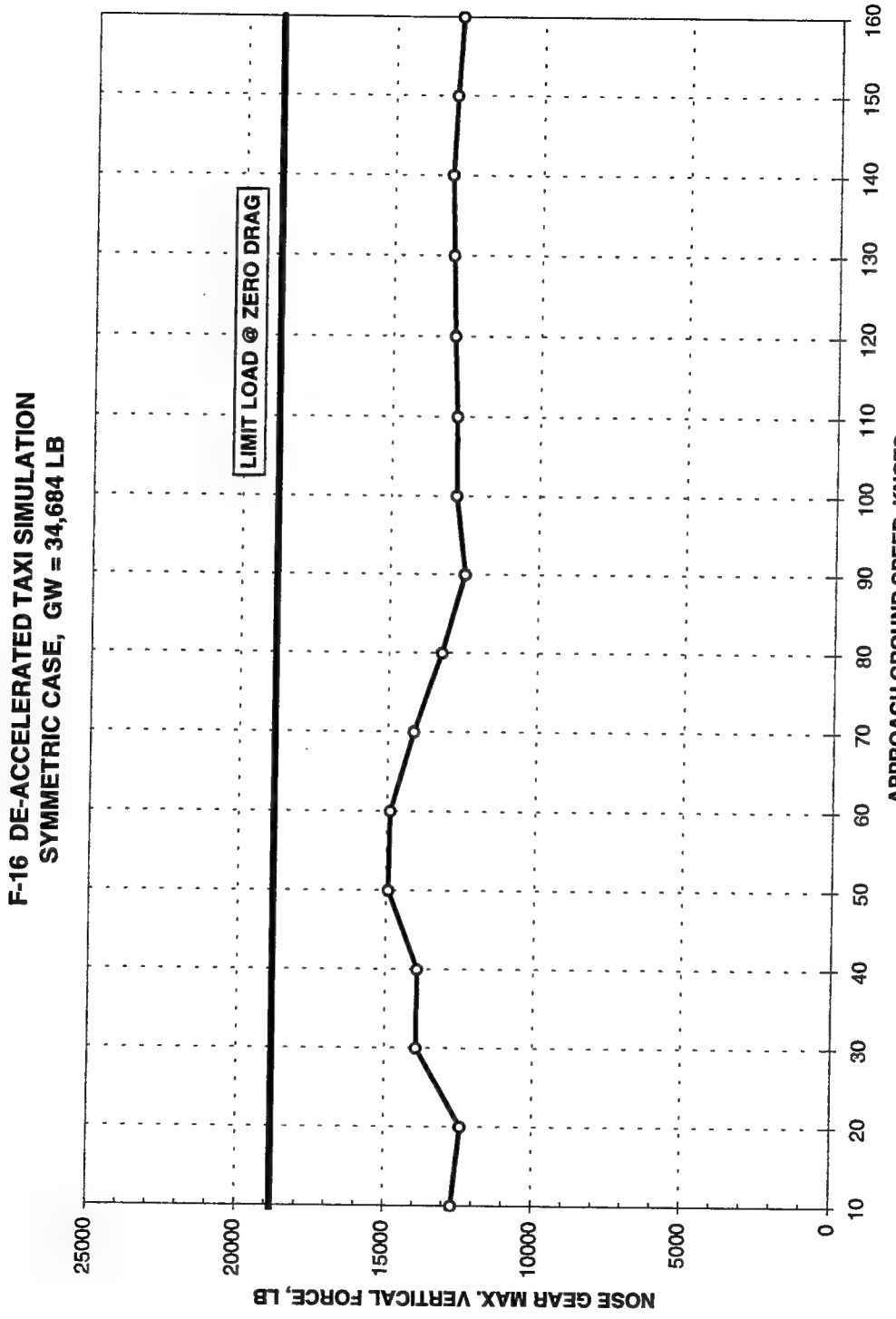

Figure A1. Nose gear forces for load case 1, deceleration (landing) mode, heavy gross weight, single mat, and 1.9-deg ramps

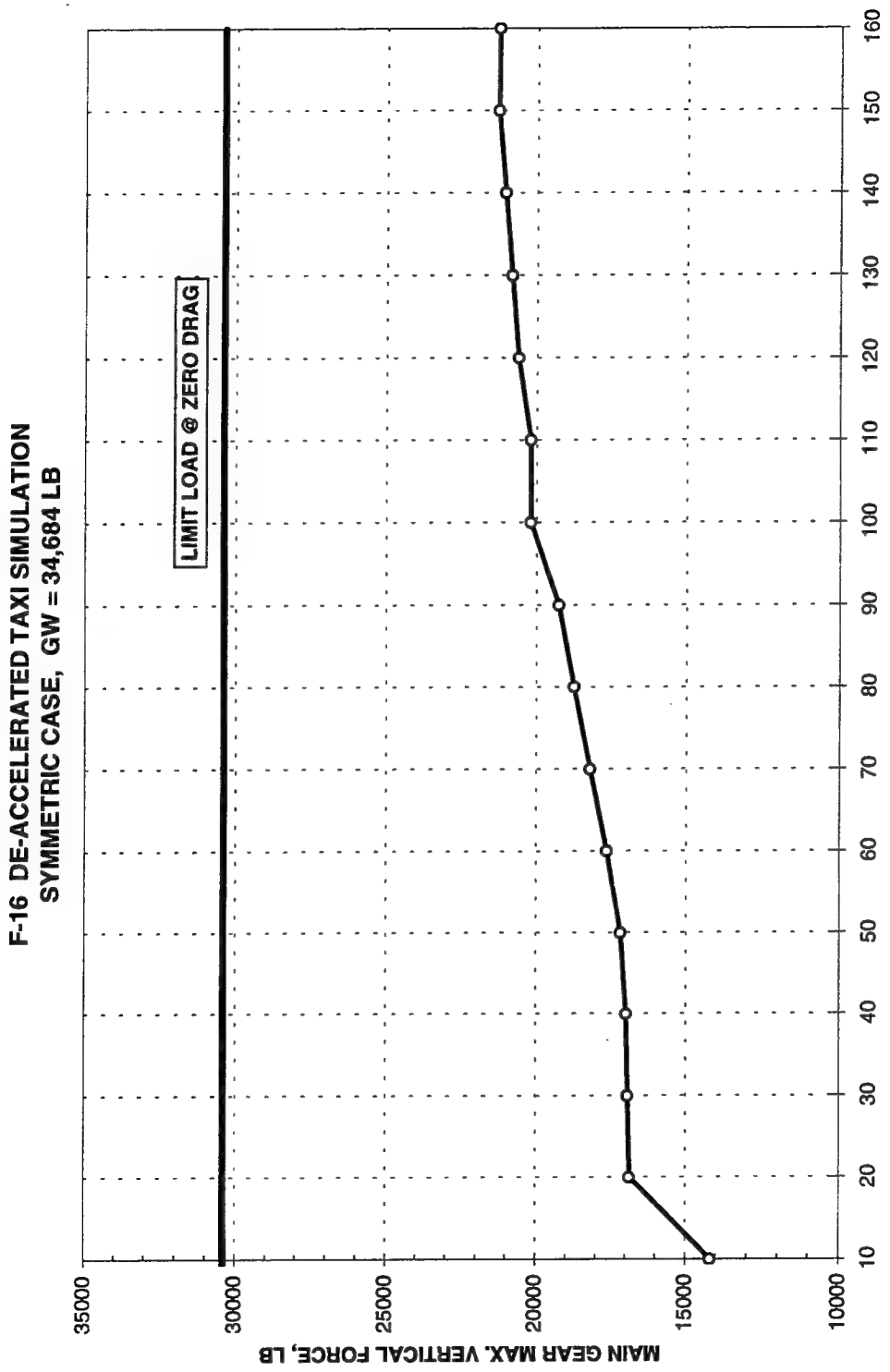

Figure A2. Main gear forces for load case 1, deceleration (landing) mode, heavy gross weight, single mat, and 1.9-deg ramps

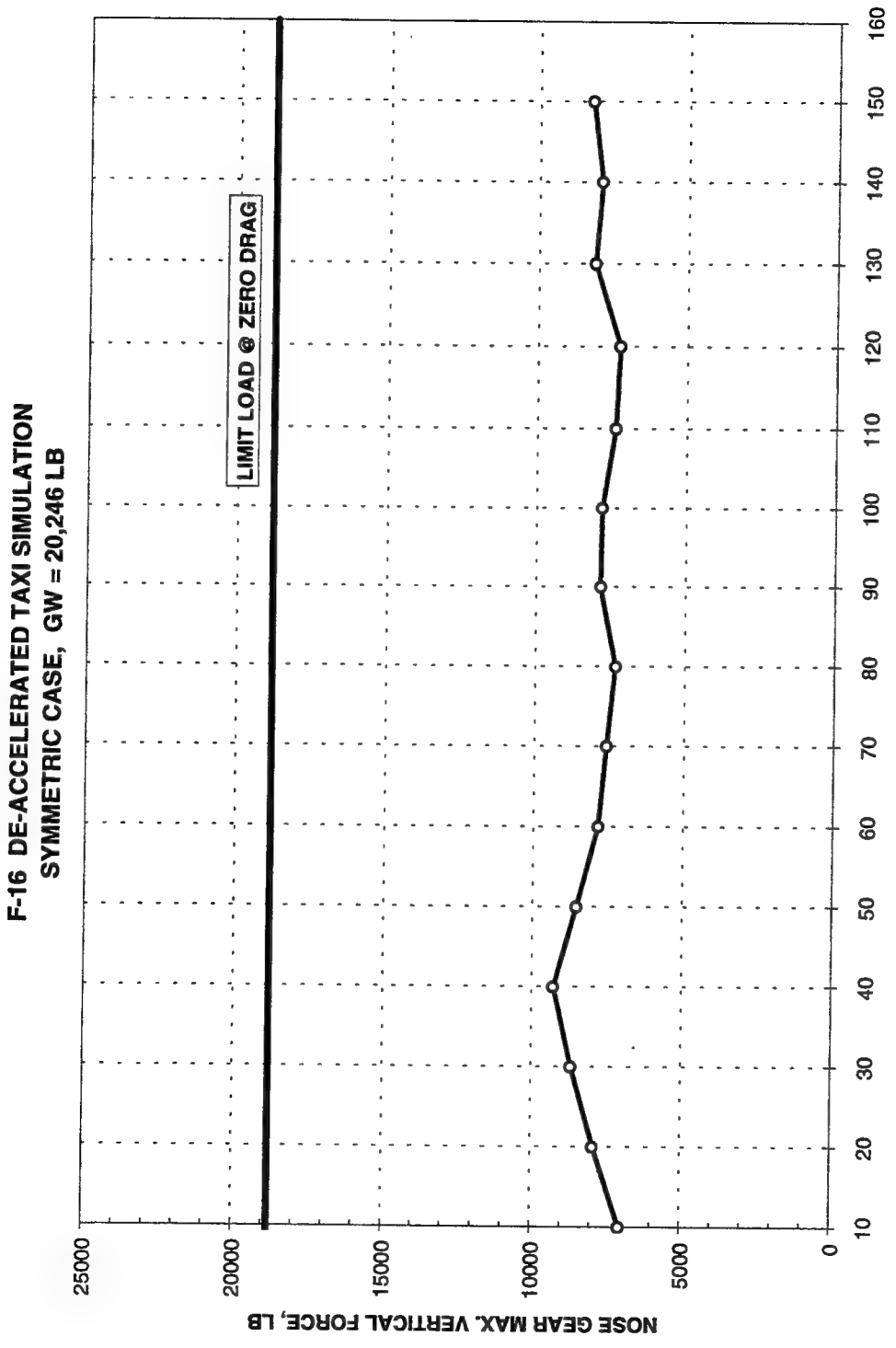

Figure A3. Nose gear forces for load case 1, deceleration (landing) mode, light gross weight, single mat, and 1.9-deg ramps

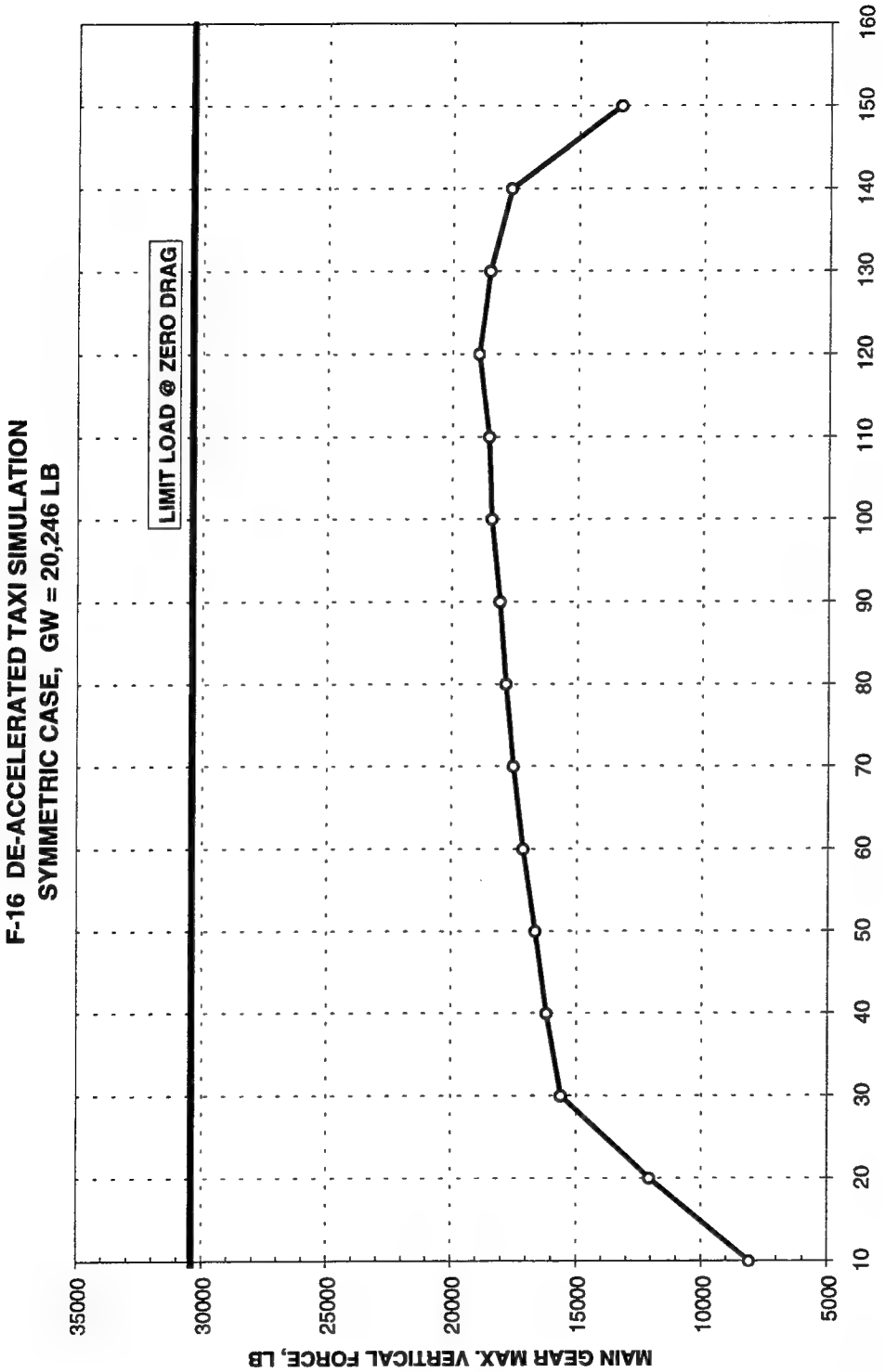

Figure A4. Main gear forces for load case 1, deceleration (landing) mode, light gross weight, single mat, and 1.9-deg ramps

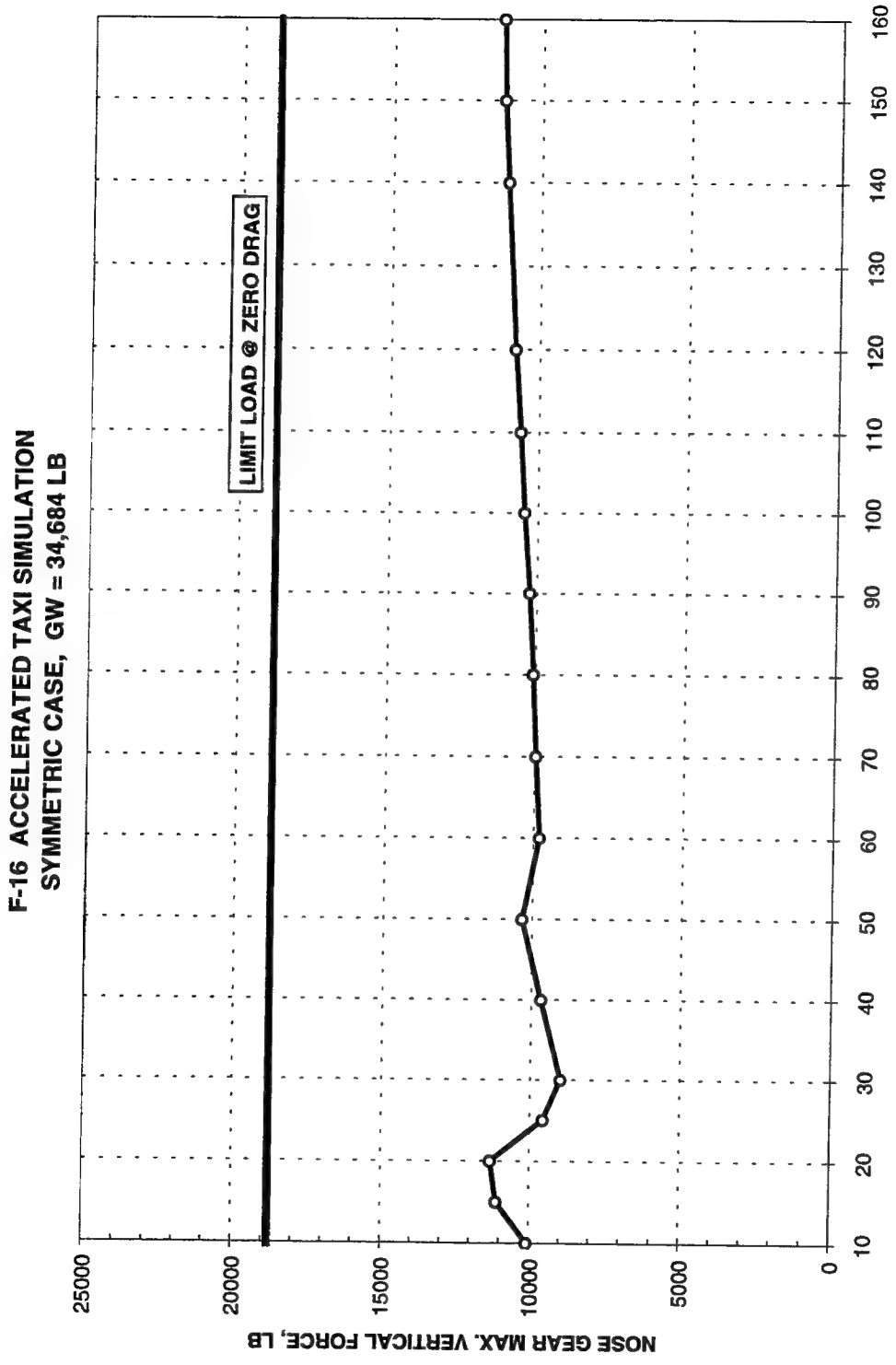

Figure A5. Nose gear forces for load case 1, acceleration (takeoff) mode, heavy gross weight, single mat, and 1.9-deg ramps

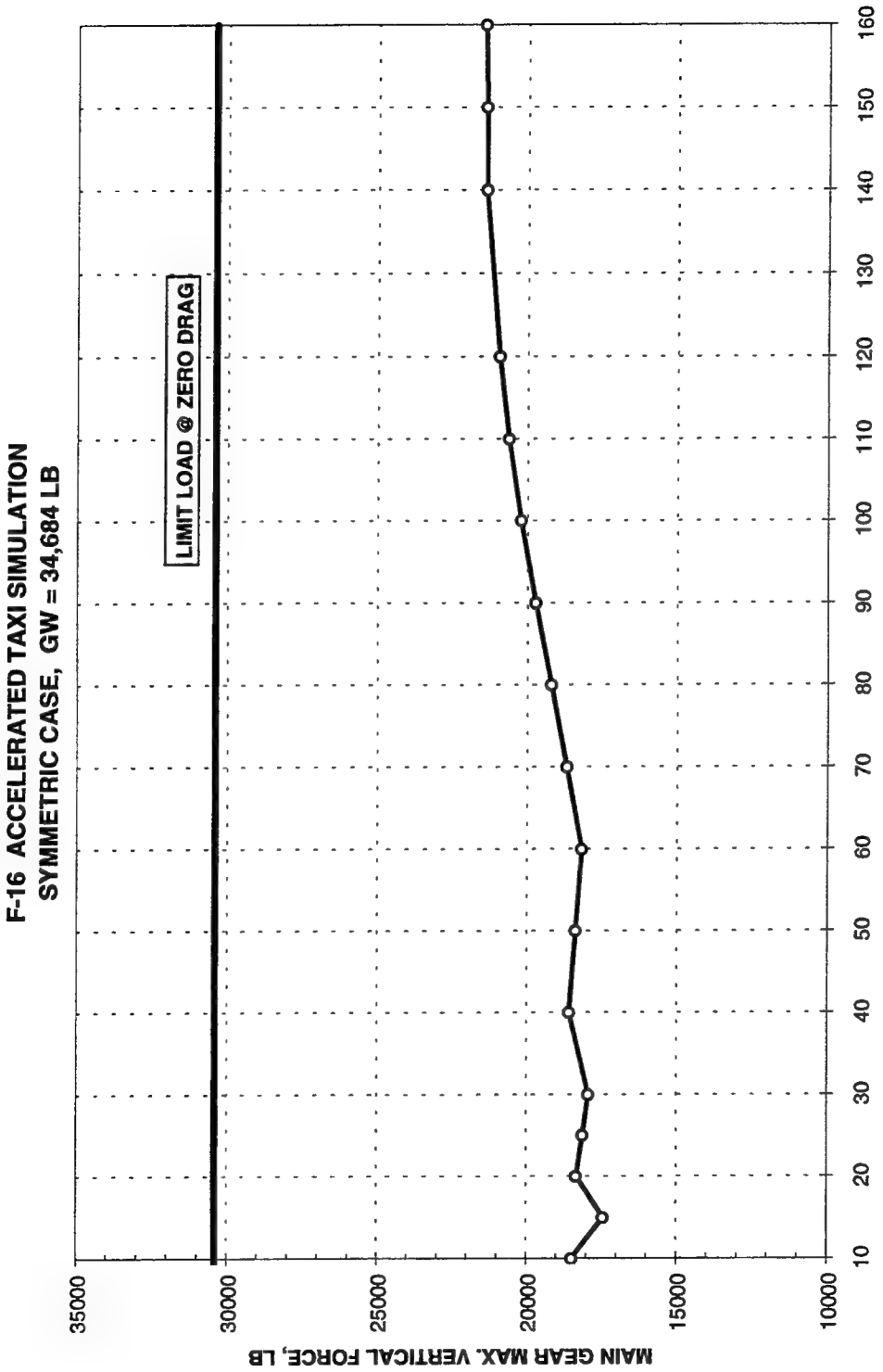

Figure A6. Main gear forces for load case 1, acceleration (takeoff) mode, heavy gross weight, single mat, and 1.9-deg ramps

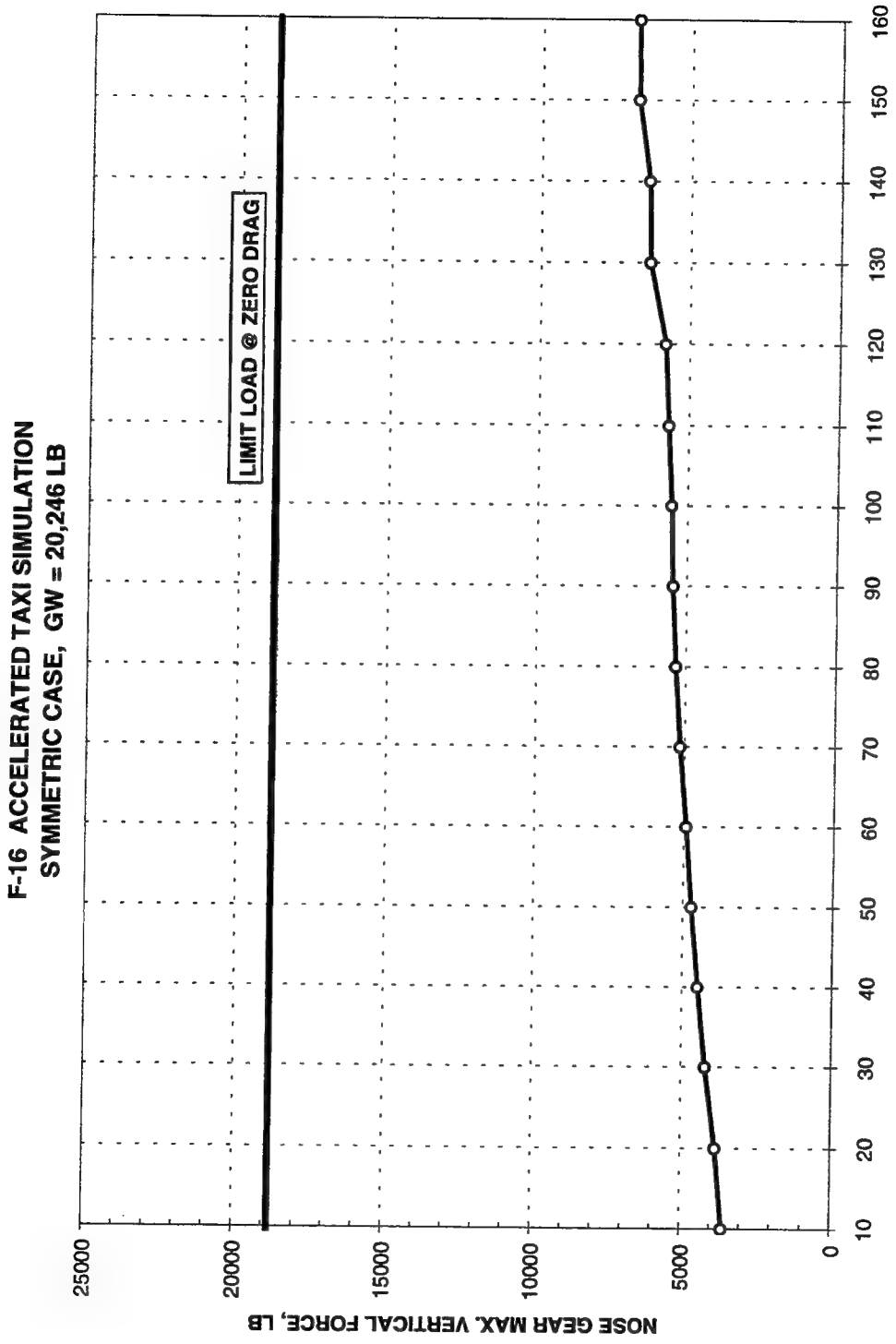

Figure A7. Nose gear forces for load case 1, acceleration (takeoff) mode, light gross weight, single mat, and 1.9-deg ramps

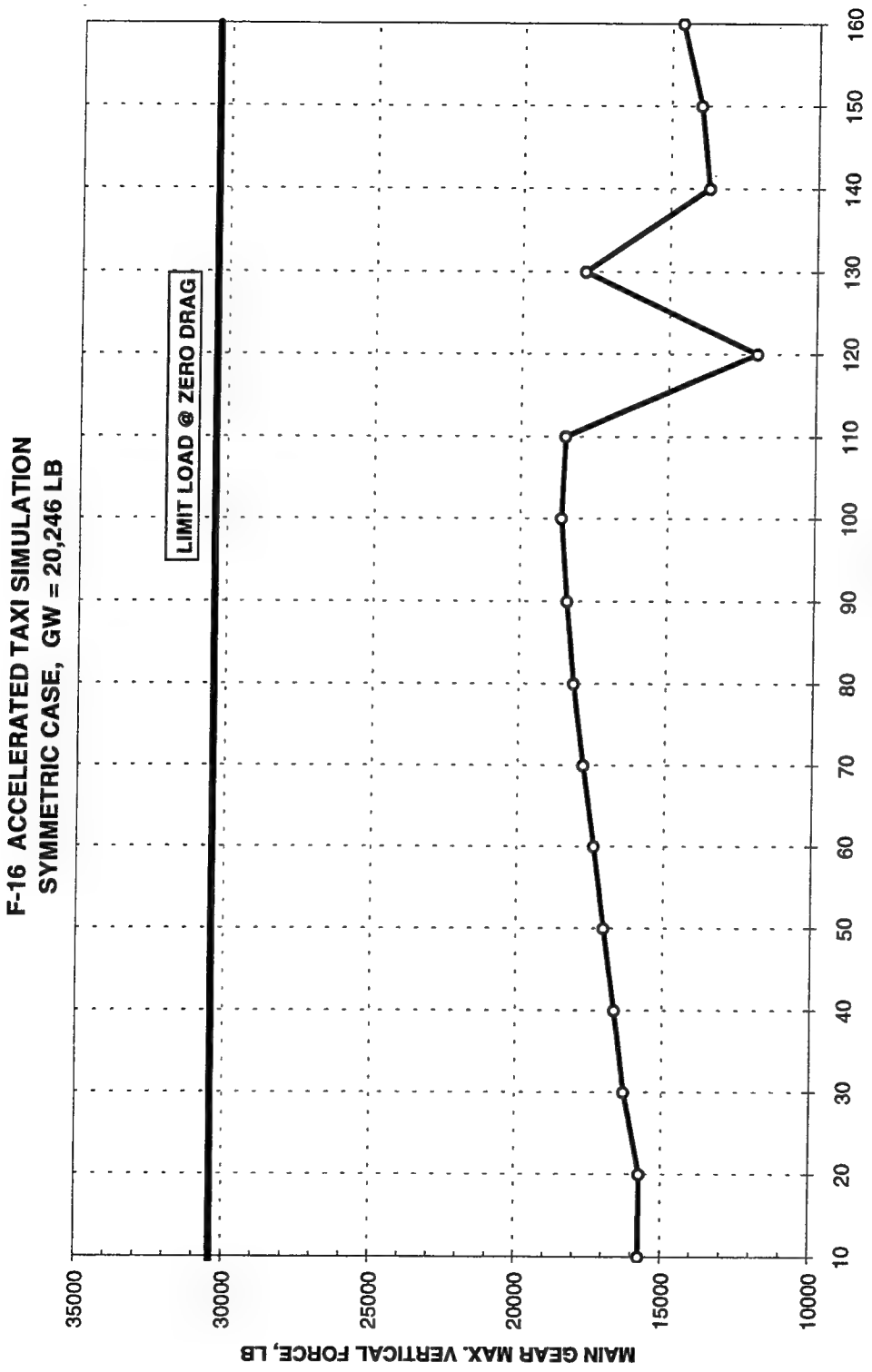

Figure A8. Main gear forces for load case 1, acceleration (takeoff) mode, light gross weight, single mat, and 1.9-deg ramps

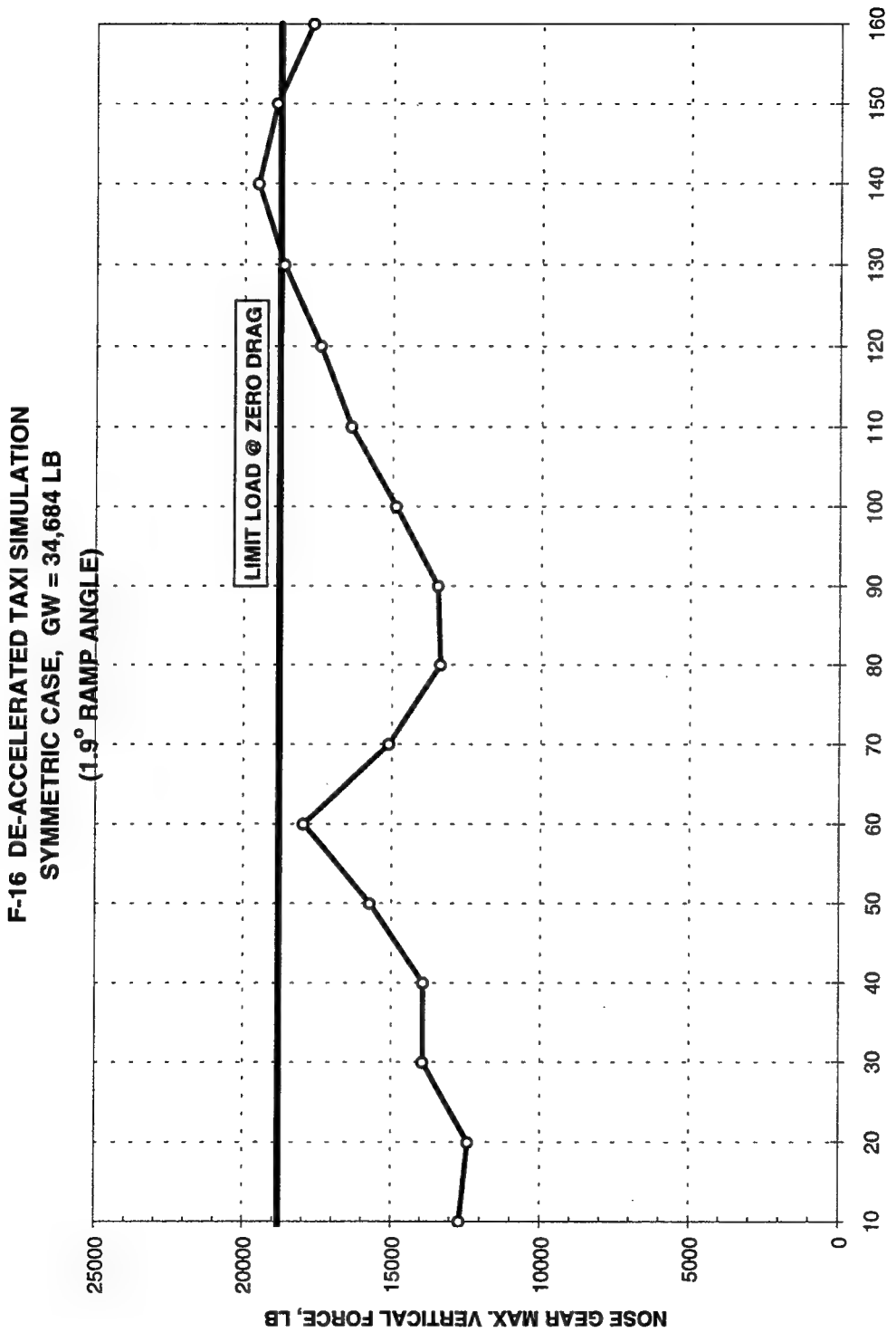

Figure A9. Nose gear forces for load case 1, deceleration (landing) mode, heavy gross weight, double mat, and 1.9-deg ramps

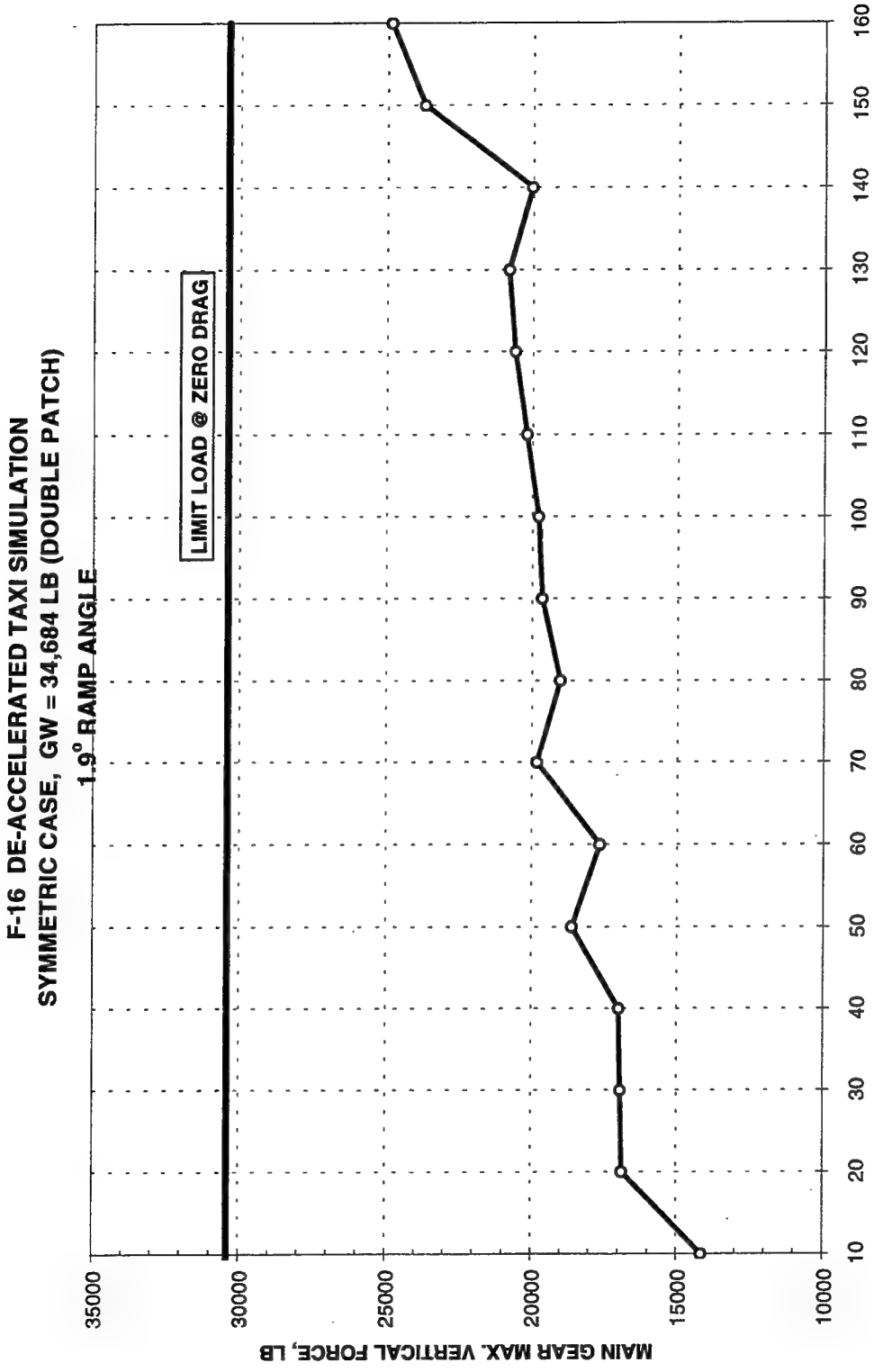

Figure A10. Main gear forces for load case 1, deceleration (landing) mode, heavy gross weight, double mat, and 1.9-deg ramps

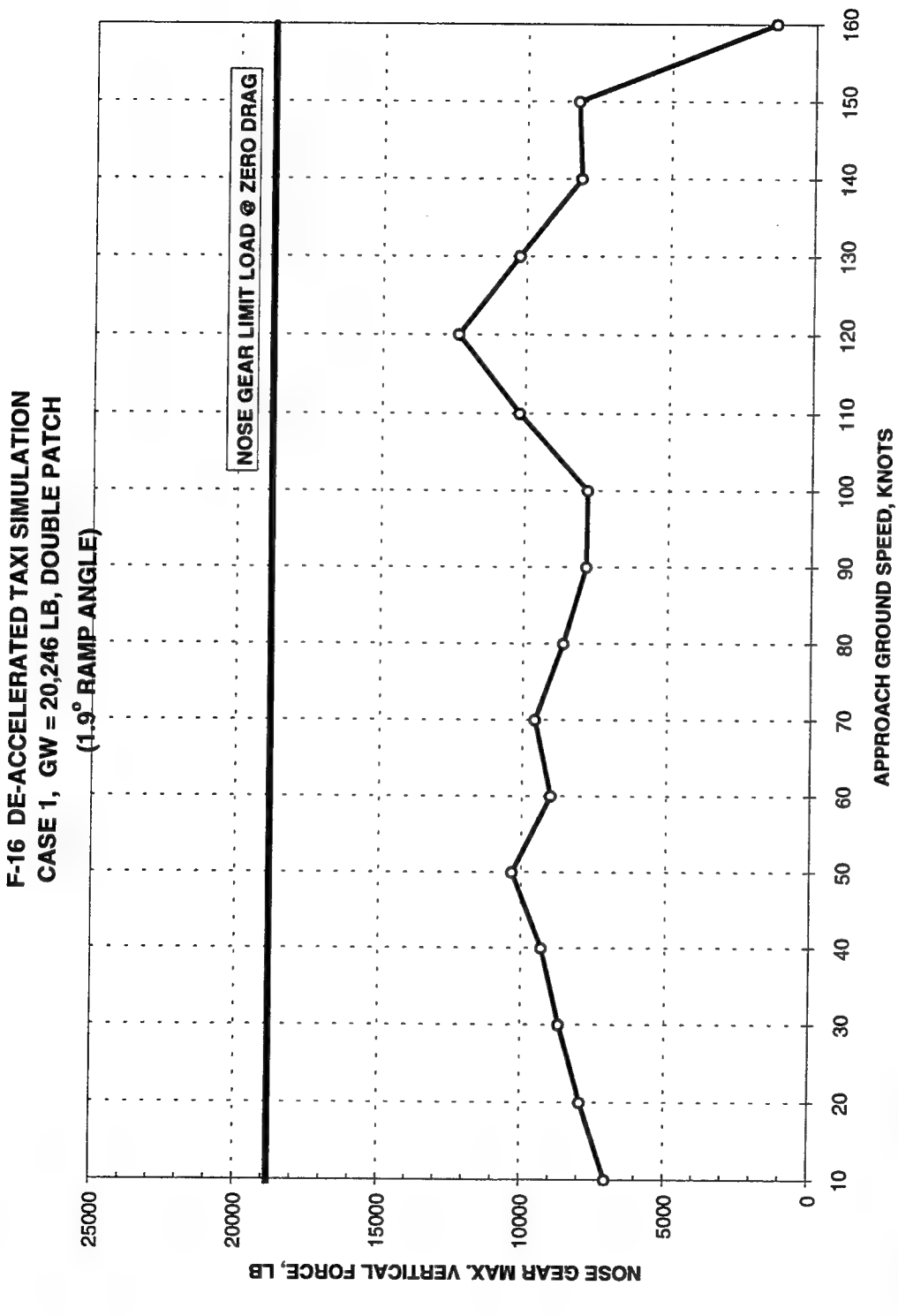

Figure A11. Nose gear forces for load case 1, deceleration (landing) mode, light gross weight, double mat, and 1.9-deg ramps

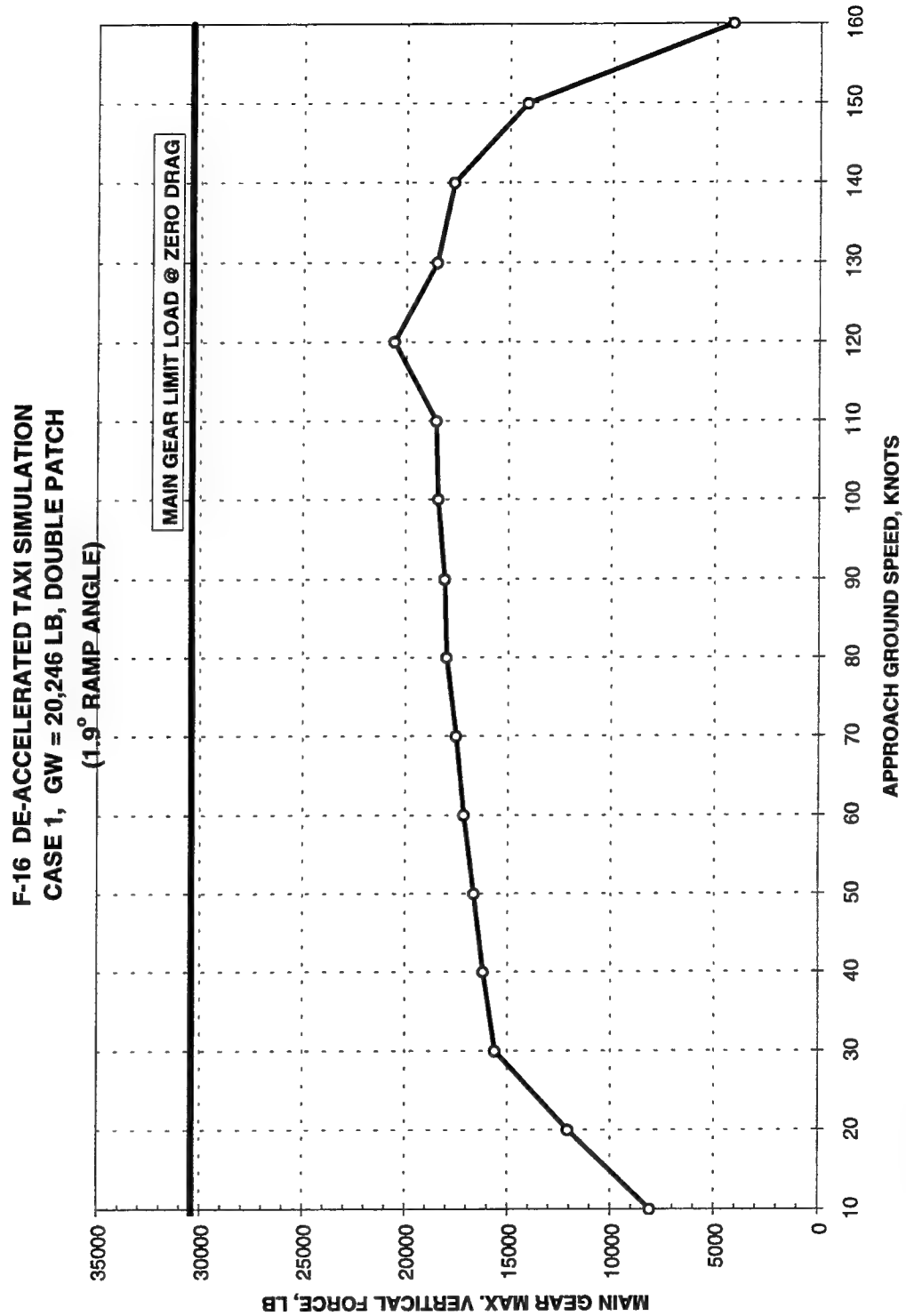

Figure A12. Main gear forces for load case 1, deceleration (landing) mode, light gross weight, double mat, and 1.9-deg ramps

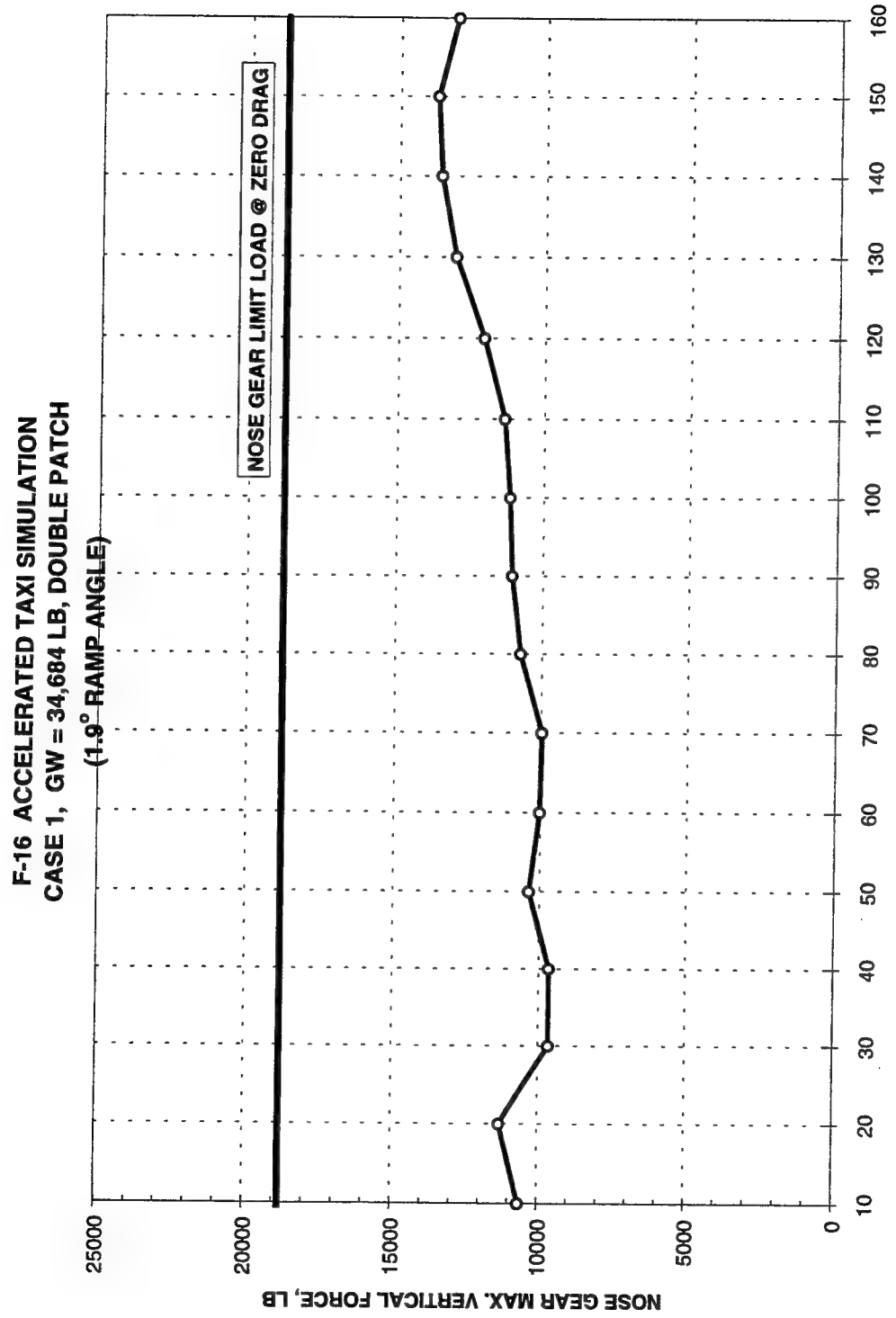

Figure A13. Nose gear forces for load case 1, acceleration (takeoff) mode, heavy gross weight, double mat, and 1.9-deg ramps

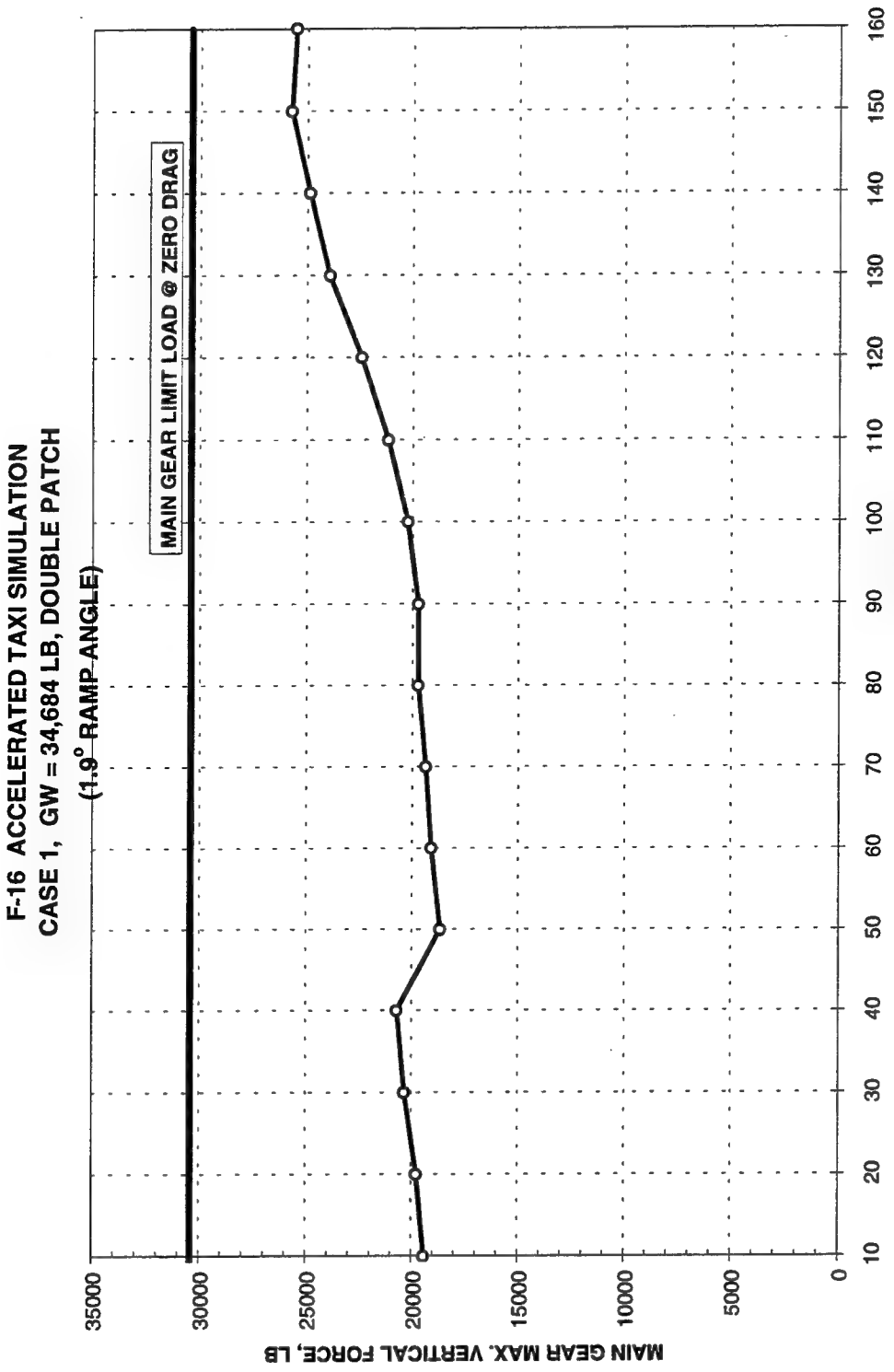

Figure A14. Main gear forces for load case 1, acceleration (takeoff) mode, heavy gross weight, double mat, and 1.9-deg ramps

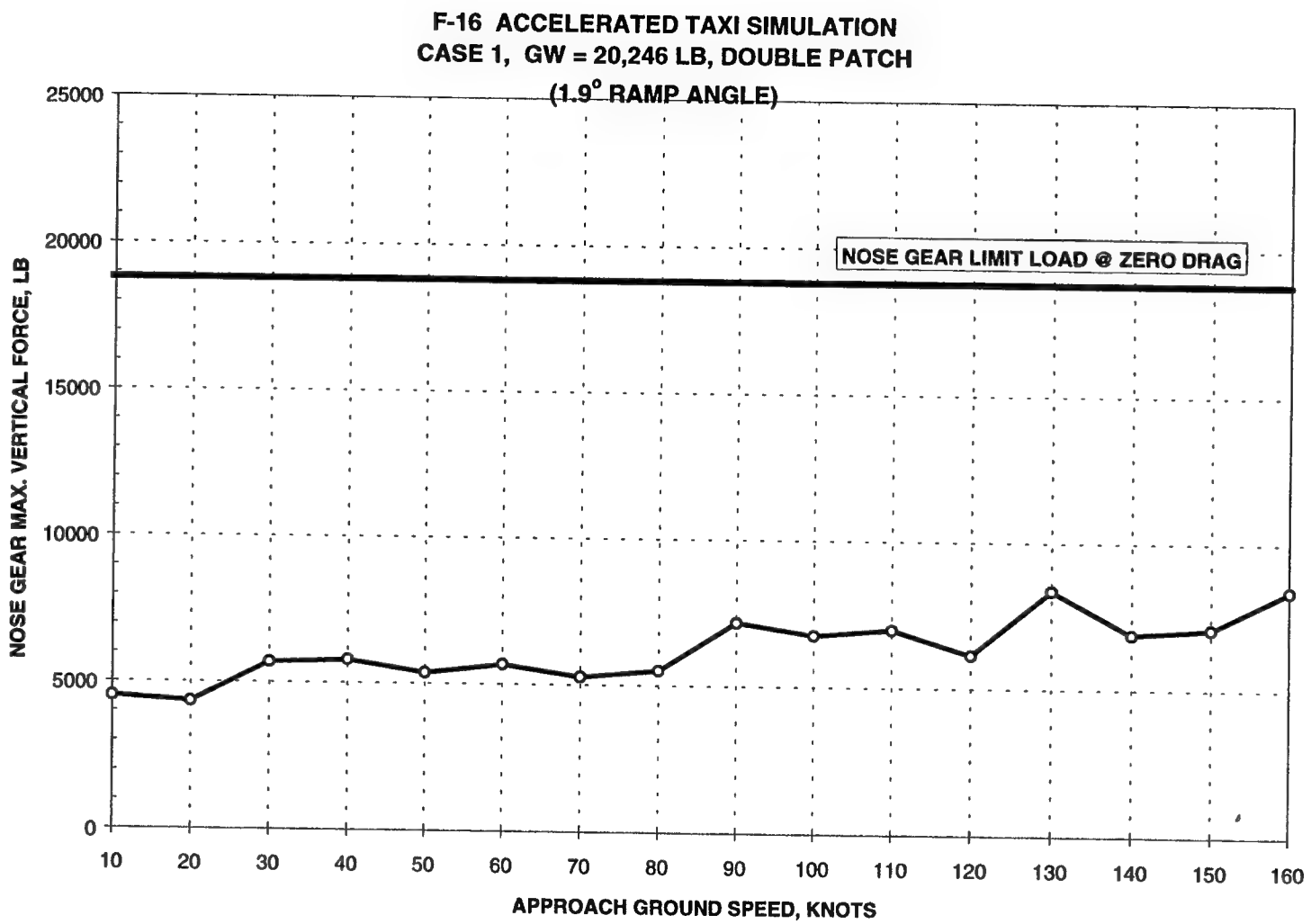

Figure A15. Nose gear forces for load case 1, acceleration (takeoff) mode, light gross weight, double mat, and 1.9-deg ramps

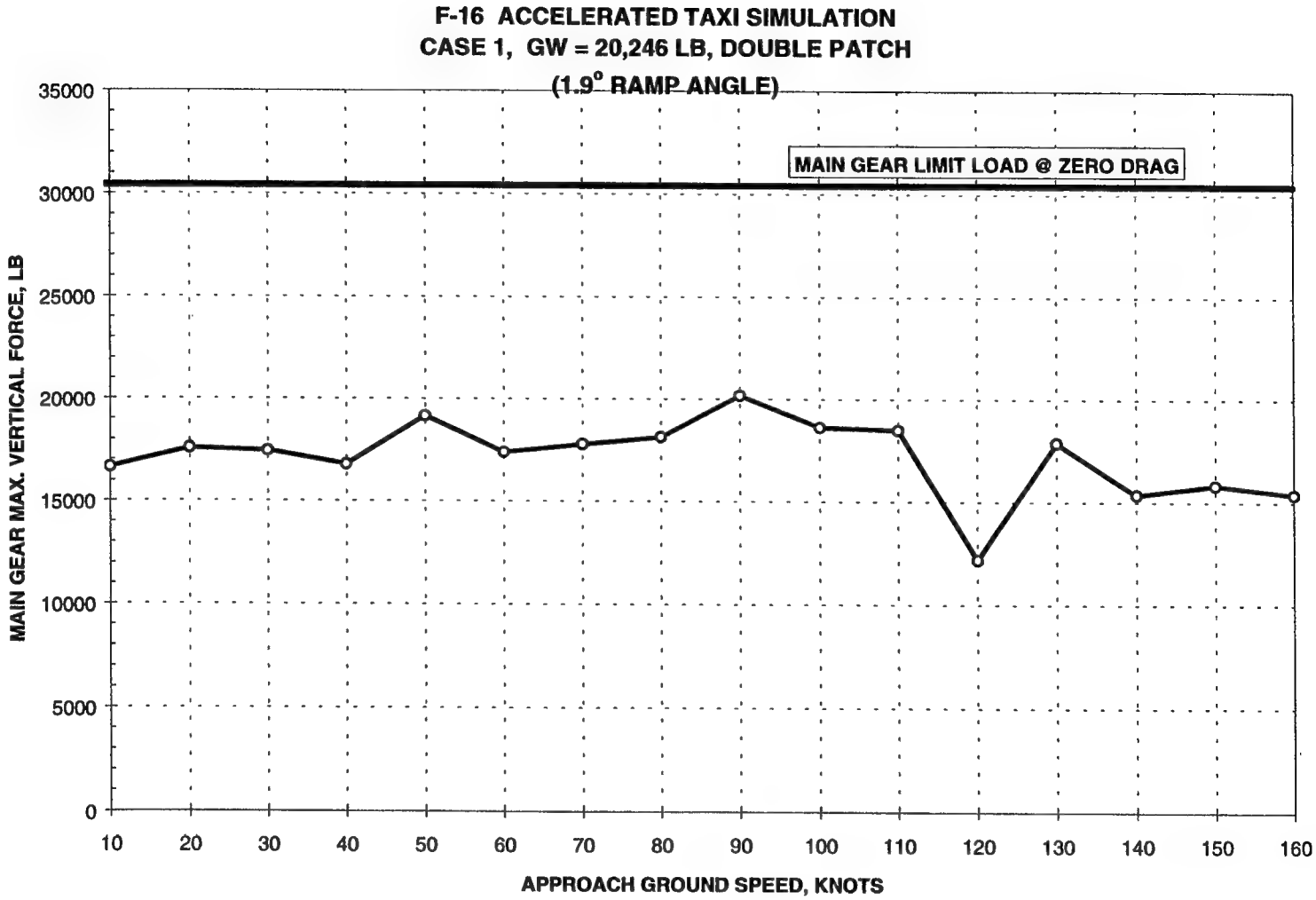

Figure A16. Main gear forces for load case 1, acceleration (takeoff) mode, light gross weight, double mat, and 1.9-deg ramps

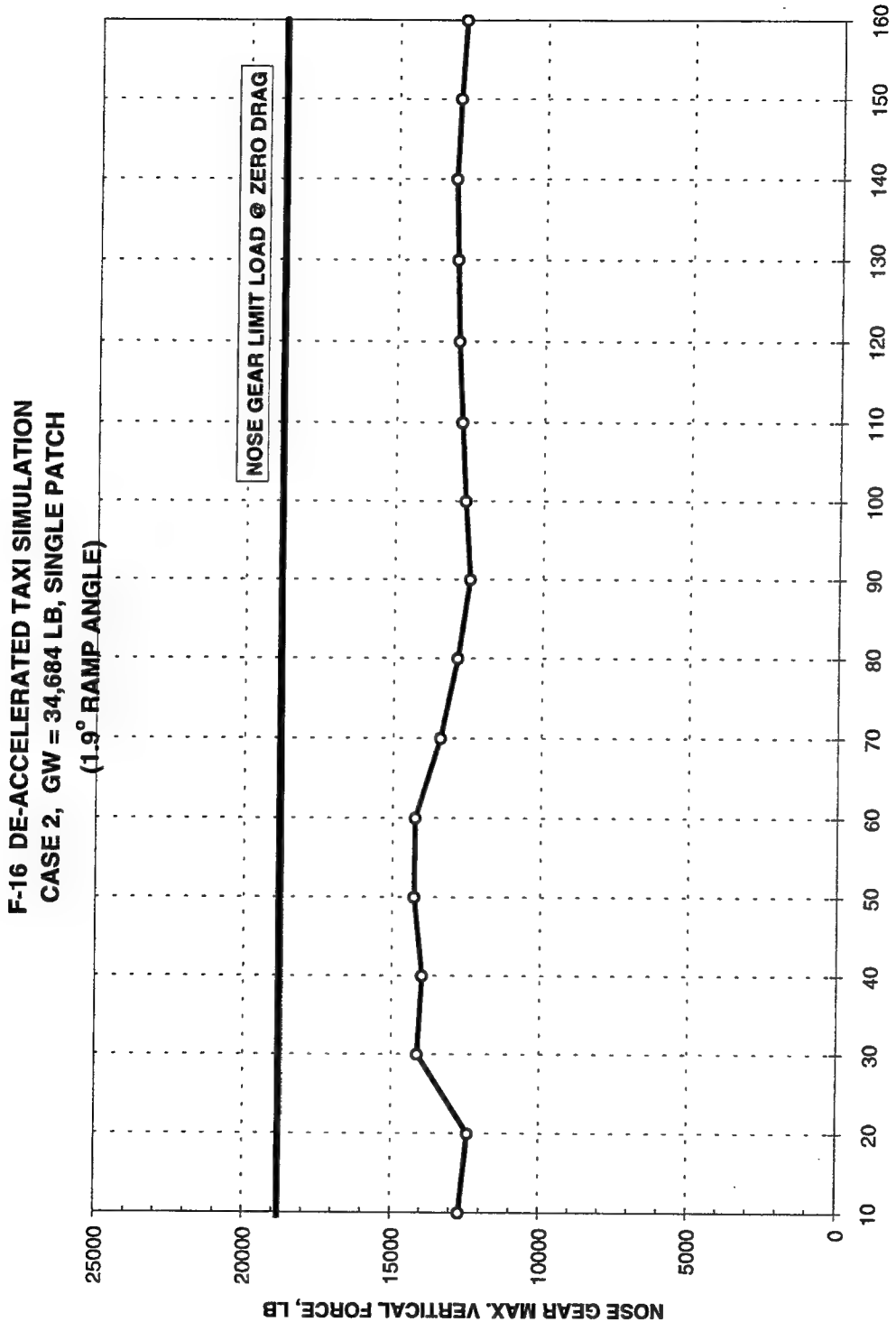

Figure A17. Nose gear forces for load case 2, deceleration (landing) mode, heavy gross weight, single mat, and 1.9-deg ramps

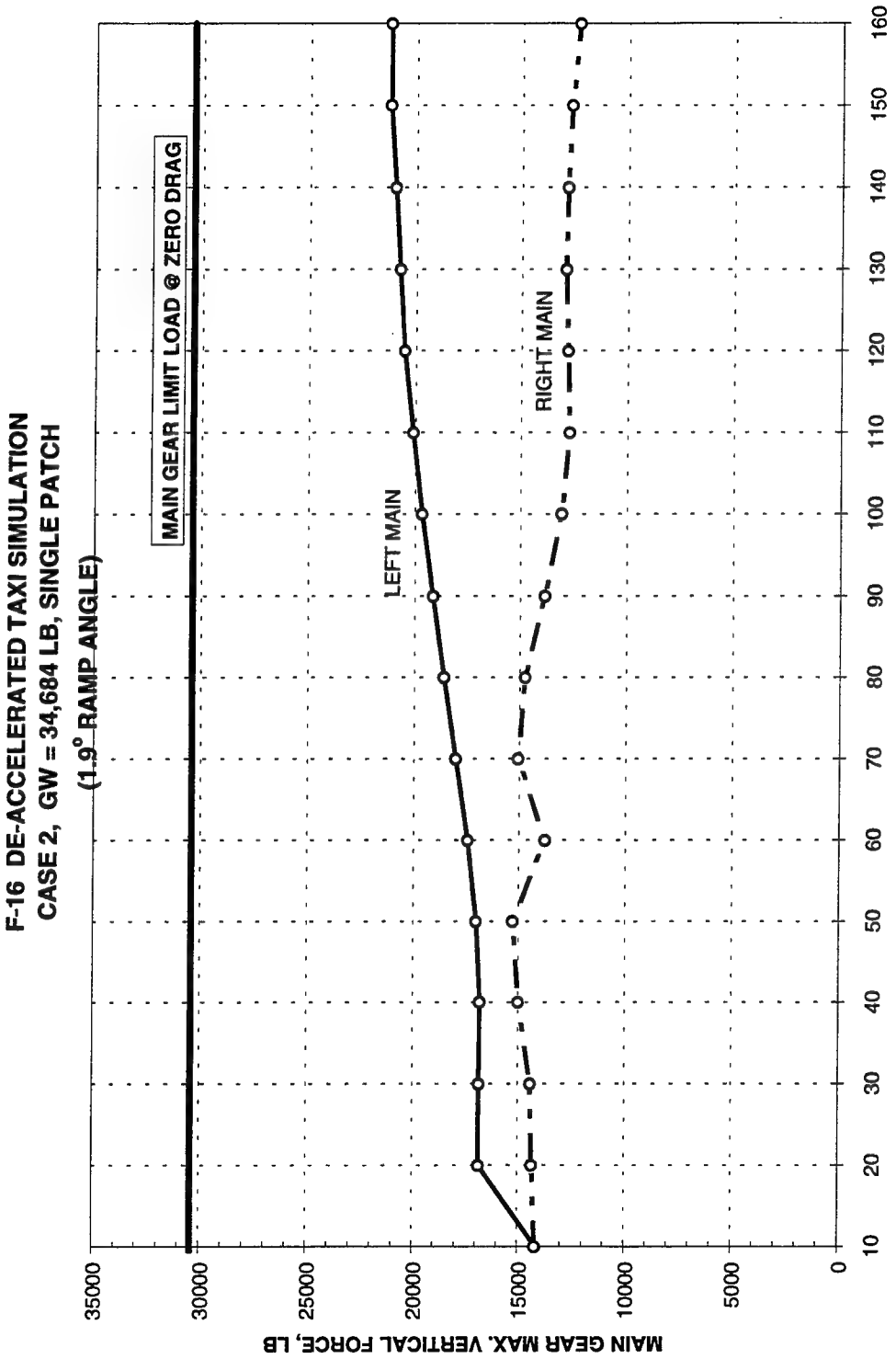

Figure A18. Main gear forces for load case 2, deceleration (landing) mode, heavy gross weight, single mat, and 1.9-deg ramps

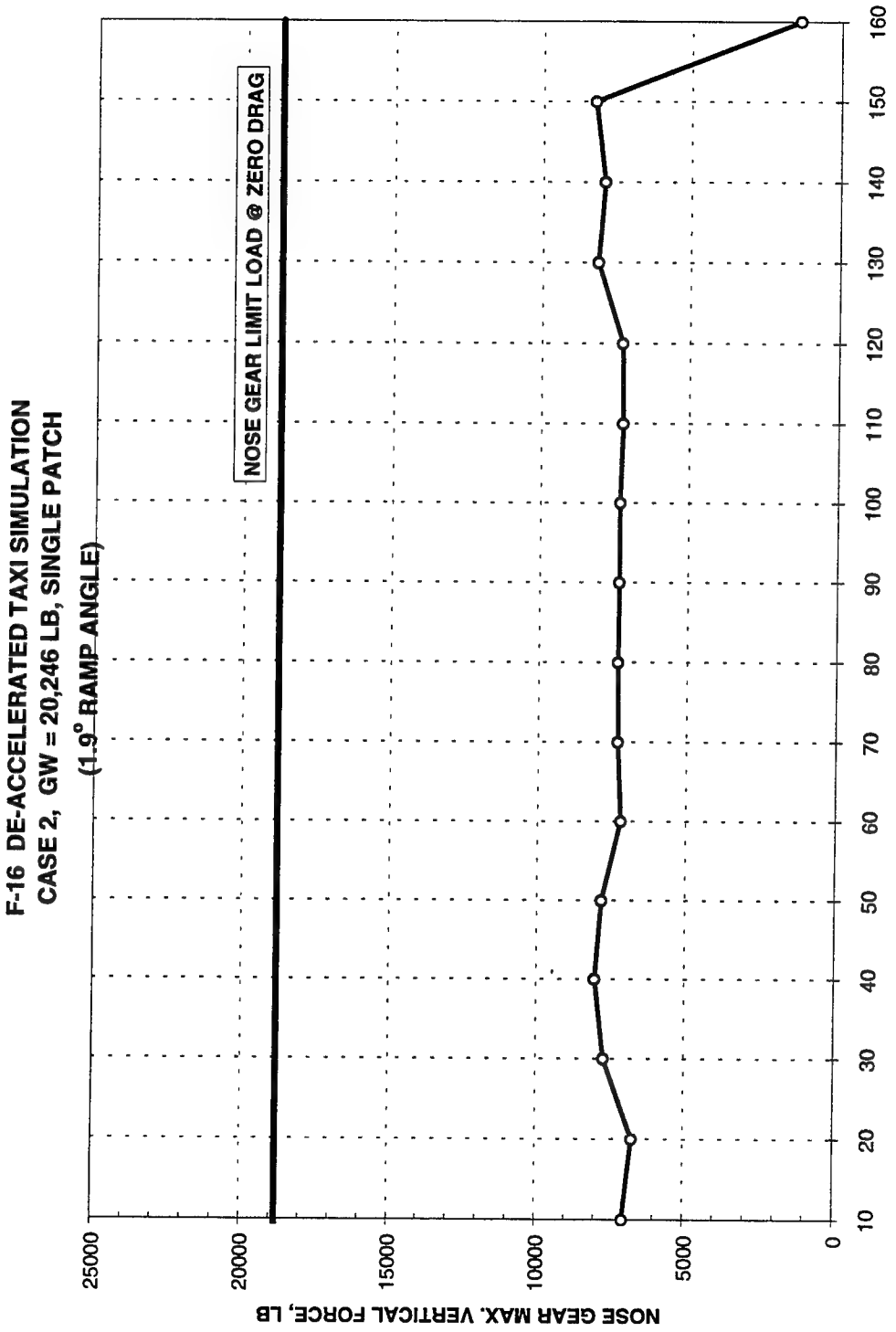

Figure A19. Nose gear forces for load case 2, deceleration (landing) mode, light gross weight, single mat, and 1.9-deg ramps

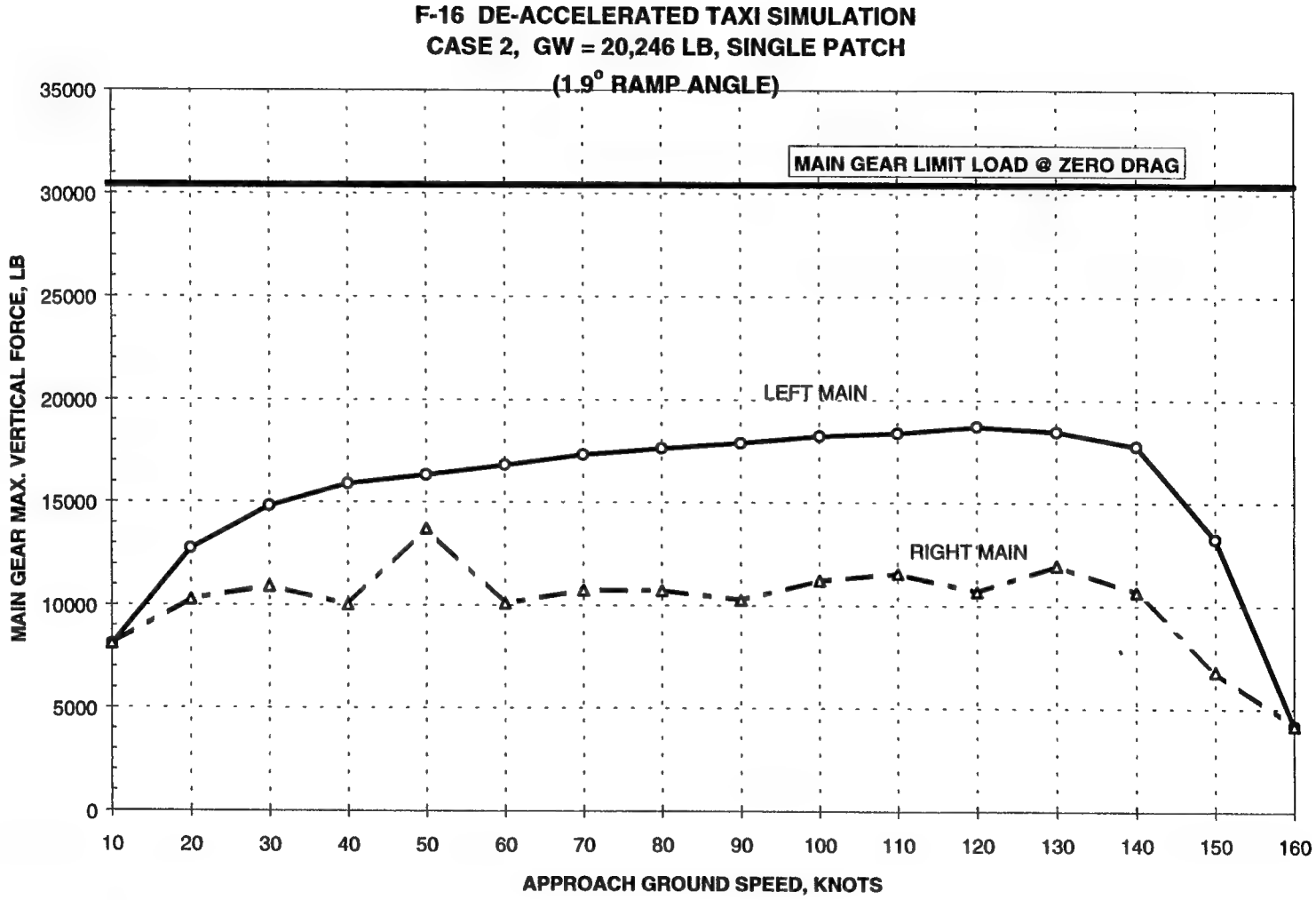

Figure A20. Main gear forces for load case 2, deceleration (landing) mode ,light gross weight, single mat, and 1.9-deg ramps

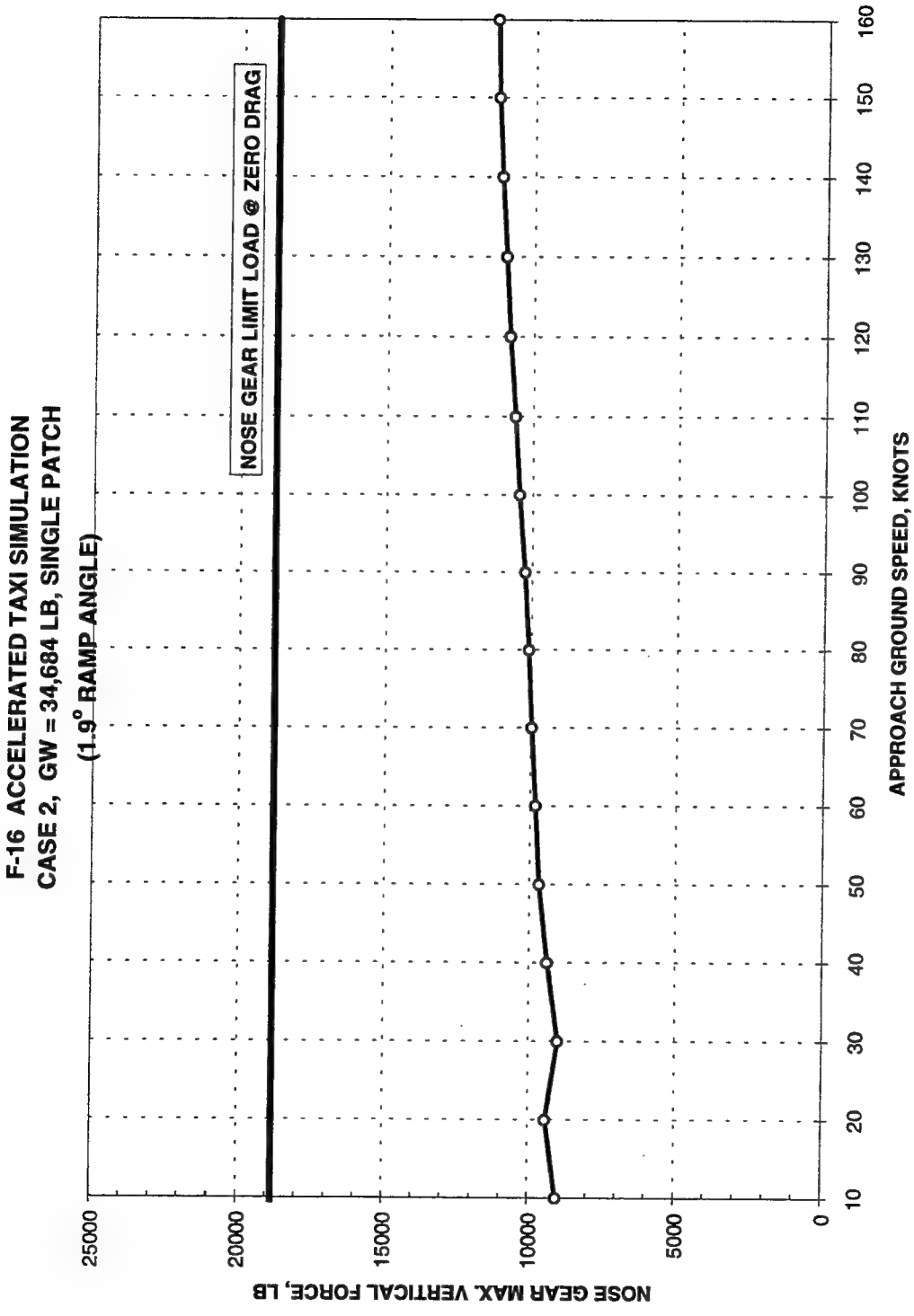

Figure A21. Nose gear forces for load case 2, acceleration (takeoff) mode, heavy gross weight, single mat, and 1.9-deg ramps

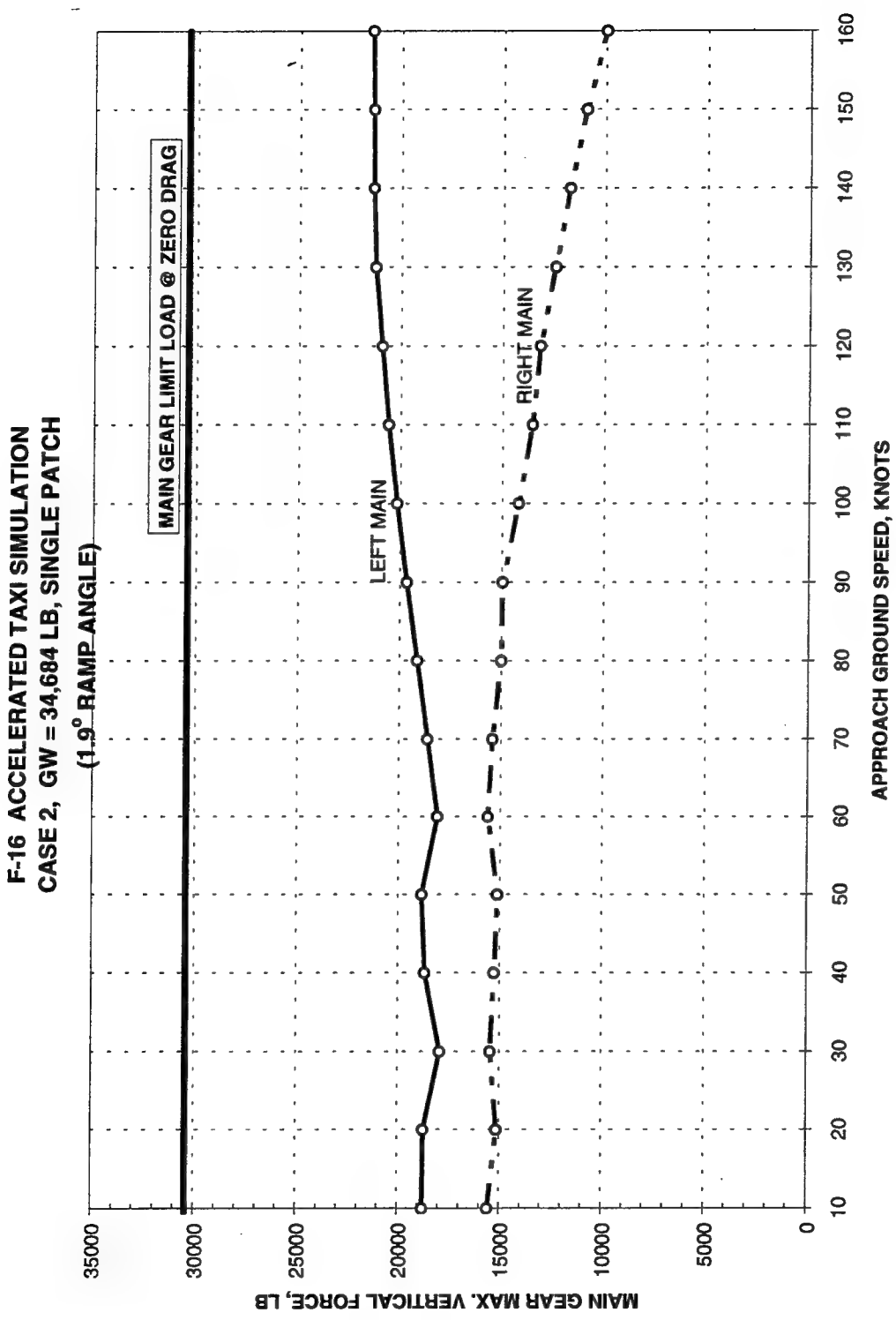

Figure A22. Main gear forces for load case 2, acceleration (takeoff) mode, heavy gross weight, single mat, and 1.9-deg ramps

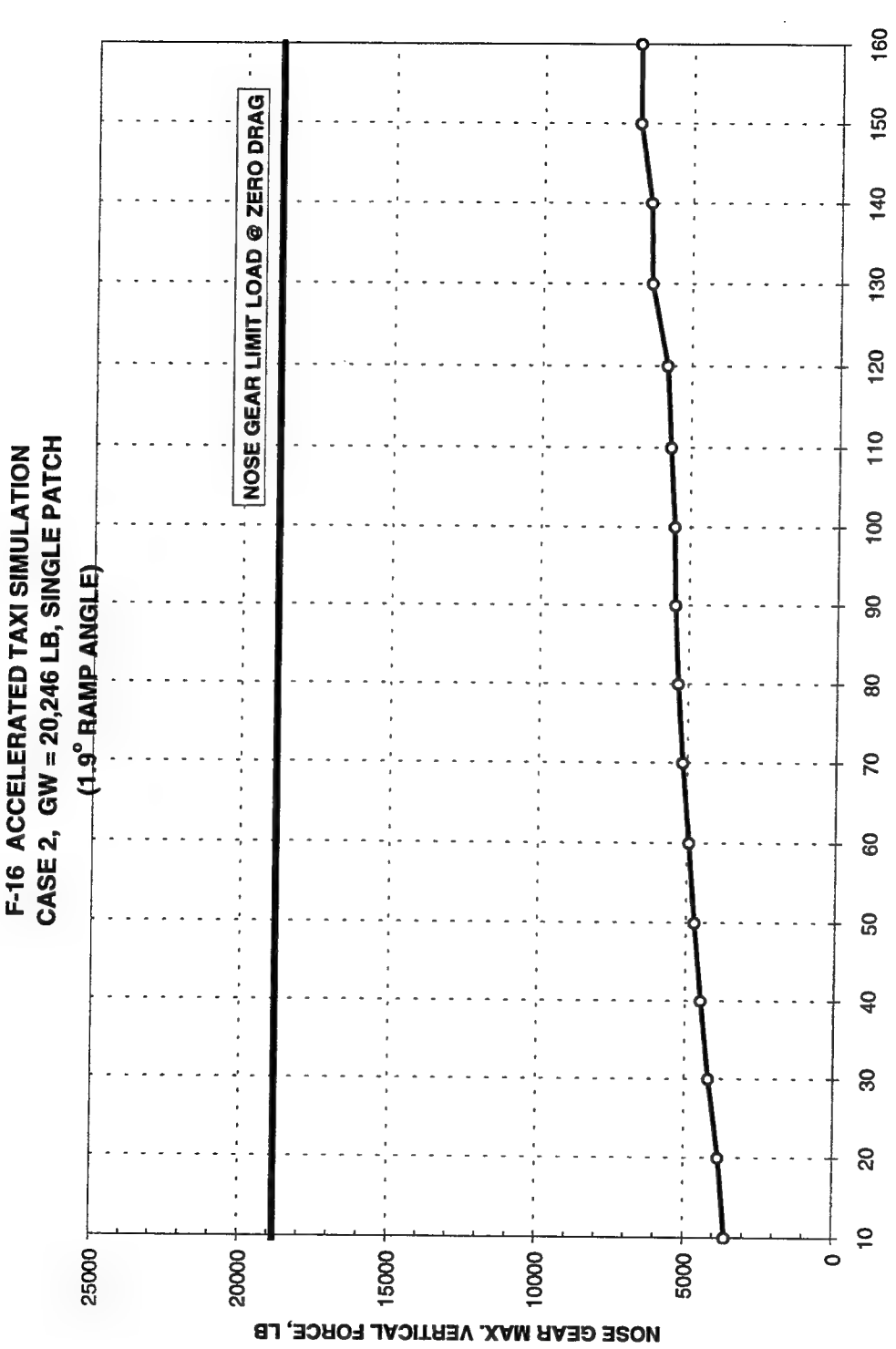

Figure A23. Nose gear forces for load case 2, acceleration (takeoff) mode, light gross weight, single mat, and 1.9-deg ramps

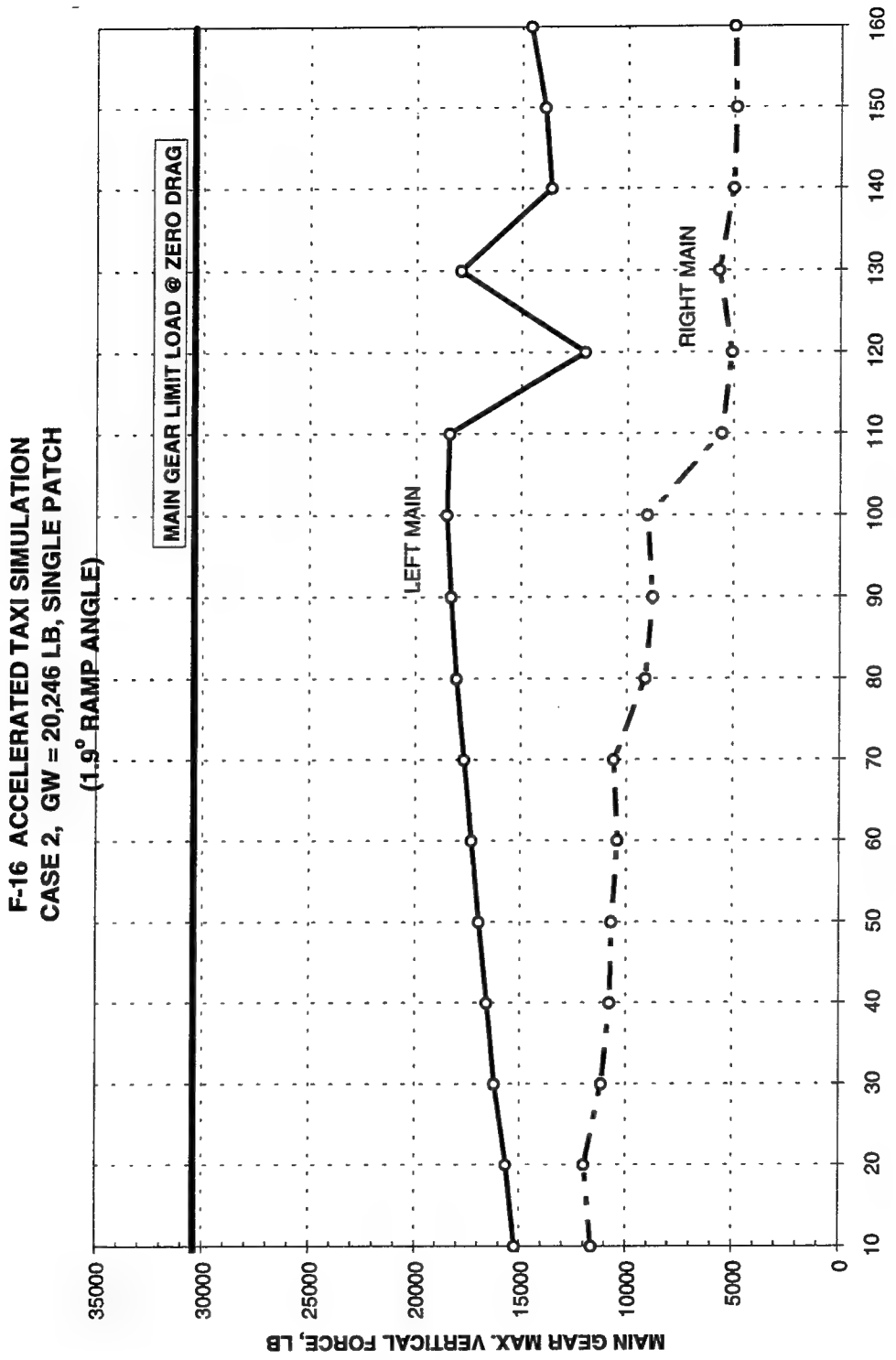

Figure A24. Main gear forces for load case 2, acceleration (takeoff) mode ,light gross weight, single mat, and 1.9-deg ramps

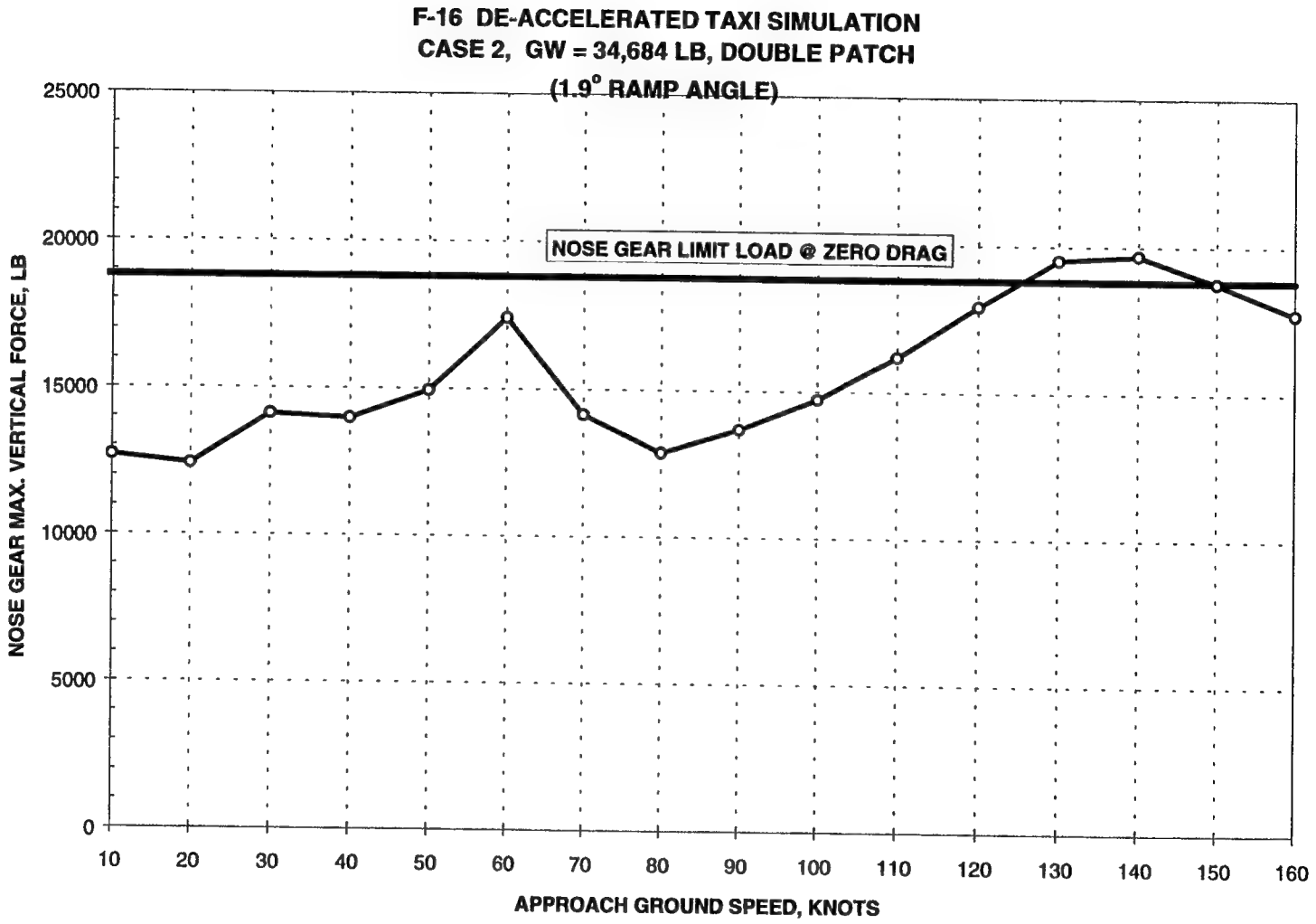

Figure A25. Nose gear forces for load case 2, deceleration (landing) mode, heavy gross weight, double mat, and 1.9-deg ramps

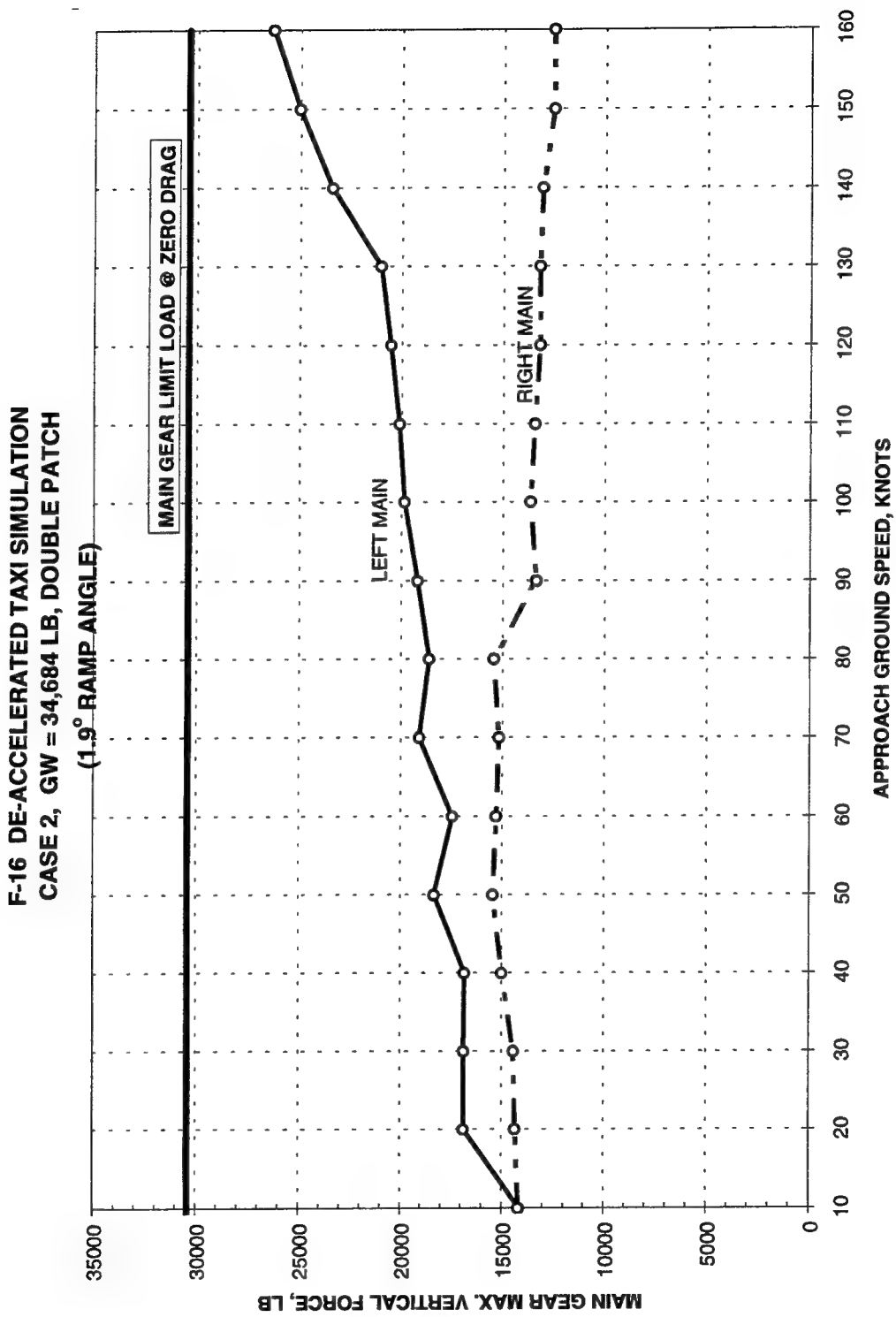

Figure A26. Main gear forces for load case 2, deceleration (landing) mode ,heavy gross weight, double mat, and 1.9-deg ramps

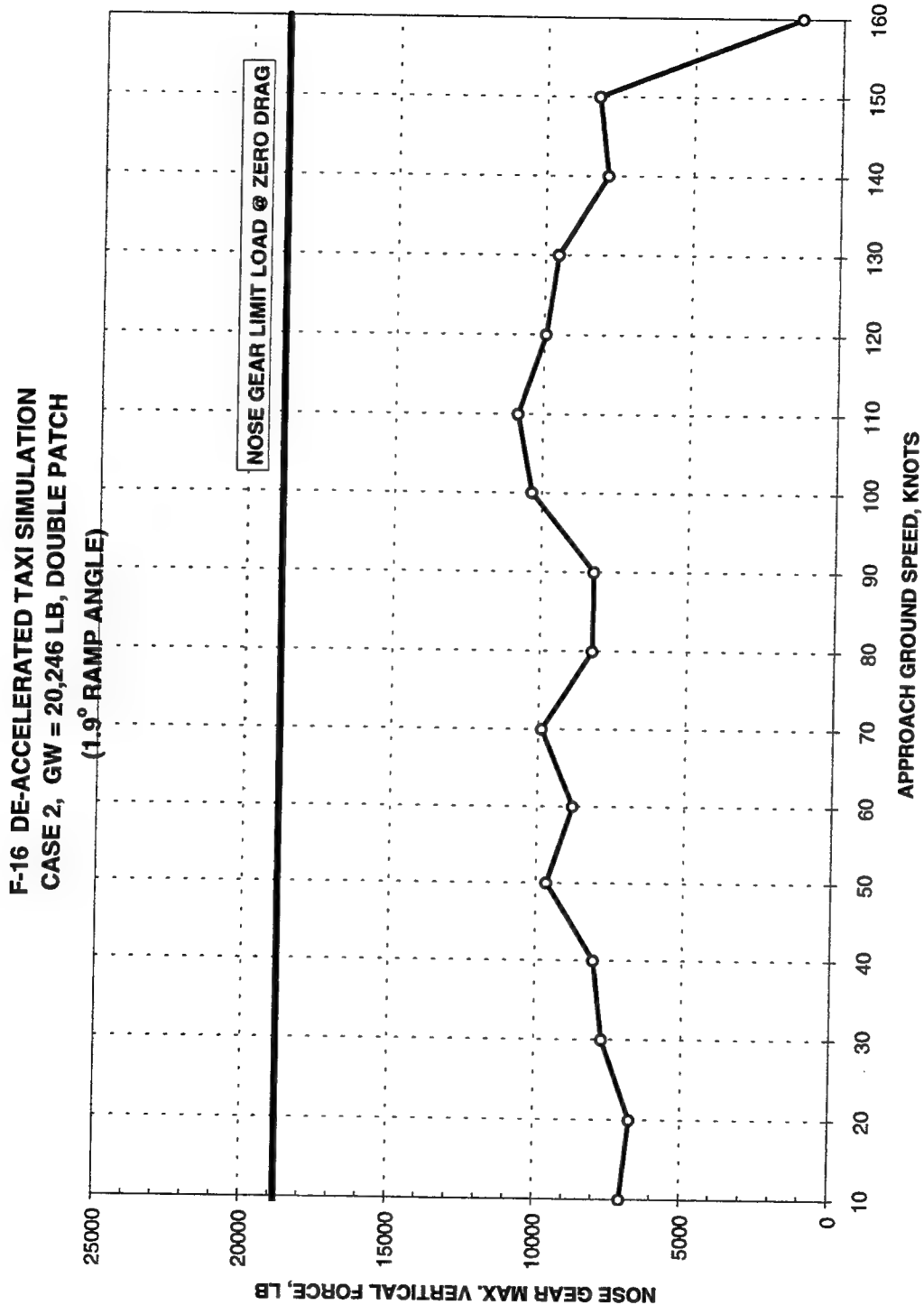

Figure A27. Nose gear forces for load case 2, deceleration (landing) mode, light gross weight, double mat, and 1.9-deg ramps

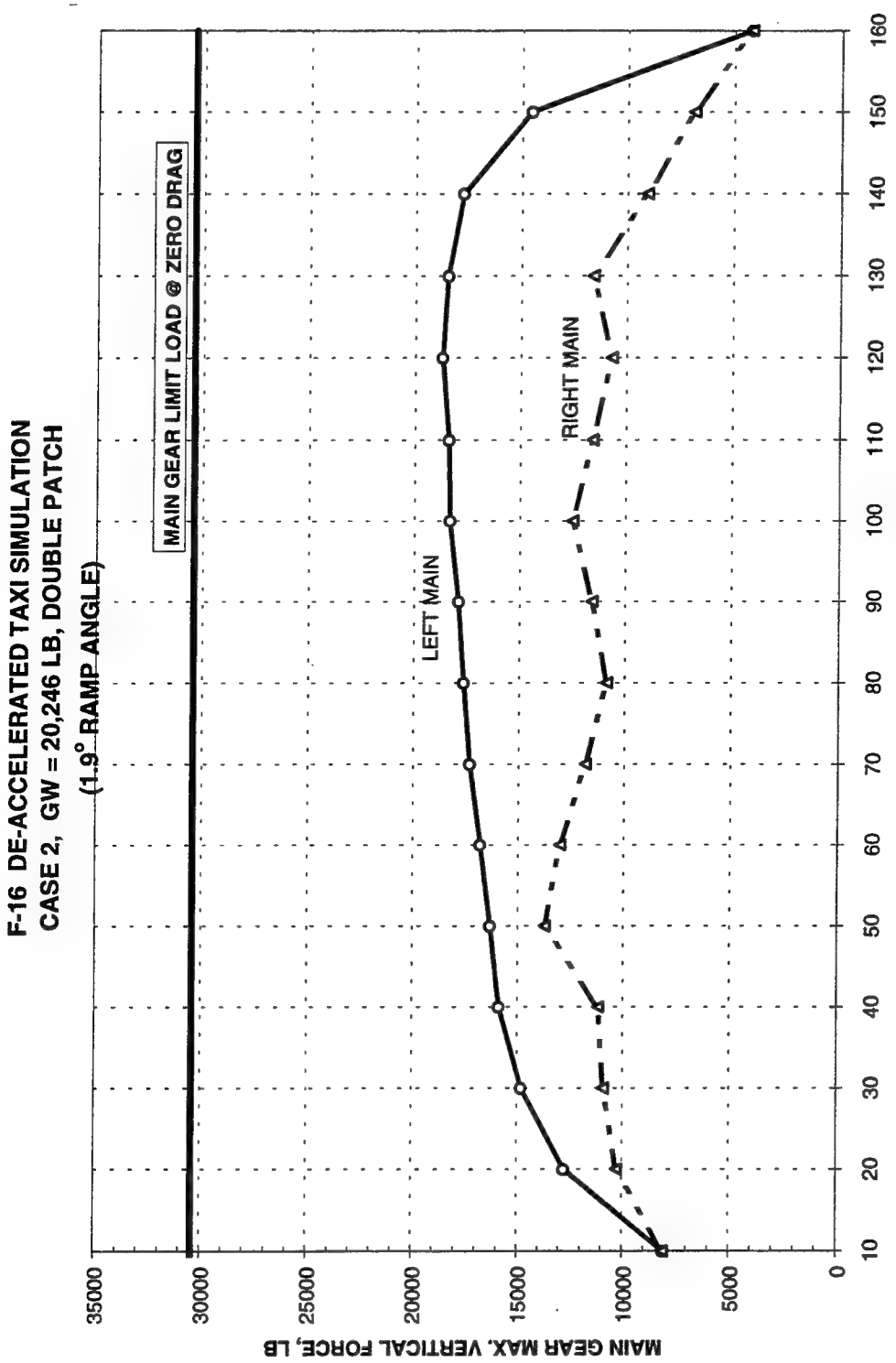

Figure A28. Main gear forces for load case 2, deceleration (landing) mode ,light gross weight, double mat, and 1.9-deg ramps

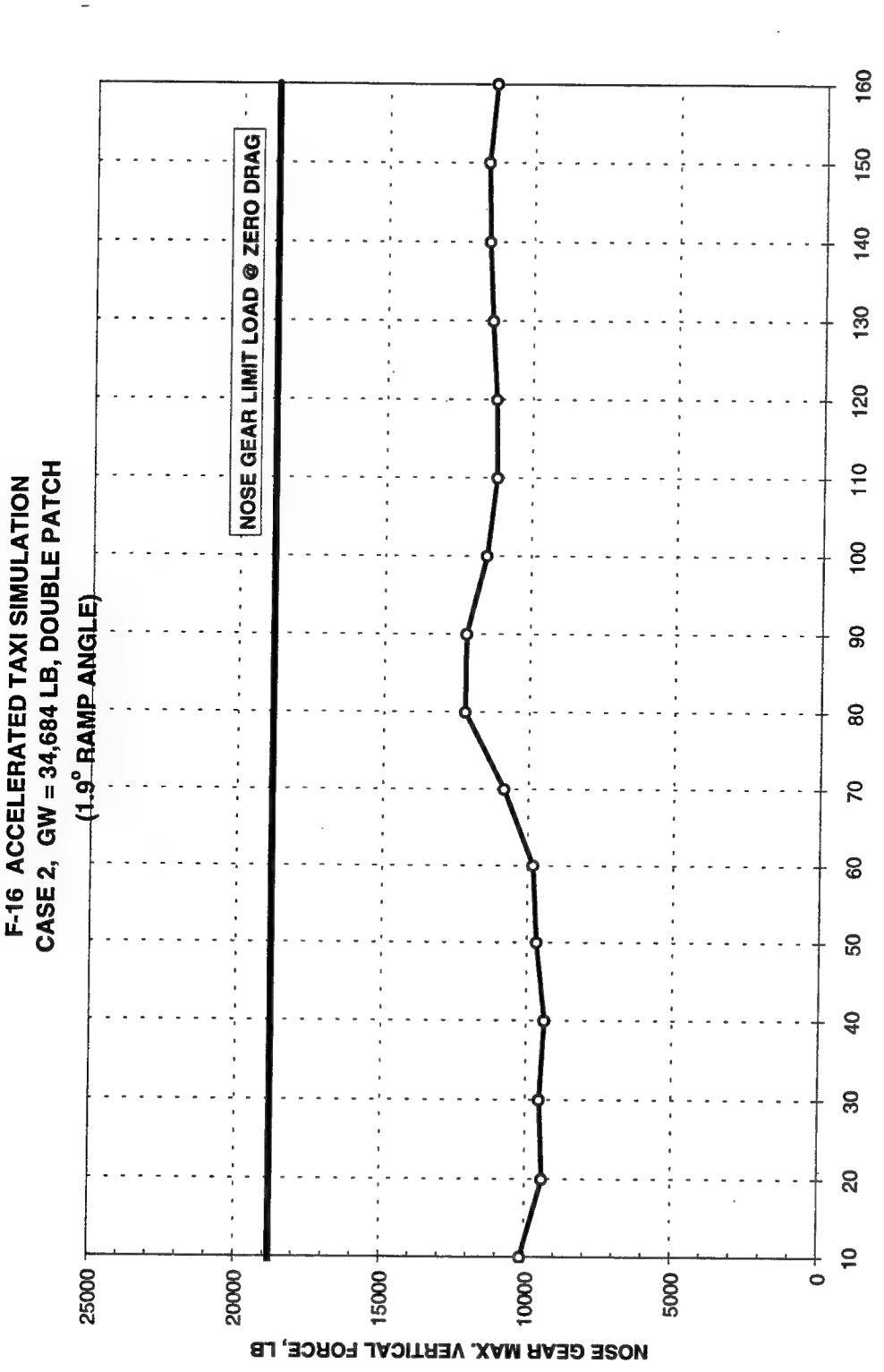

Figure A29. Nose gear forces for load case 2, acceleration (takeoff) mode, heavy gross weight, double mat, and 1.9-deg ramps

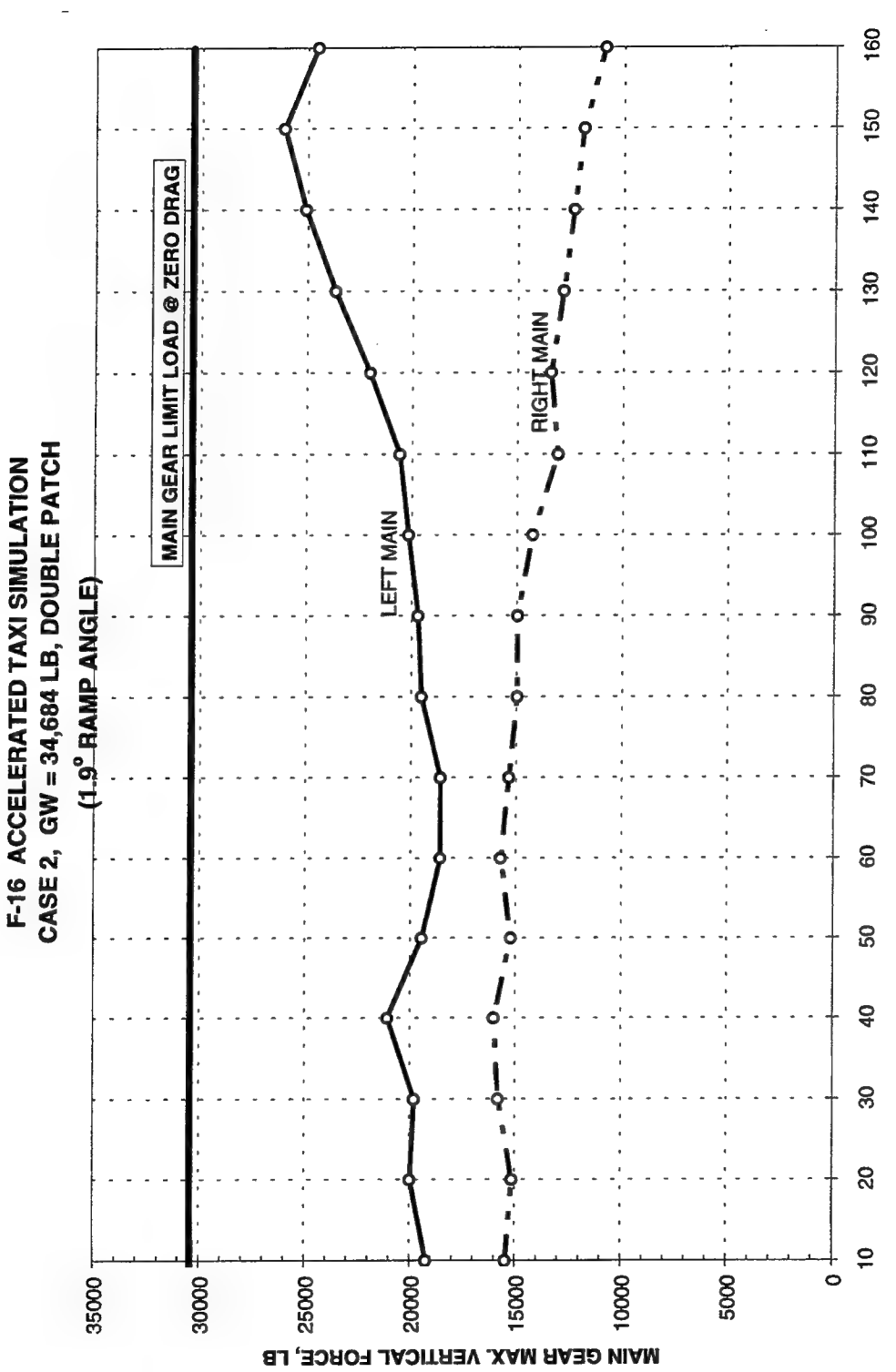

Figure A30. Main gear forces for load case 2, acceleration (takeoff) mode , heavy gross weight, double mat, and 1.9-deg ramps

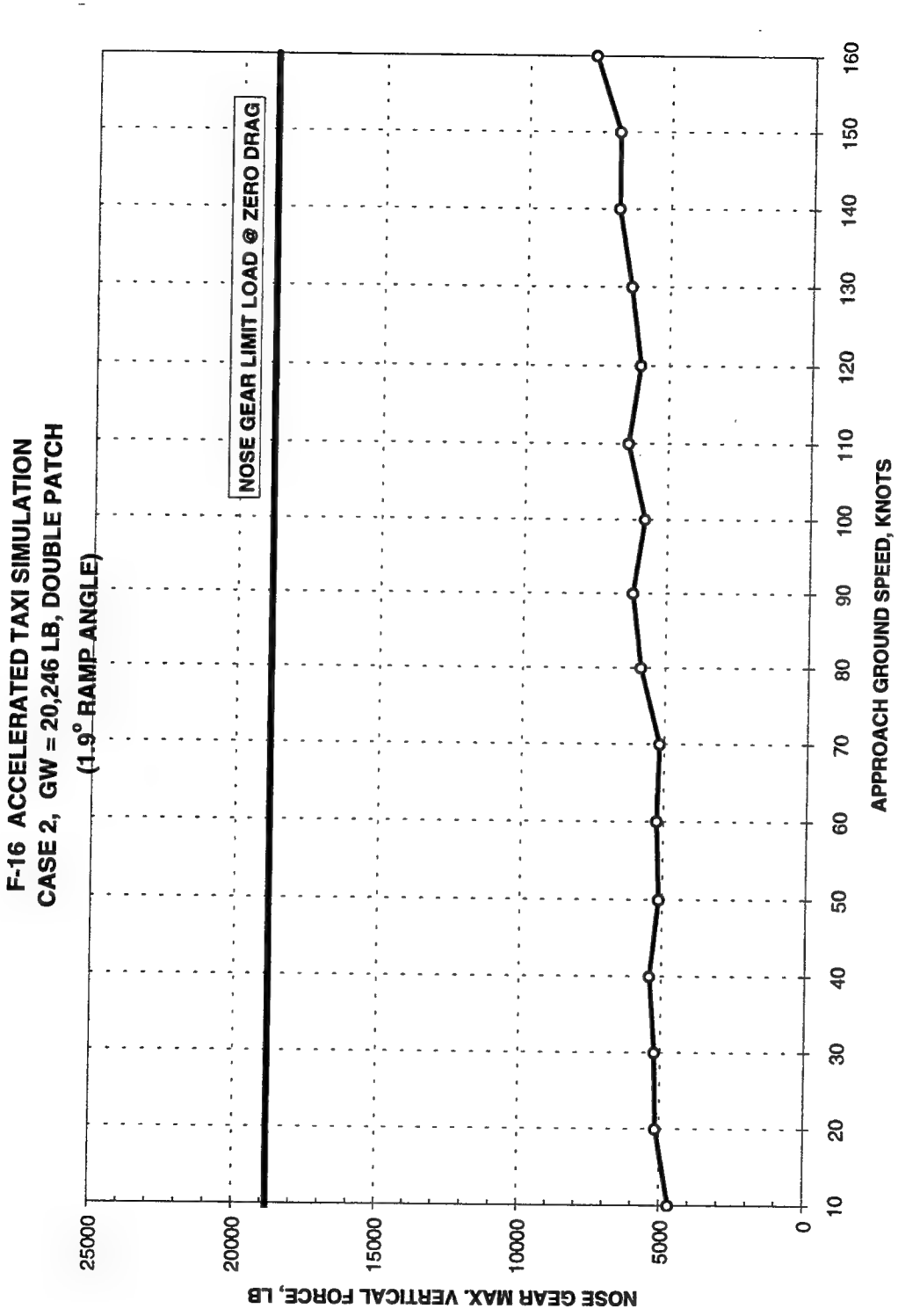

Figure A31. Nose gear forces for load case 2, acceleration (takeoff) mode, light gross weight, double mat, and 1.9-deg ramps

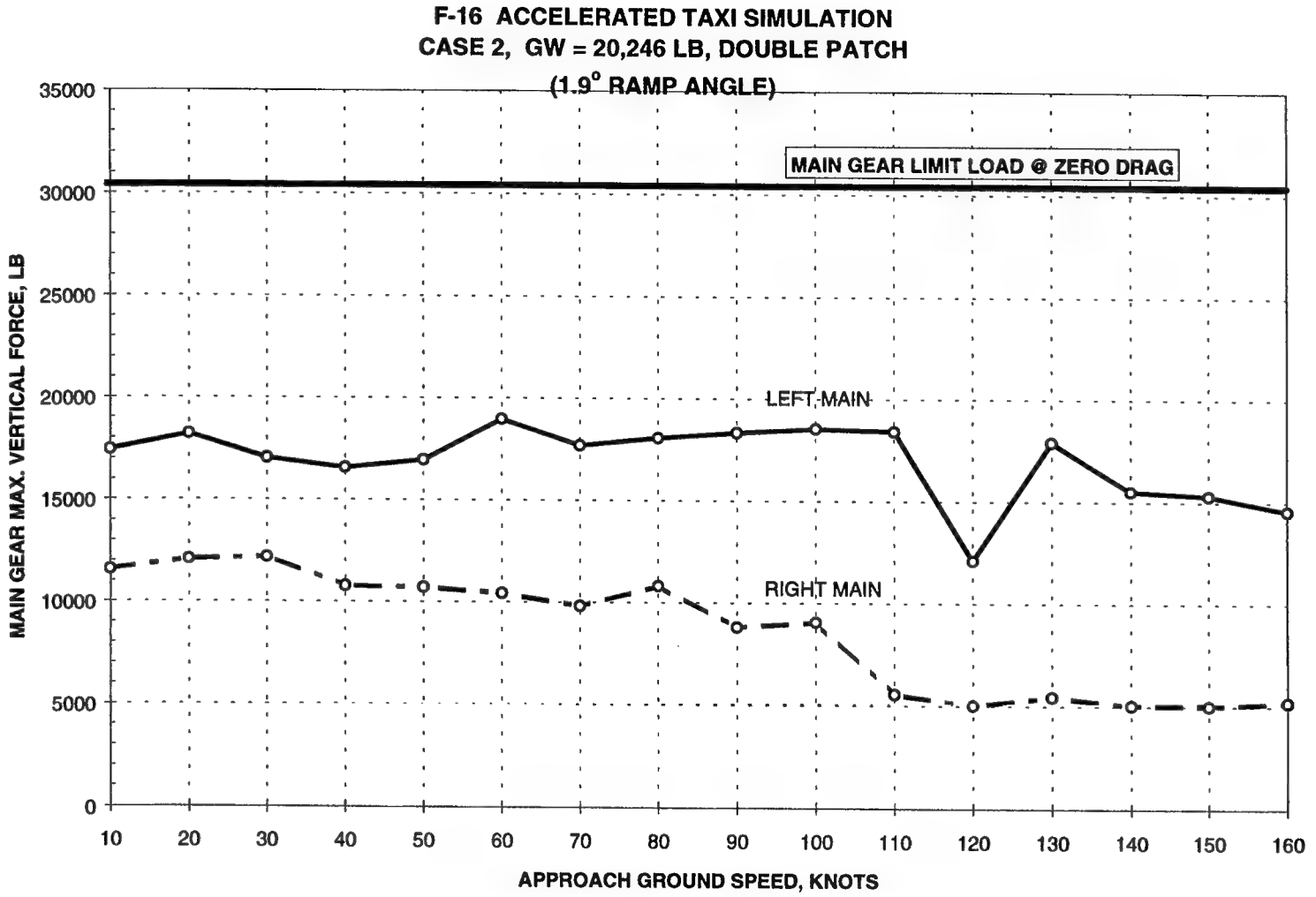

Figure A32. Main gear forces for load case 2, acceleration (takeoff) mode ,light gross weight, double mat, and 1.9-deg ramps

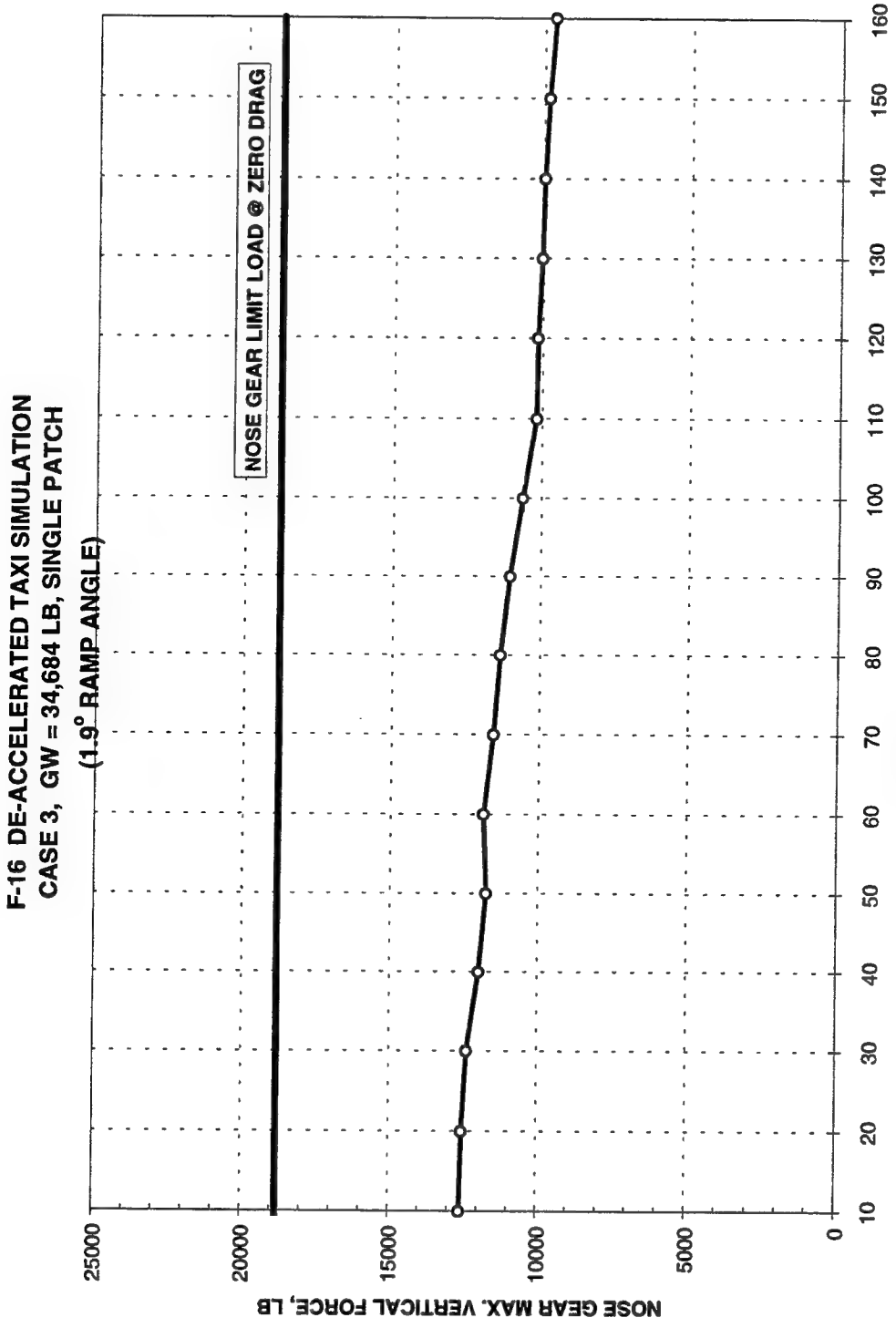

Figure A33. Nose gear forces for load case 3, deceleration (landing) mode, heavy gross weight, single mat, and 1.9-deg ramps

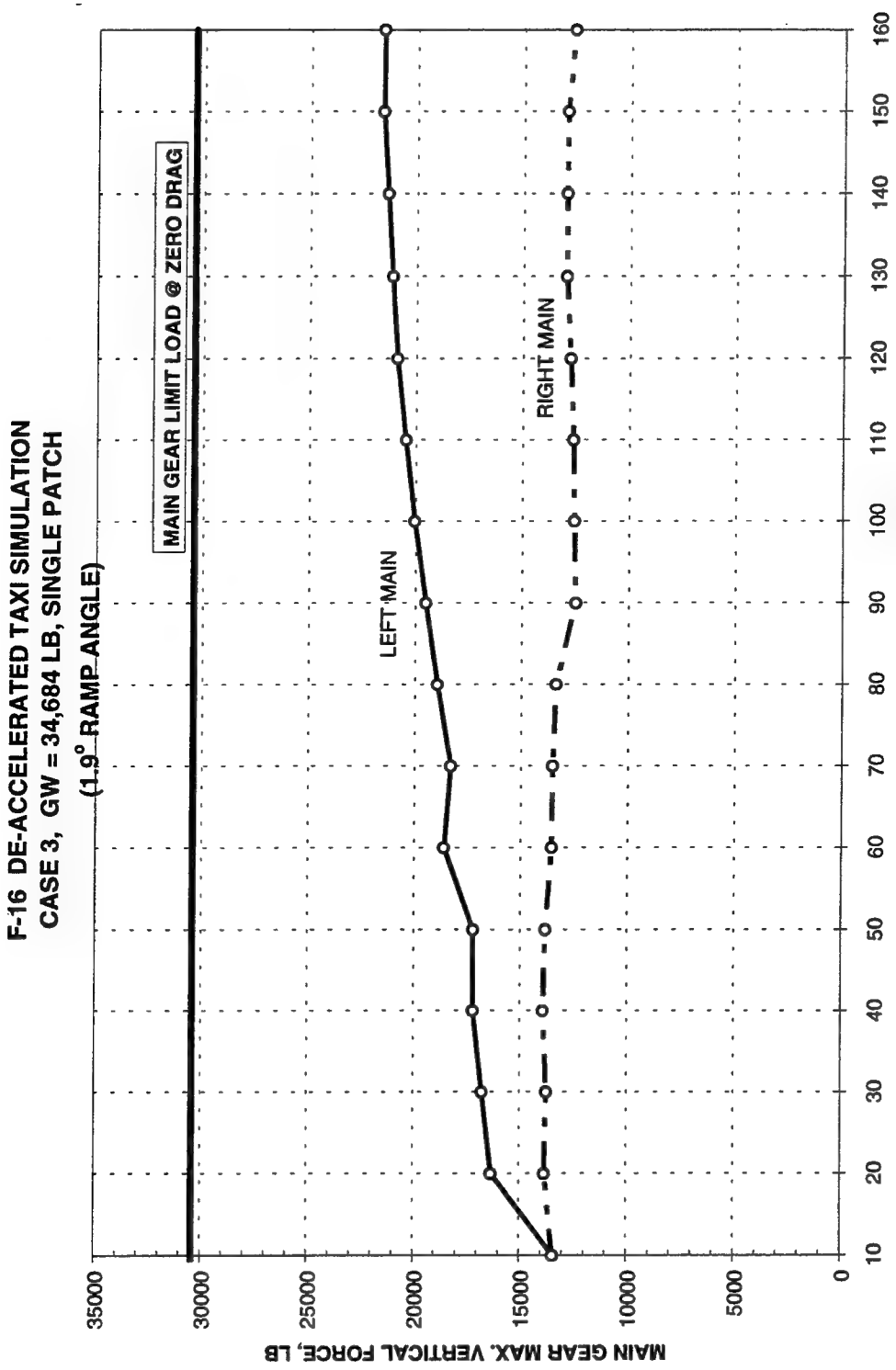

Figure A34. Main gear forces for load case 3, deceleration (landing) mode , heavy gross weight, single mat, and 1.9-deg ramps

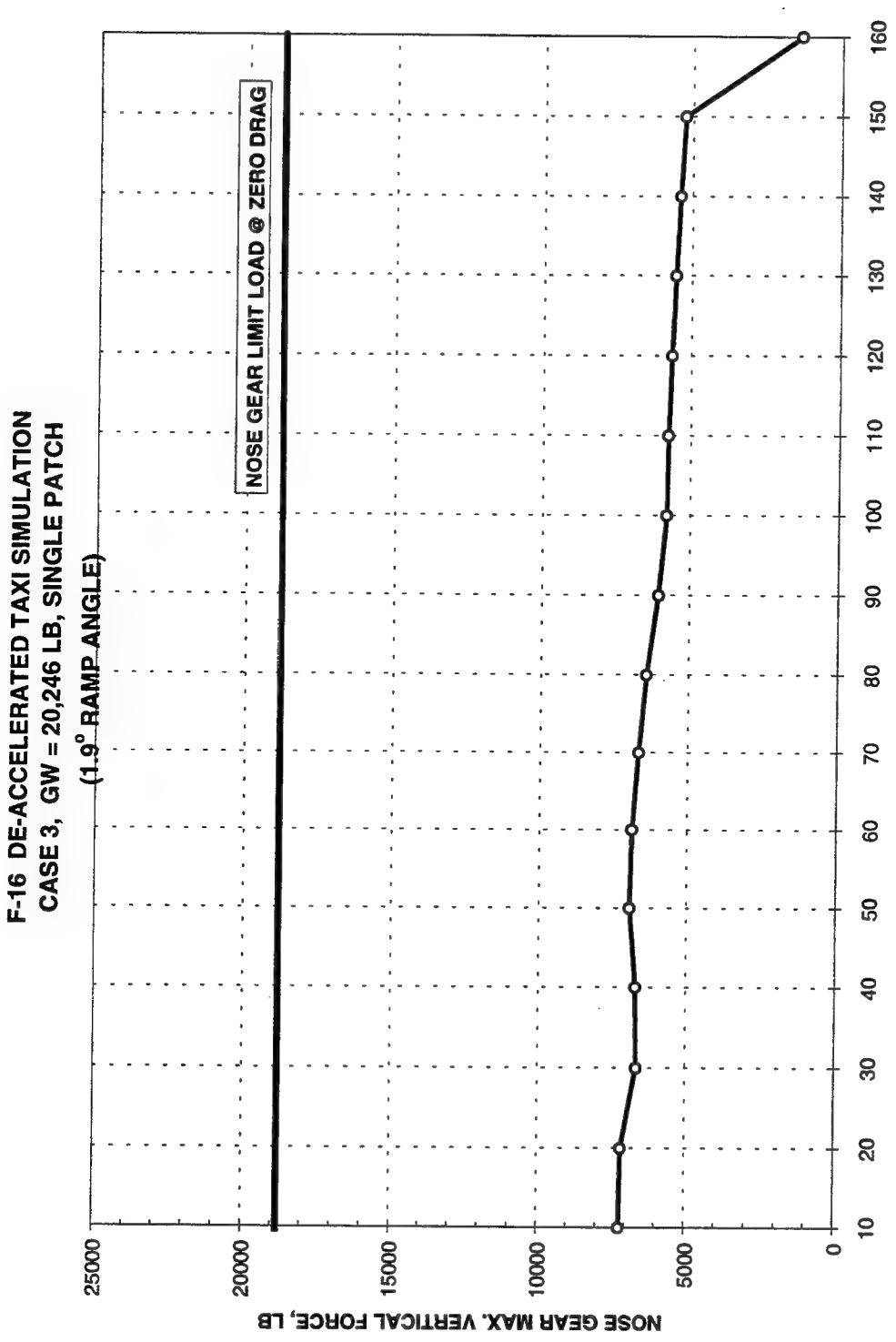

Figure A35. Nose gear forces for load case 3, deceleration (landing) mode, light gross weight, single mat, and 1.9-deg ramps

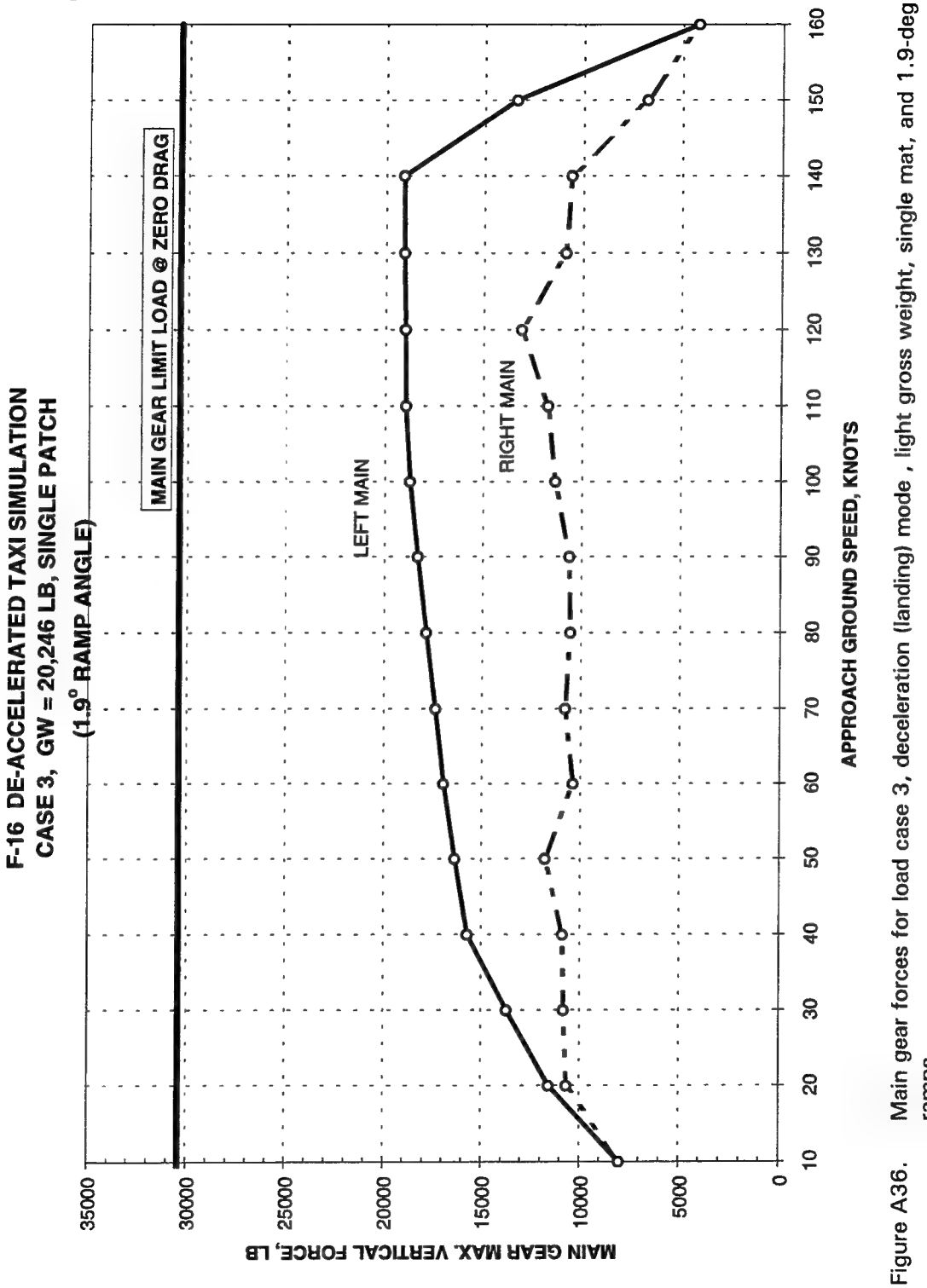

Figure A36. Main gear forces for load case 3, deceleration (landing) mode , light gross weight, single mat, and 1.9-deg ramps

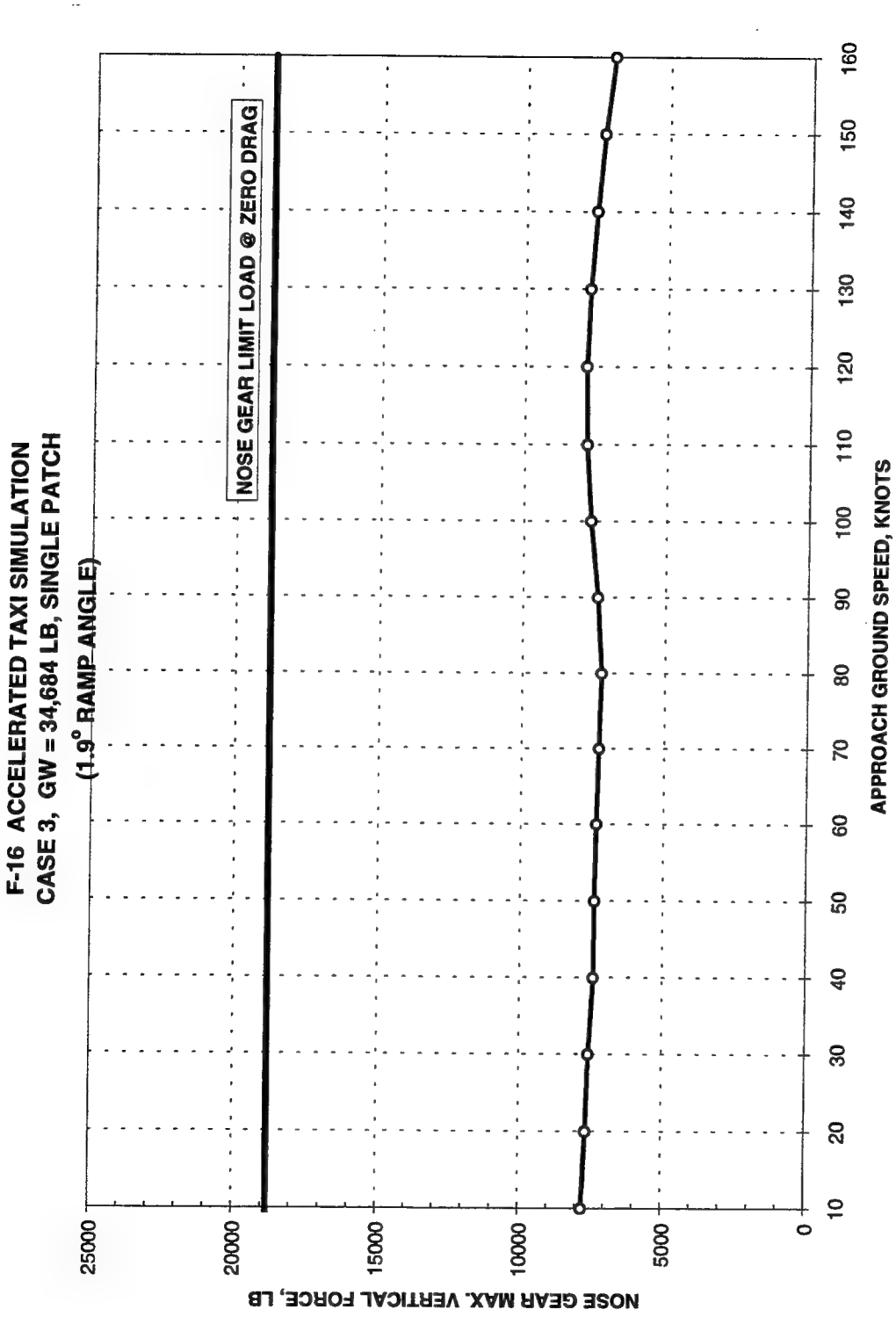

Figure A37. Nose gear forces for load case 3, acceleration (takeoff) mode , heavy gross weight, single mat, and 1.9-deg ramps

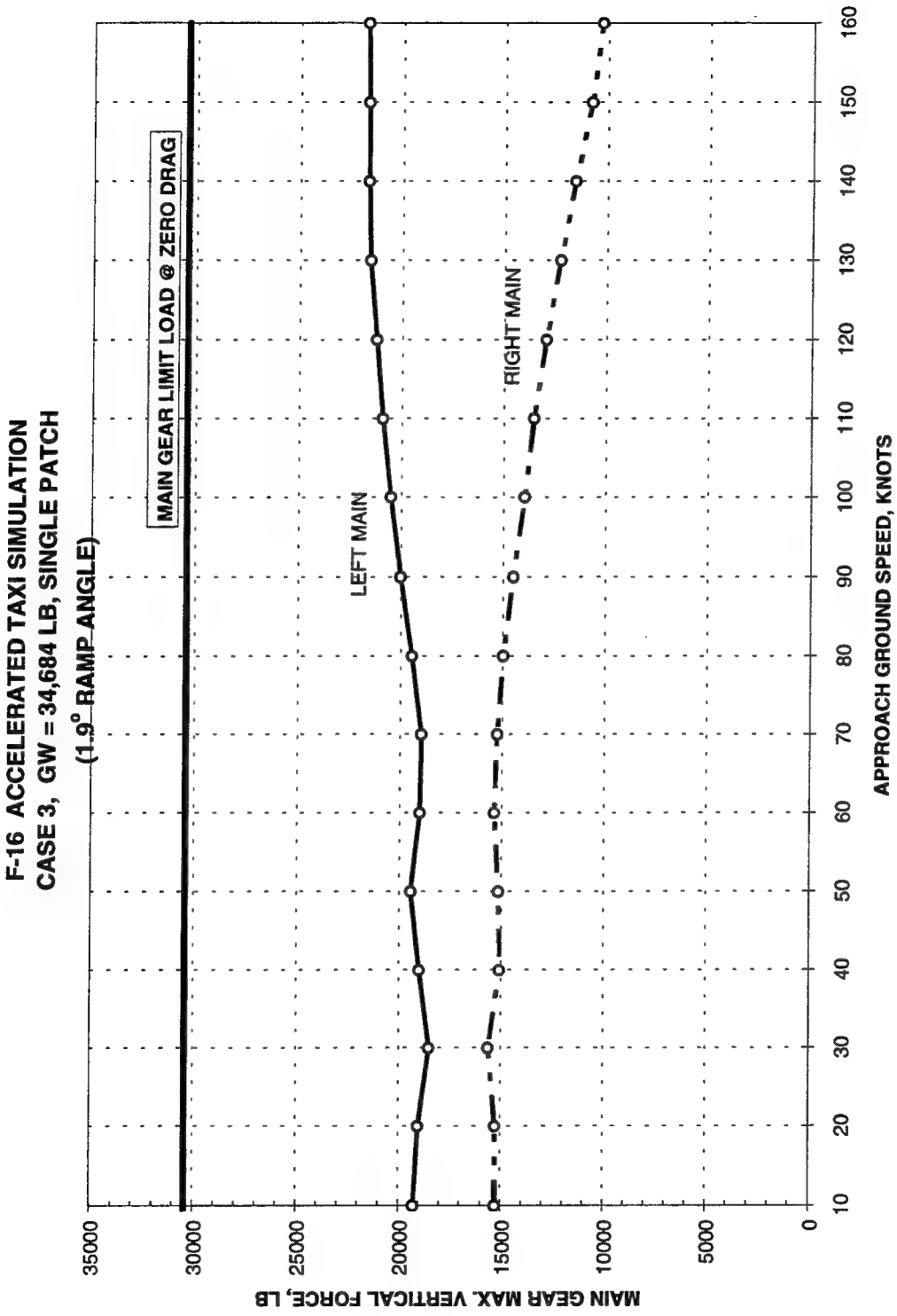

Figure A38. Main gear forces for load case 3, acceleration (takeoff) mode , heavy gross weight, single mat, and 1.9-deg ramps

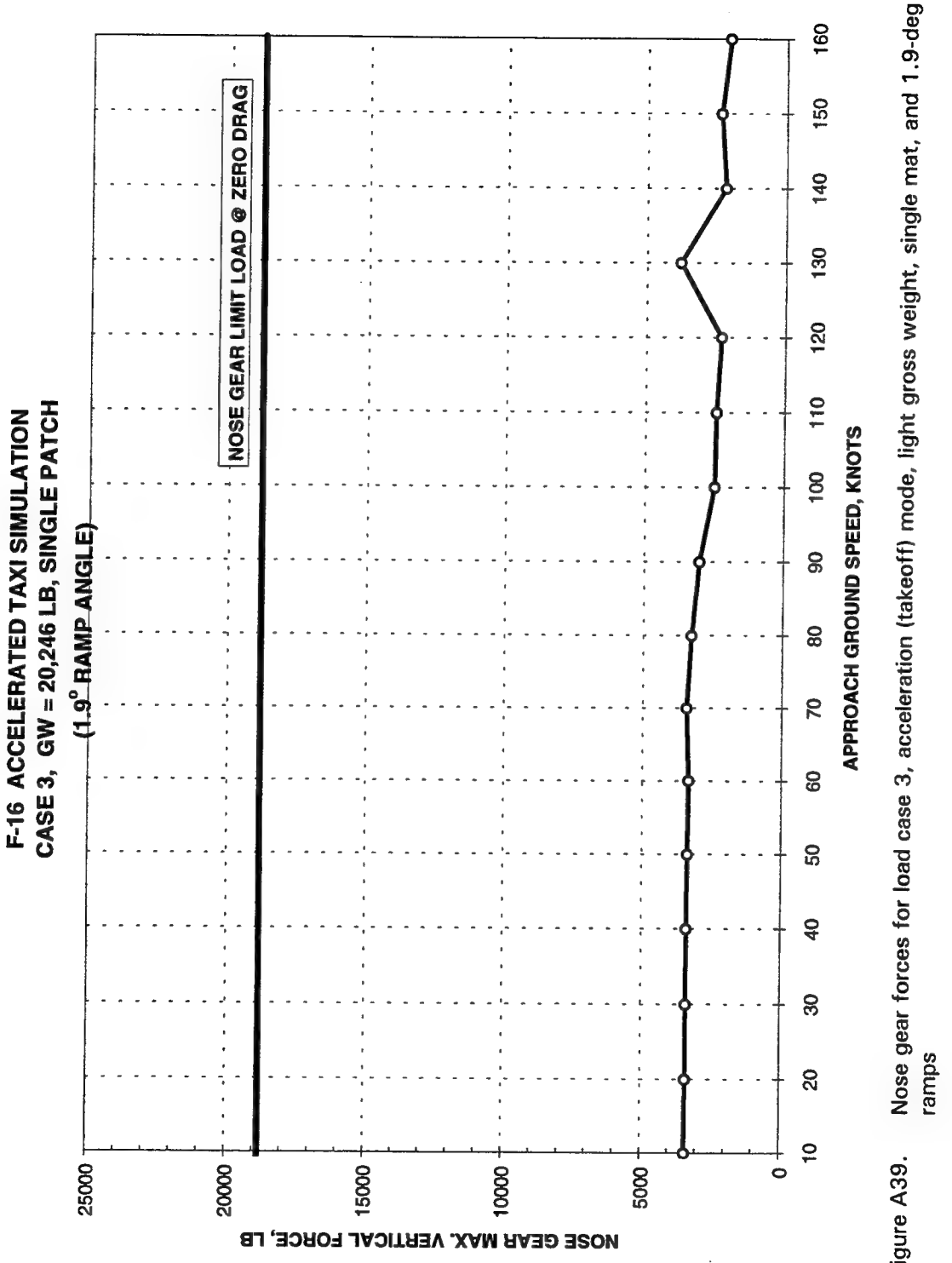

Figure A39. Nose gear forces for load case 3, acceleration (takeoff) mode, light gross weight, single mat, and 1.9-deg ramps

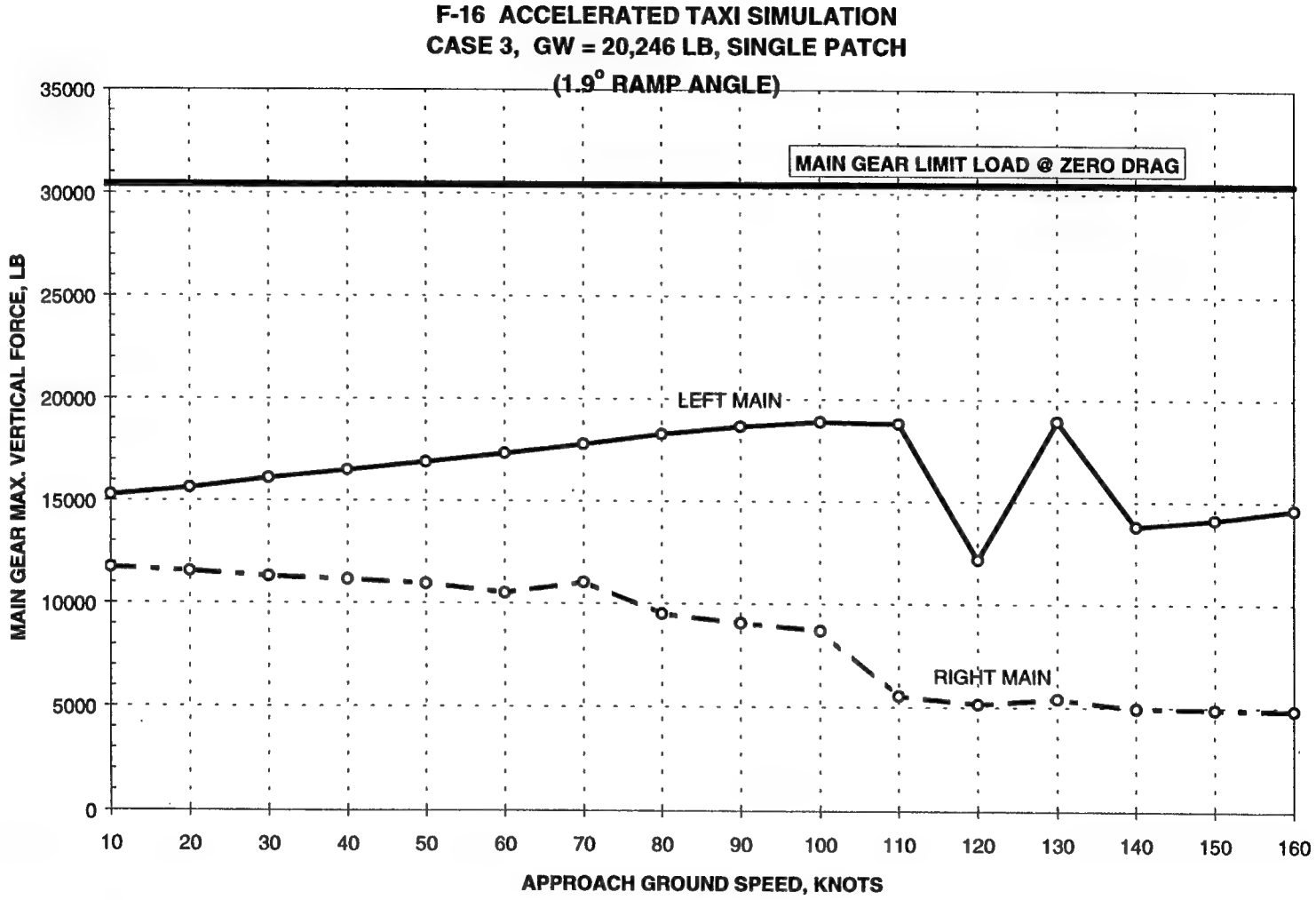

Figure A40. Main gear forces for load case 3, acceleration (takeoff) mode , light gross weight, single mat, and 1.9-deg ramps

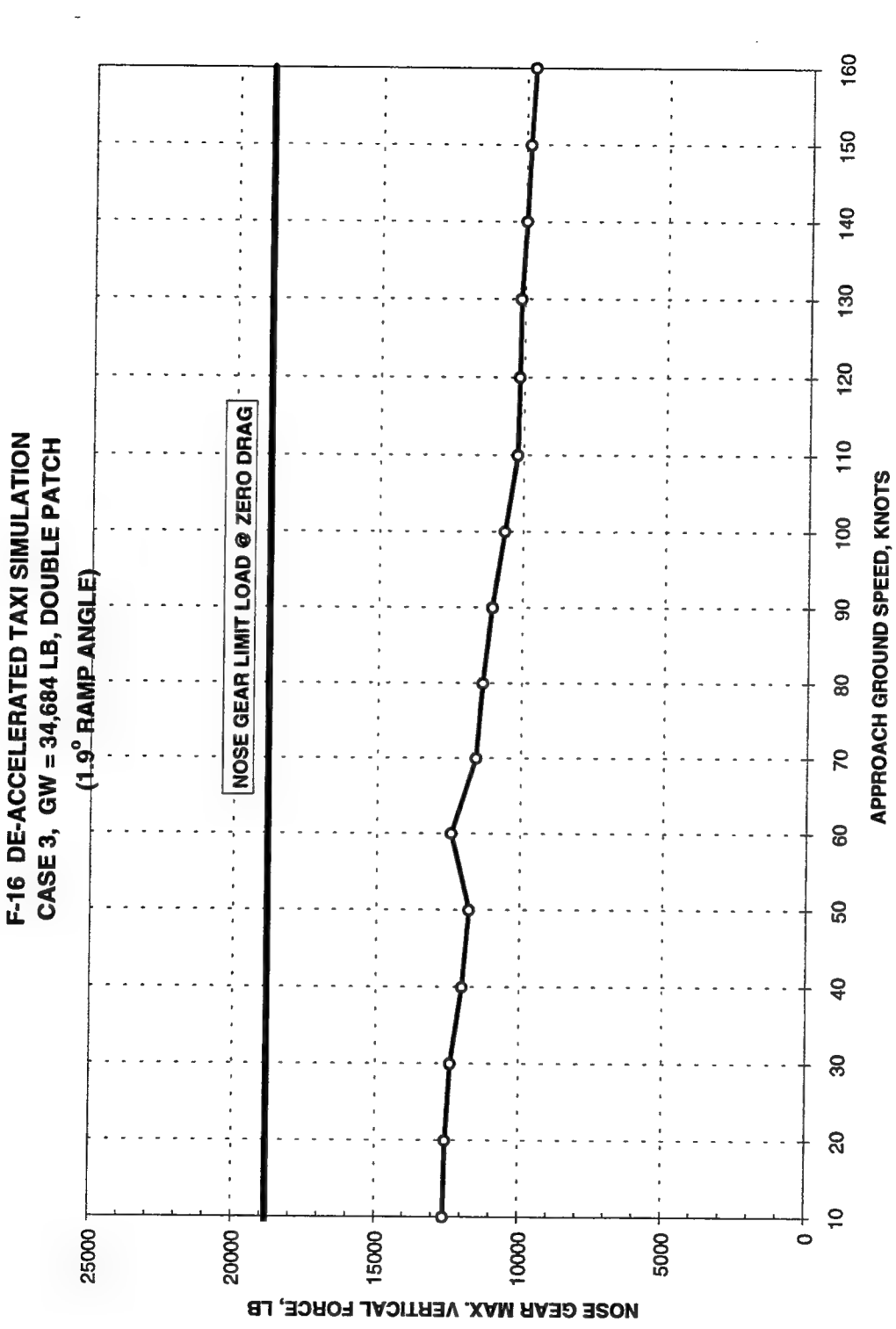

Figure A41. Nose gear forces for load case 3, deceleration (landing) mode, heavy gross weight, double mat, and 1.9-deg ramps

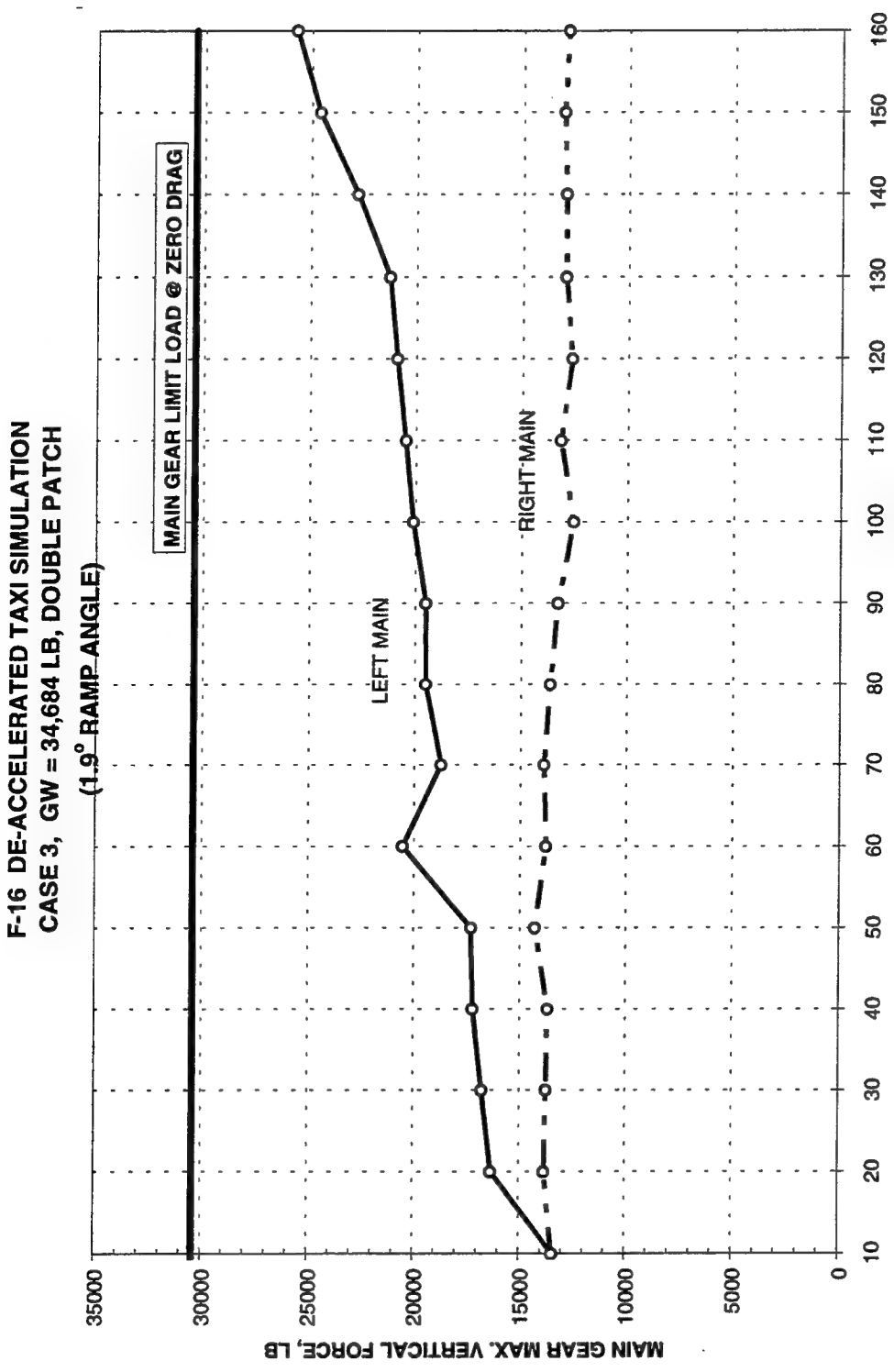

Figure A42. Main gear forces for load case 3, deceleration (landing) mode , heavy gross weight, double mat, and 1.9-deg ramps

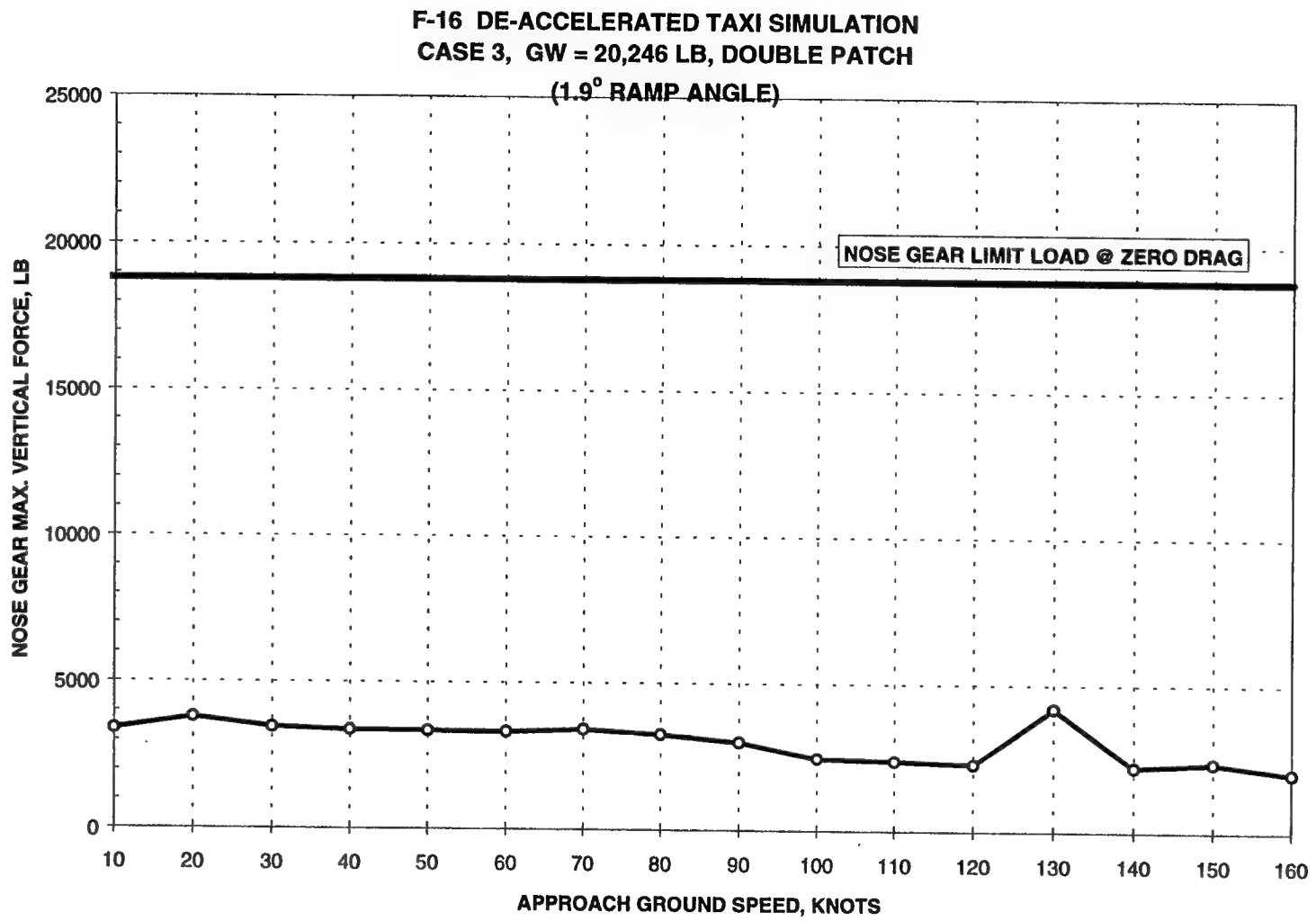

Figure A43. Nose gear forces for load case 3, deceleration (landing) mode, light gross weight, double mat, and 1.9-deg ramps

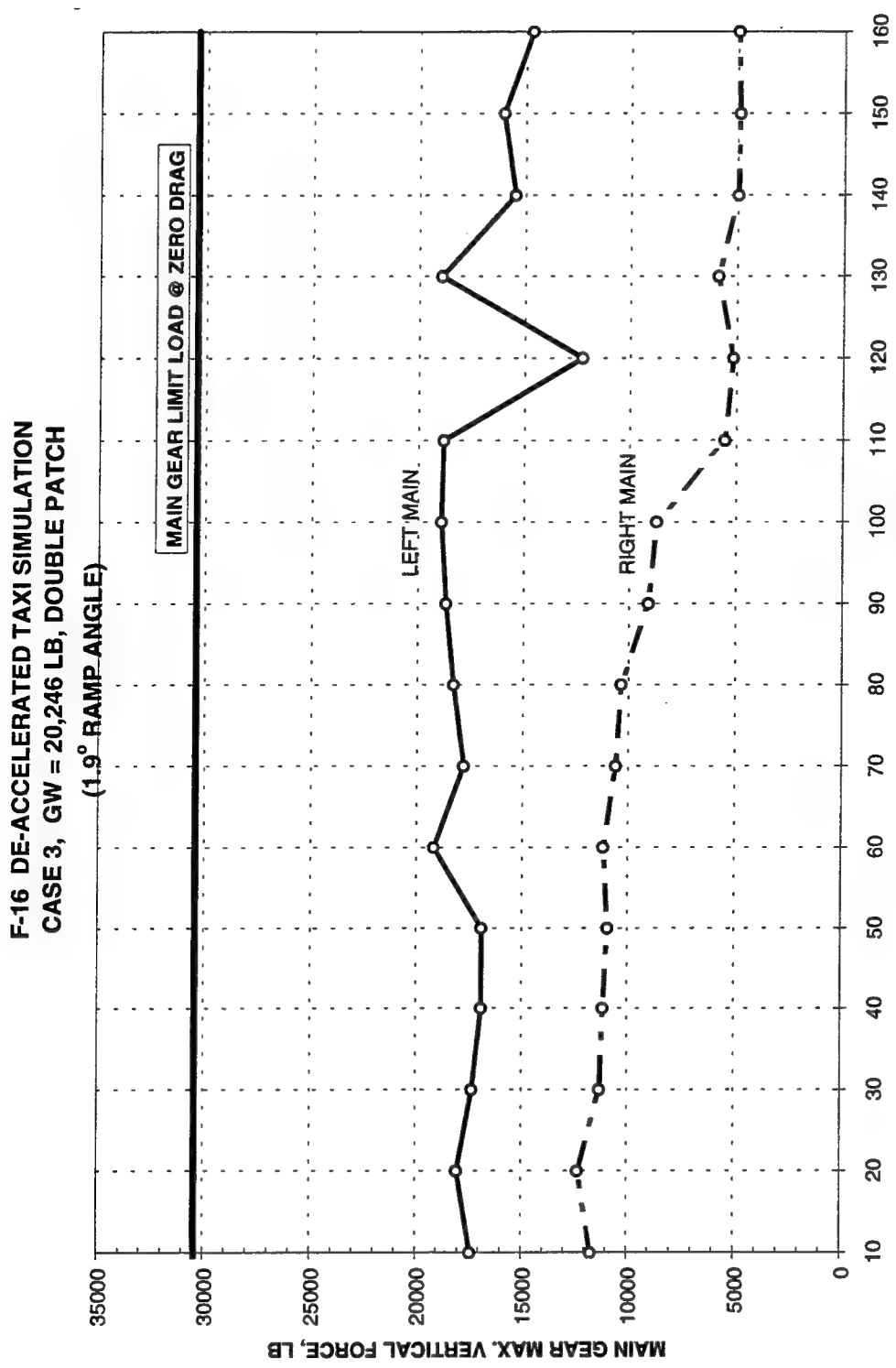

Figure A44. Main gear forces for load case 3, deceleration (landing) mode , light gross weight, double mat, and 1.9-deg ramps

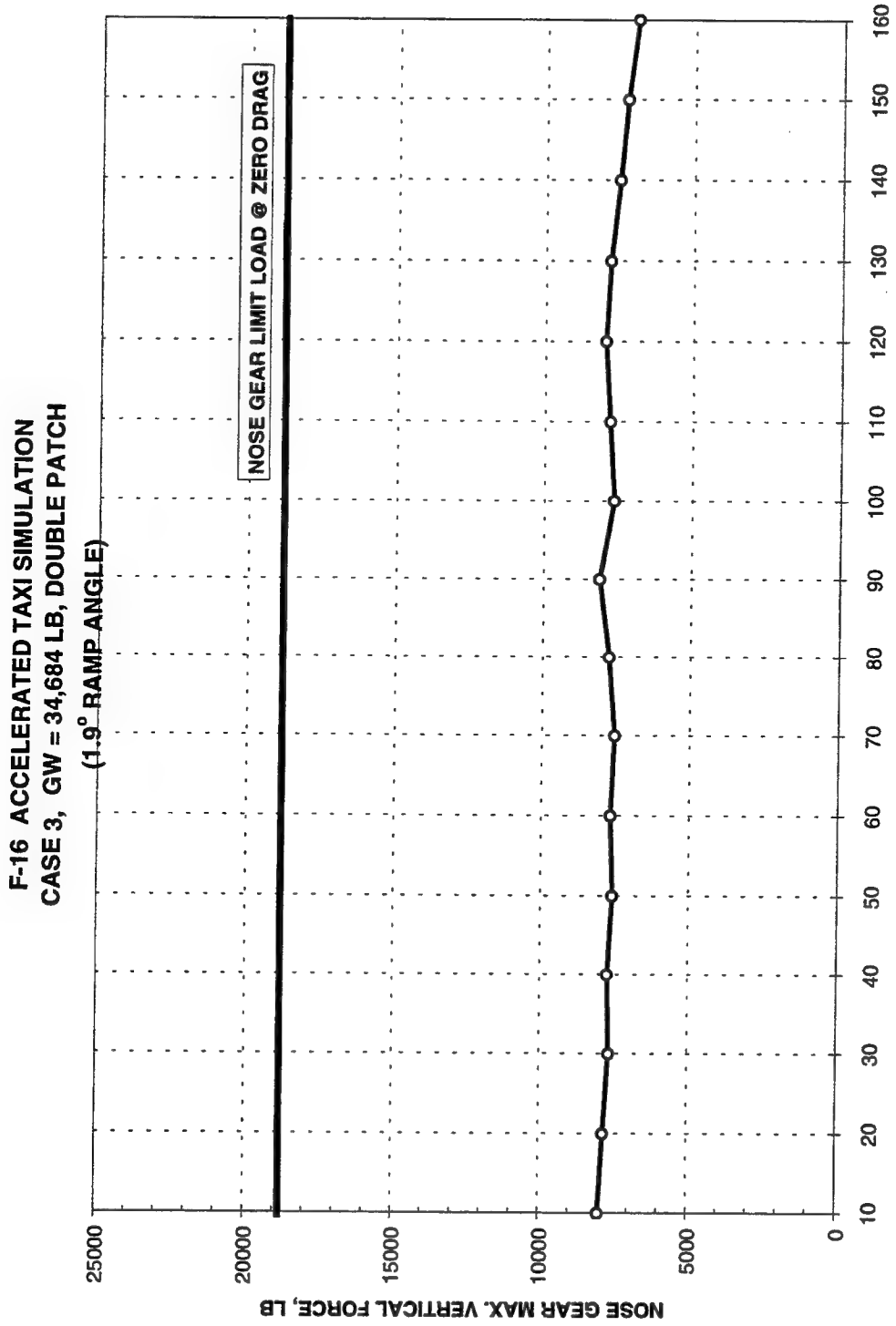

Figure A45. Nose gear forces for load case 3, acceleration (takeoff) mode, heavy gross weight, double mat, and 1.9-deg ramps

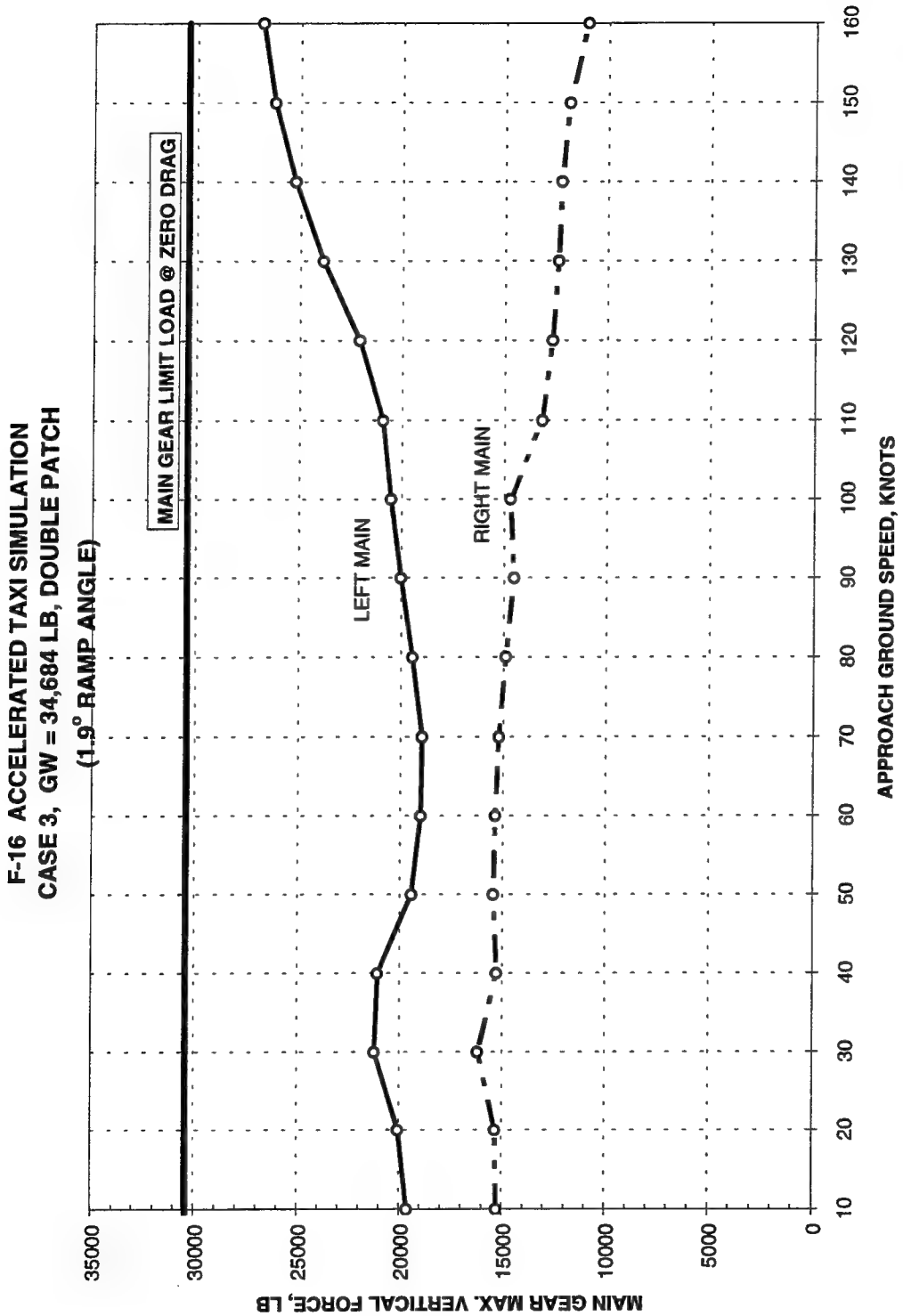

Figure A46. Main gear forces for load case 3, acceleration (takeoff) mode , heavy gross weight, double mat, and 1.9-deg ramps

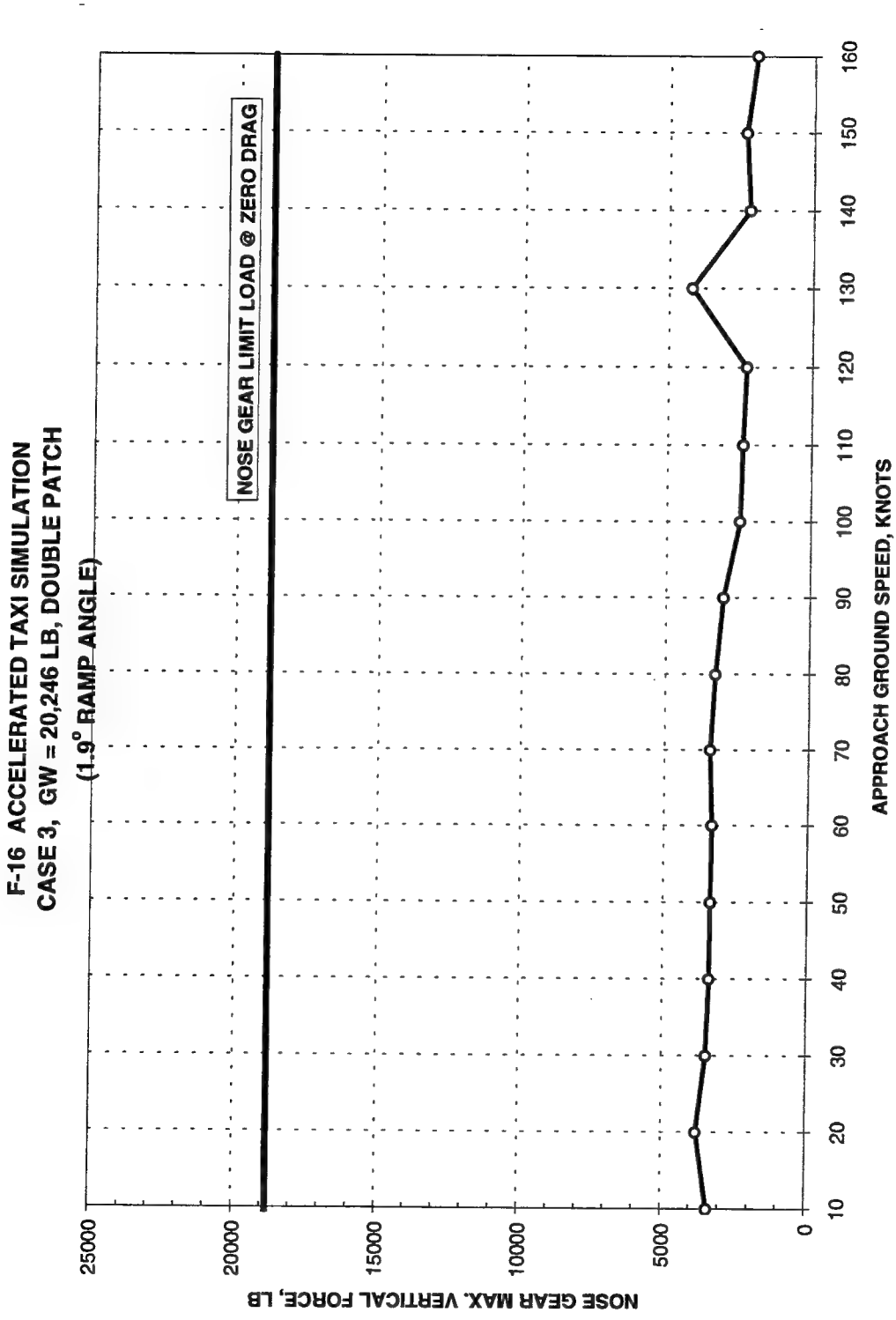

Figure A47. Nose gear forces for load case 3, acceleration (takeoff) mode, light gross weight, double mat, and 1.9-deg ramps

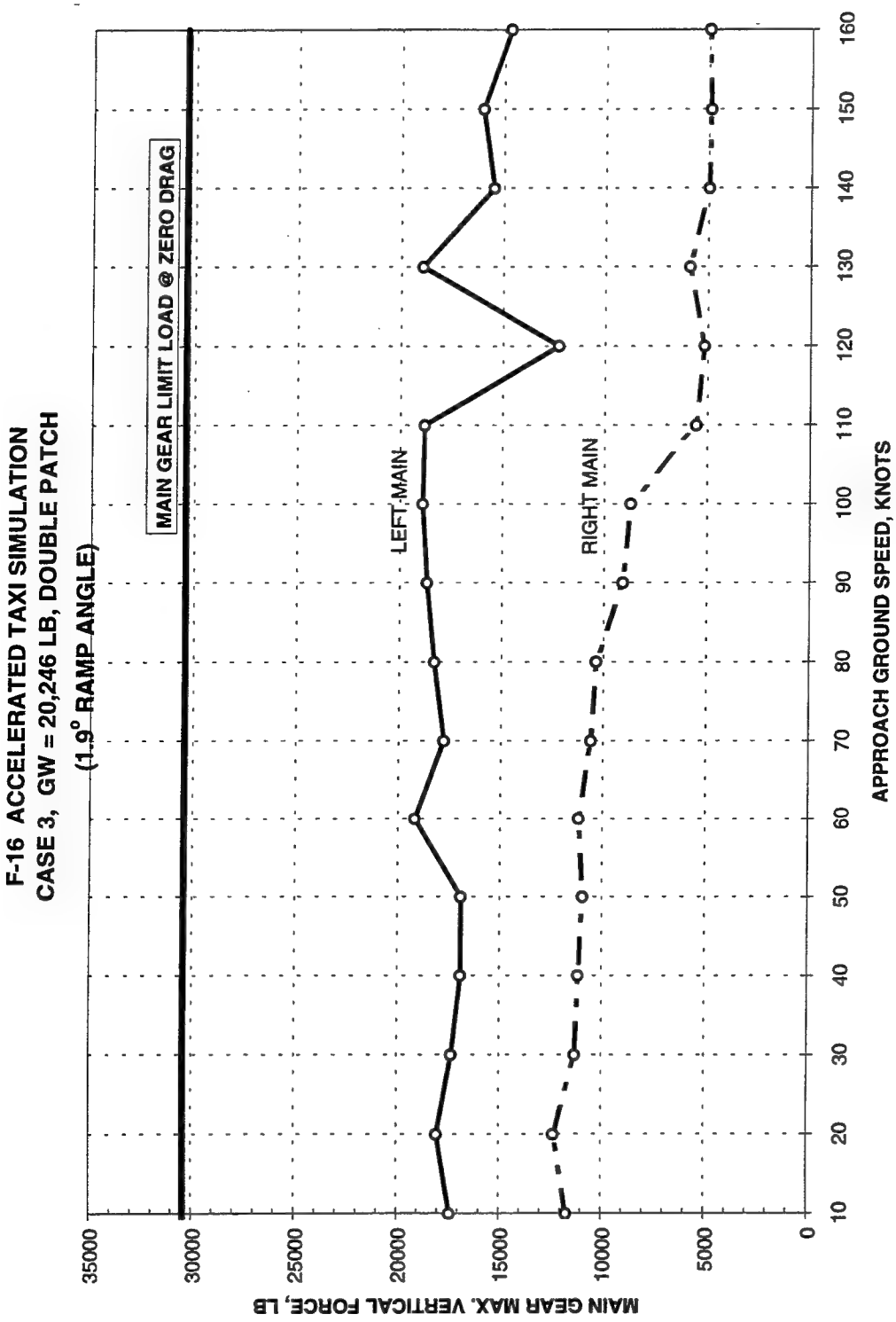

Figure A48. Main gear forces for load case 3, acceleration (takeoff) mode , light gross weight, double mat, and 1.9-deg ramps

Appendix B
Relationships of Maximum Calculated Gear Forces Versus Approach Ground Speed for 0.9-Deg Ramps

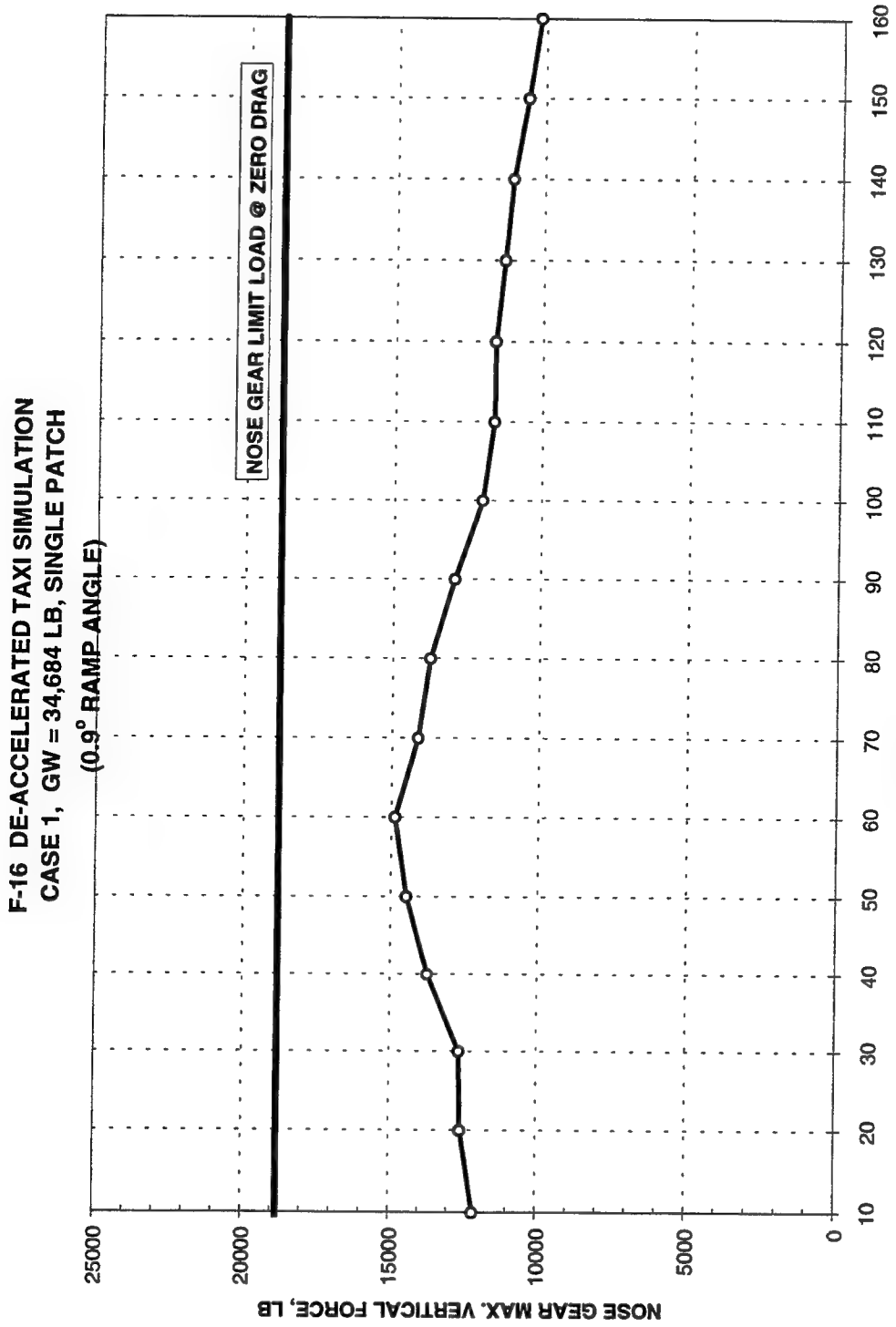

Figure B1. Nose gear forces for load case 1, deceleration (landing) mode, heavy gross weight, single mat, and 0.9-deg ramps

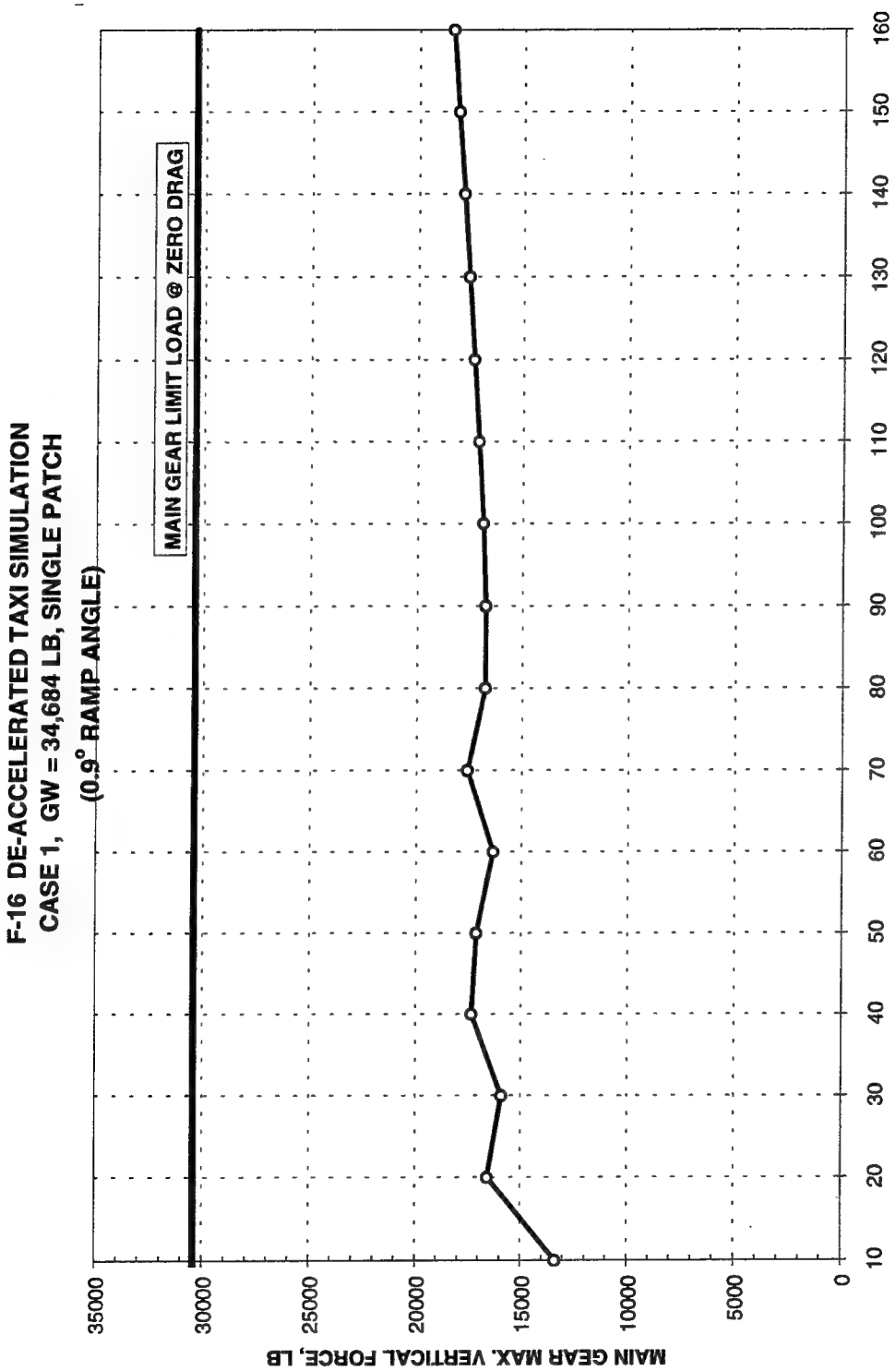

Figure B2. Main gear forces for load case 1, deceleration (landing) mode, heavy gross weight, single mat, and 0.9-deg ramps

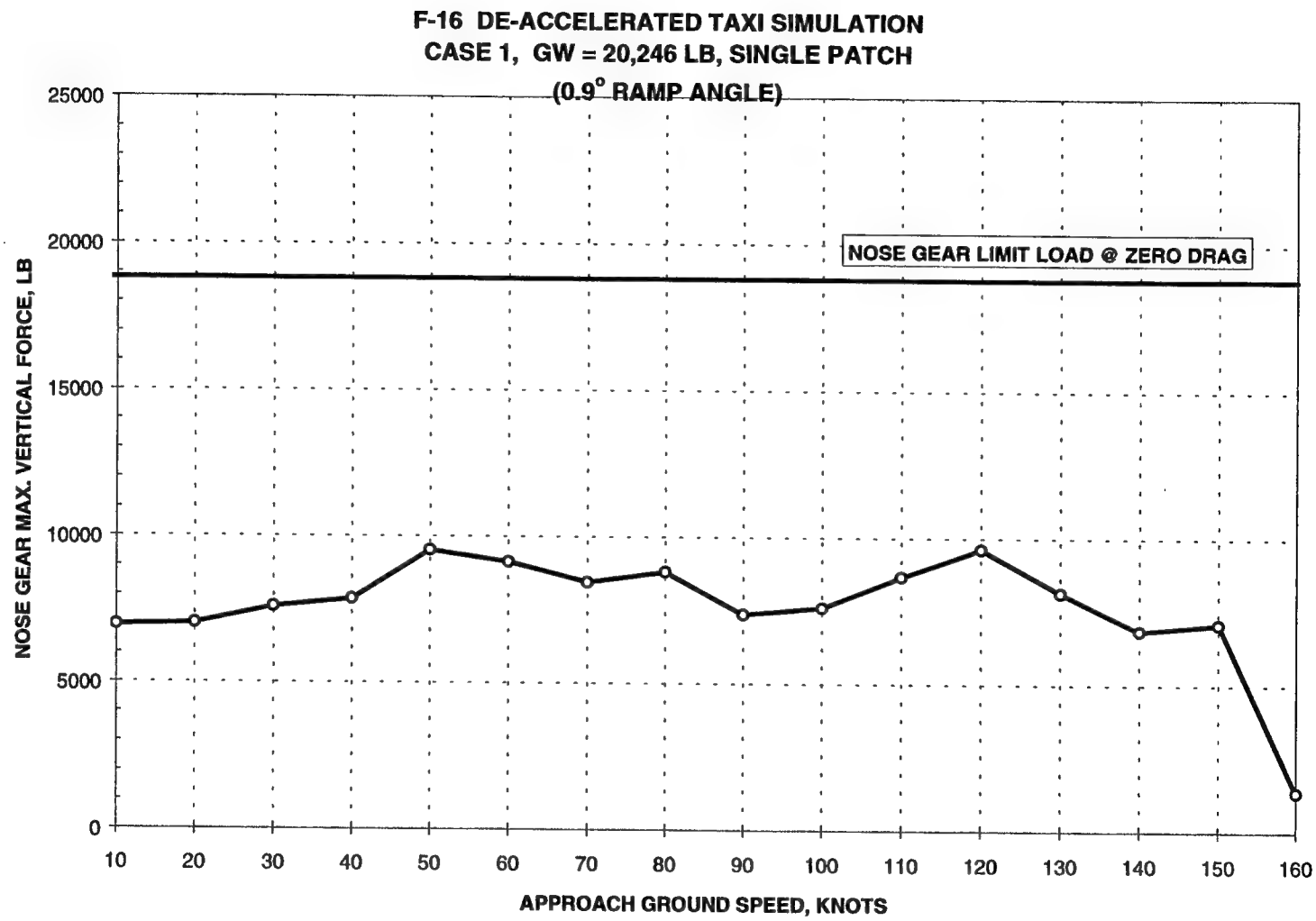

Figure B3. Nose gear forces for load case 1, deceleration (landing) mode, light gross weight, single mat, and 0.9-deg ramps

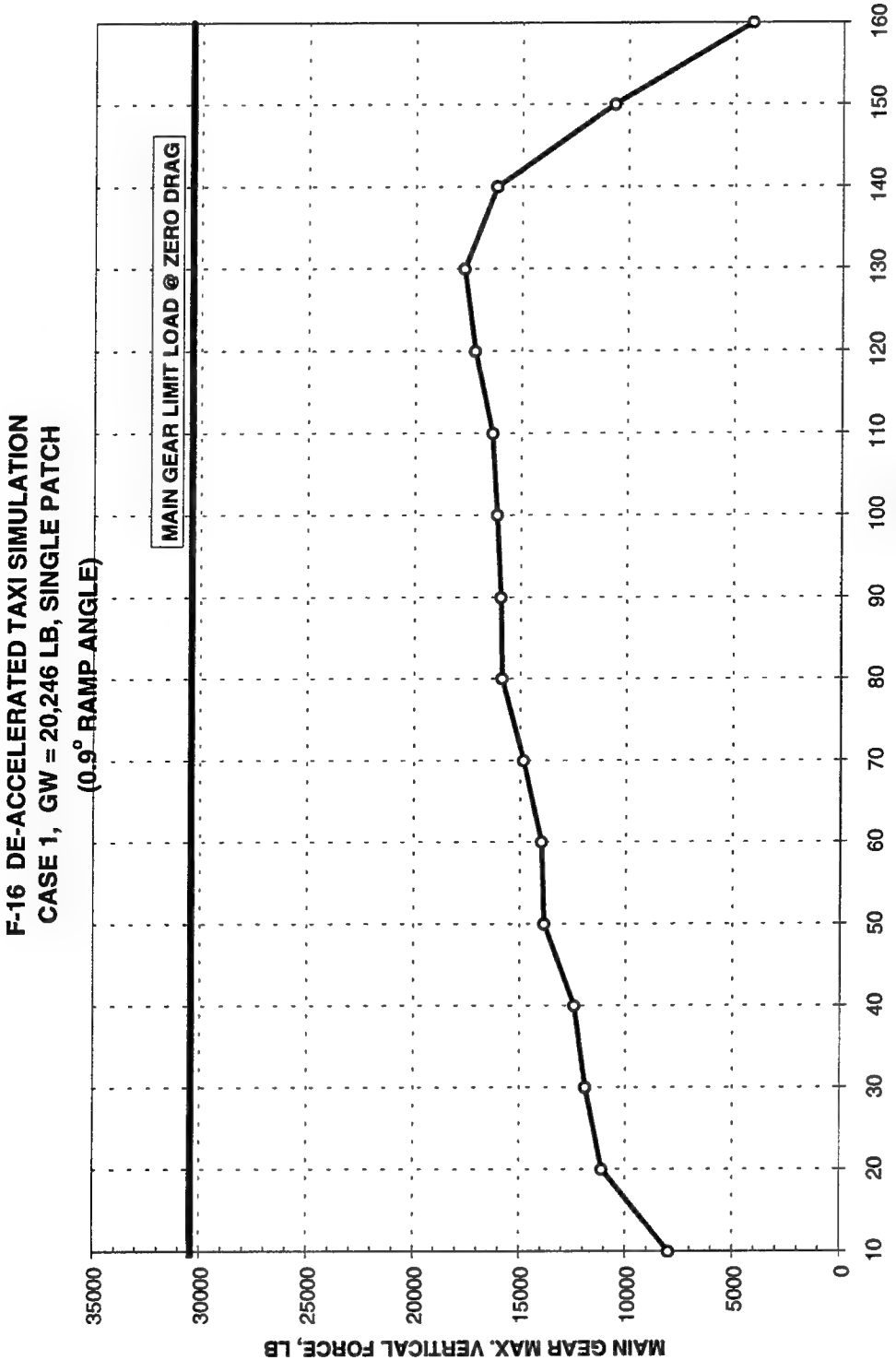

Figure B4. Main gear forces for load case 1, deceleration (landing) mode, light gross weight, single mat, and 0.9-deg ramps

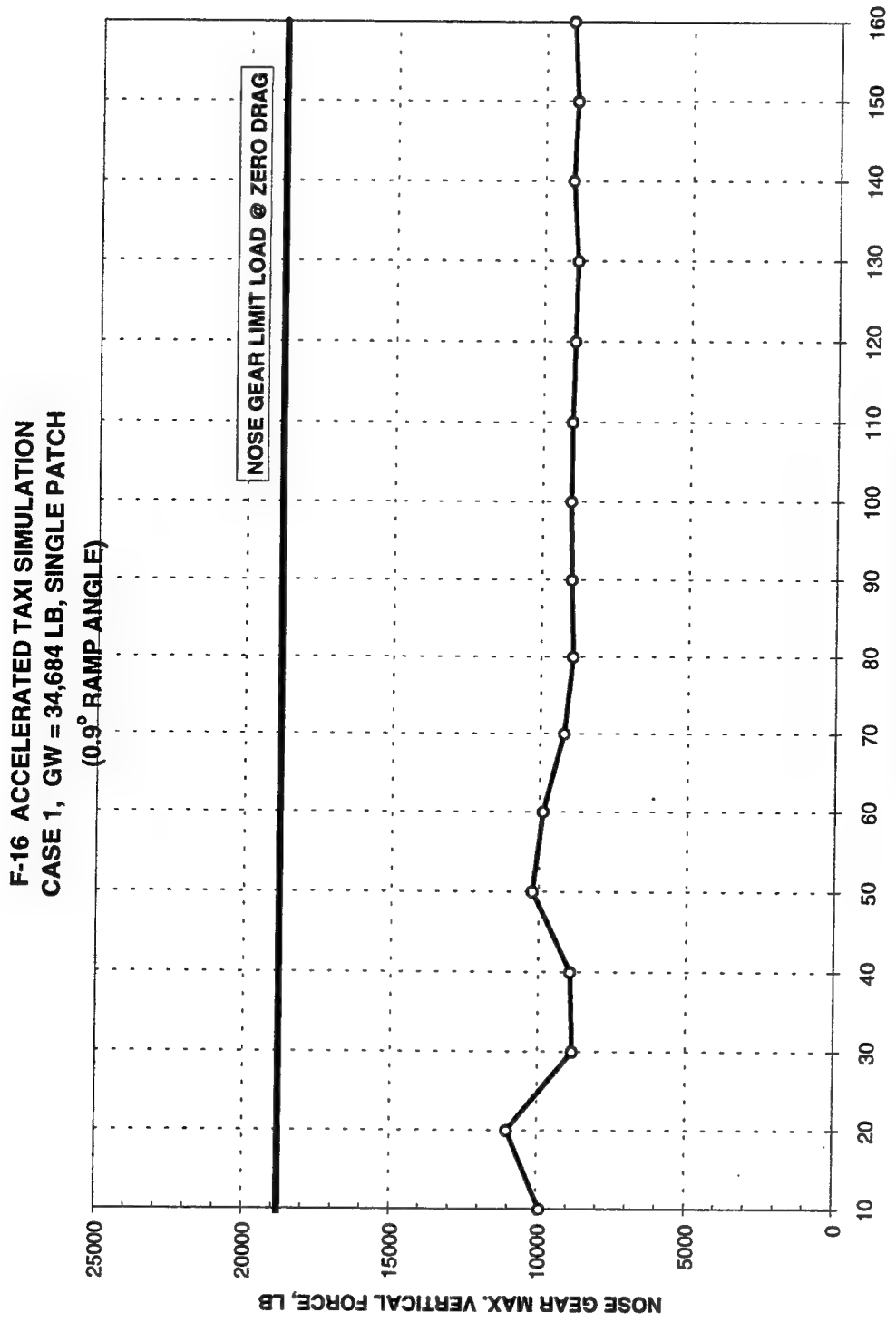

Figure B5. Nose gear forces for load case 1, acceleration (takeoff) mode, heavy gross weight, single mat, and 0.9-deg ramps

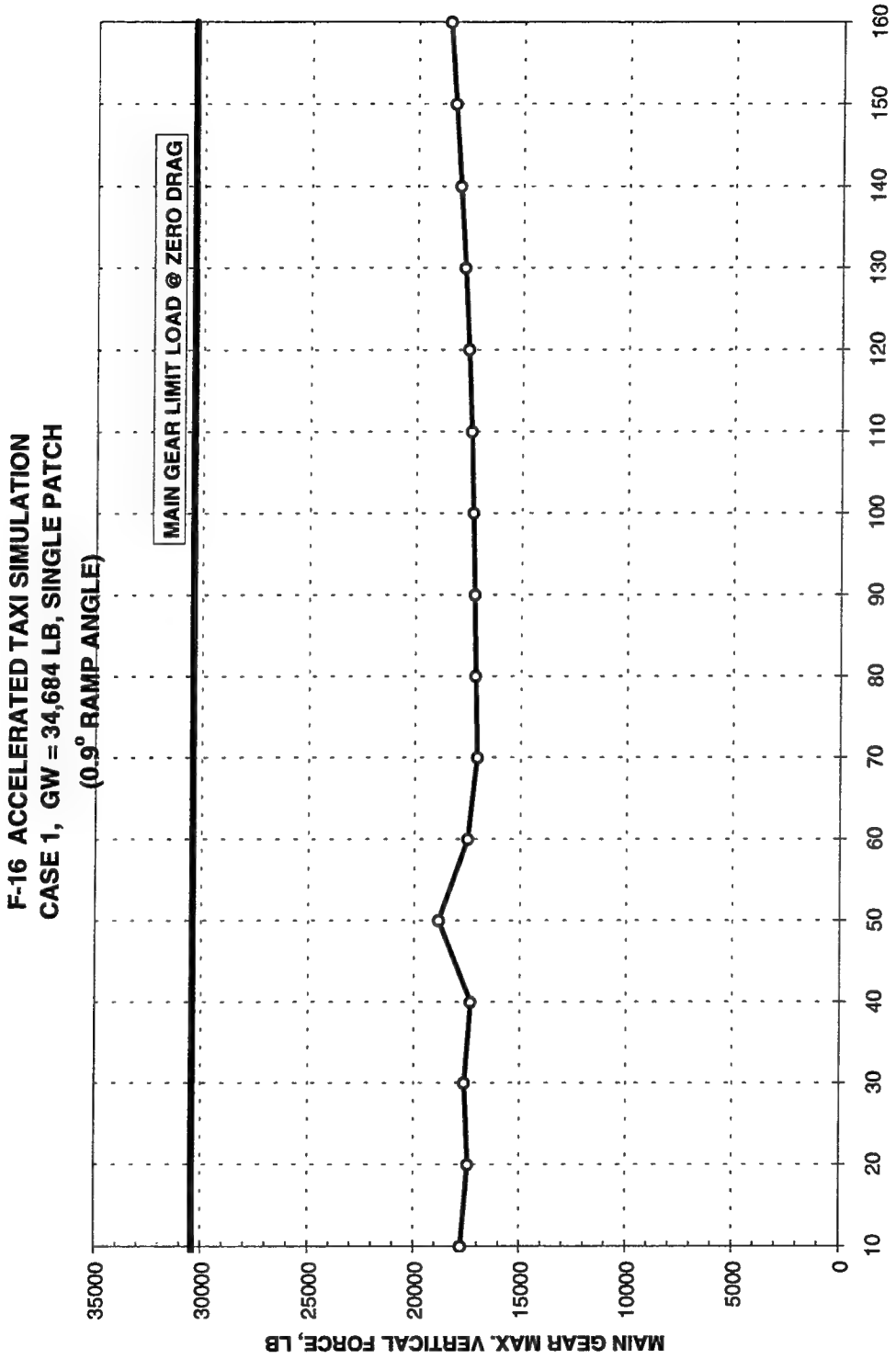

Figure B6. Main gear forces for load case 1, acceleration (takeoff) mode, heavy gross weight, single mat, and 0.9-deg ramps

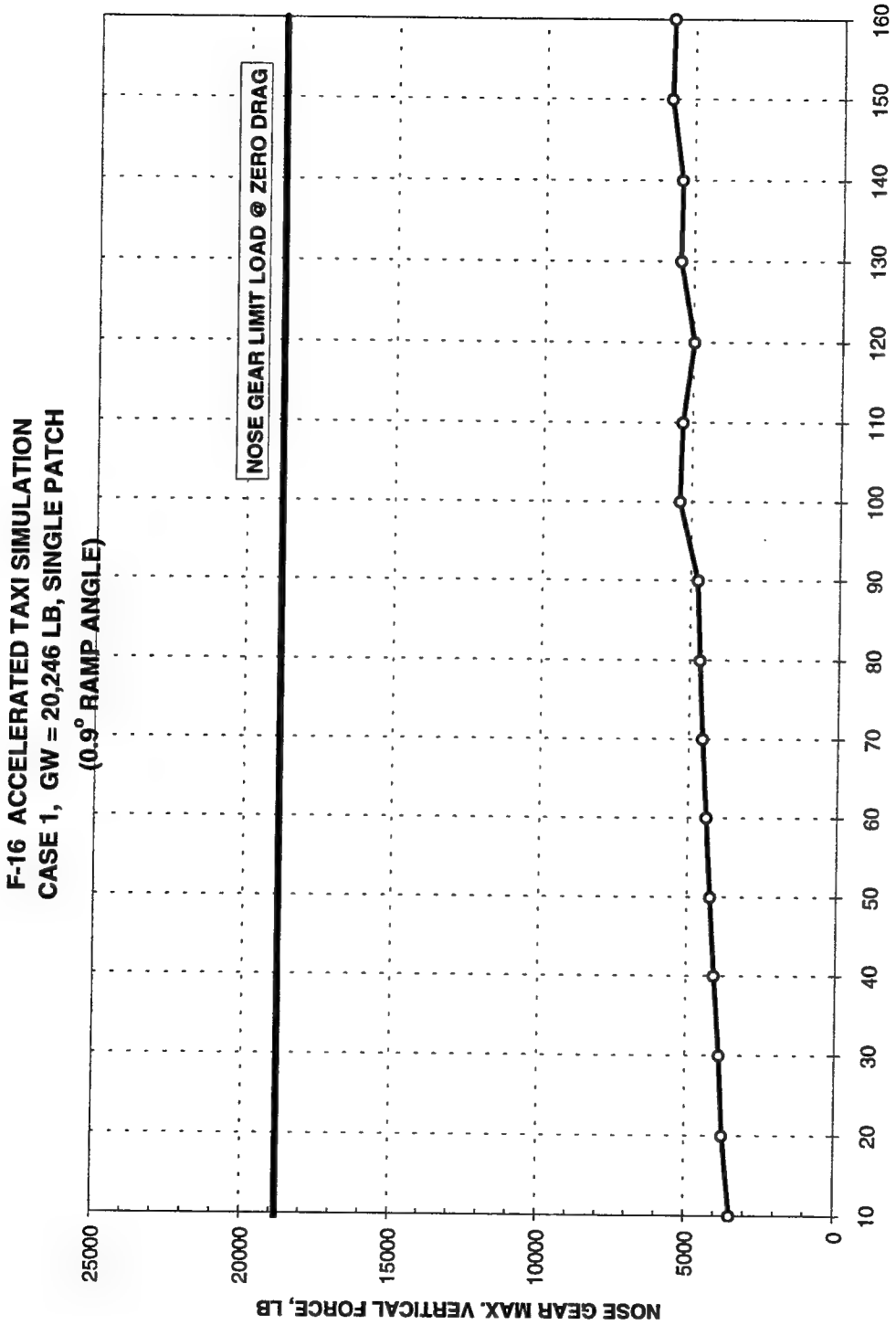

Figure B7. Nose gear forces for load case 1, acceleration (takeoff) mode, light gross weight, single mat, and 0.9-deg ramps

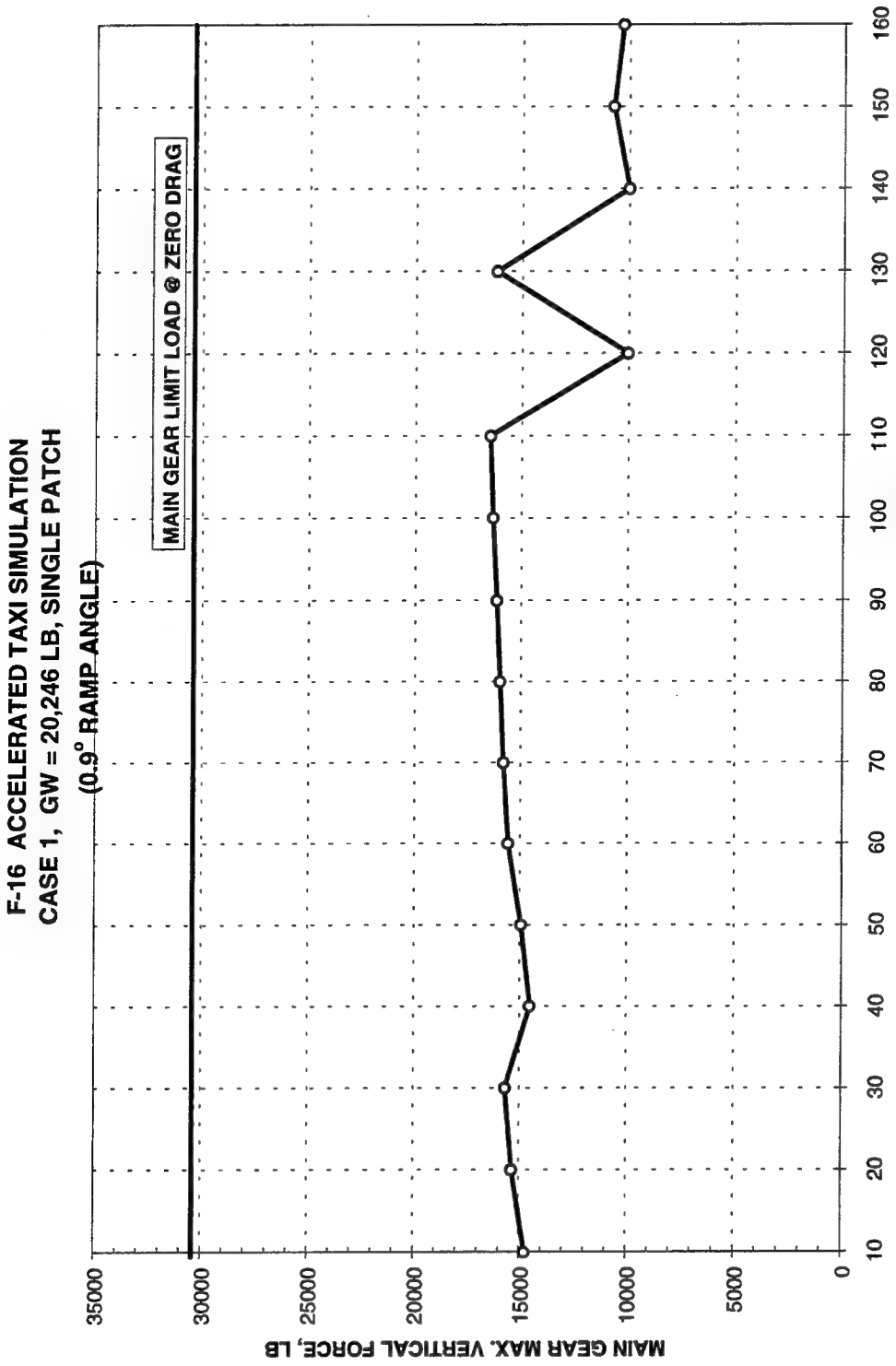

Figure B8. Main gear forces for load case 1, acceleration (takeoff) mode, light gross weight, single mat, and 0.9-deg ramps

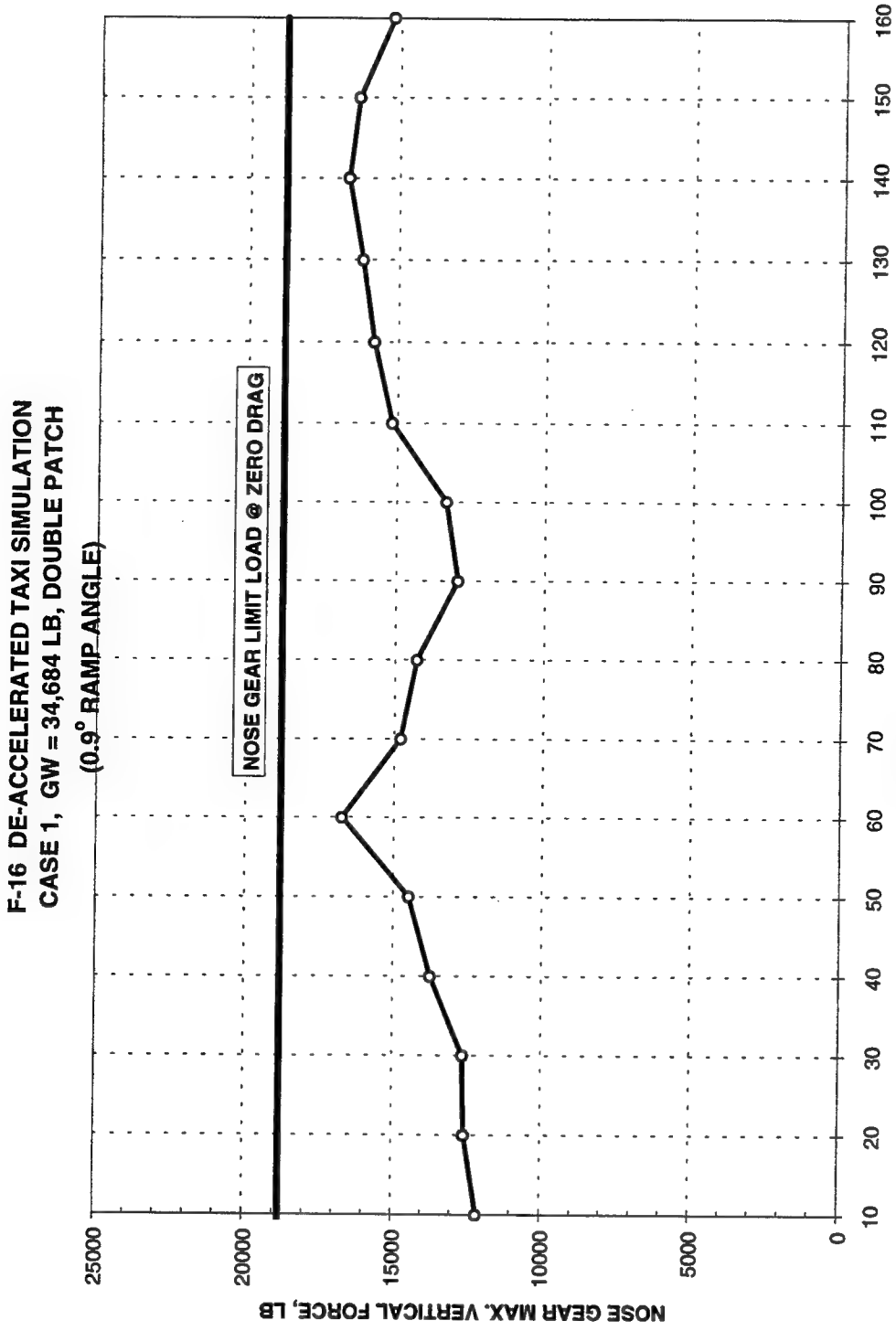

Figure B9. Nose gear forces for load case 1, deceleration (landing) mode, heavy gross weight, double mat, and 0.9-deg ramps

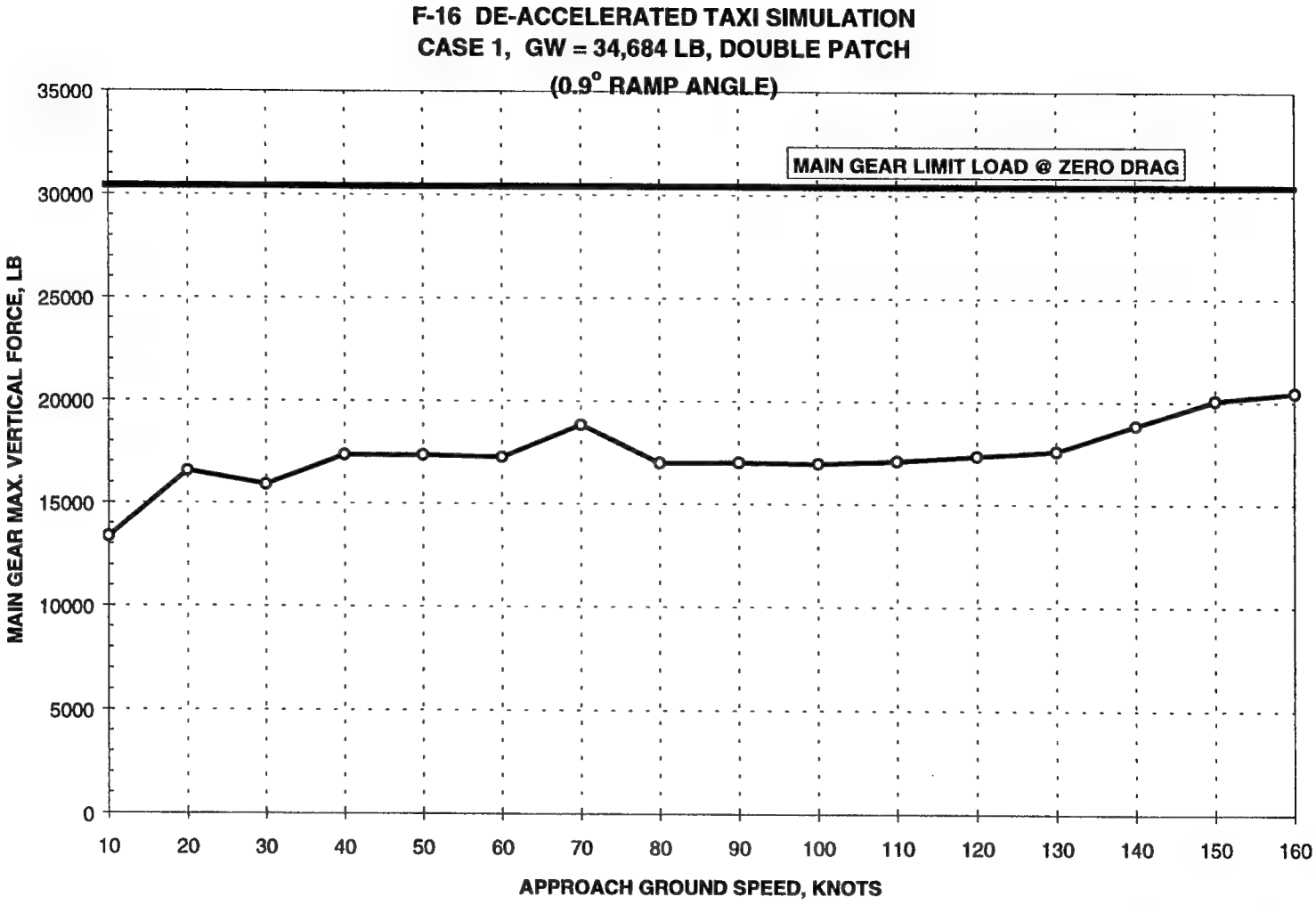

Figure B10. Main gear forces for load case 1, deceleration (landing) mode, heavy gross weight, double mat, and 0.9-deg ramps

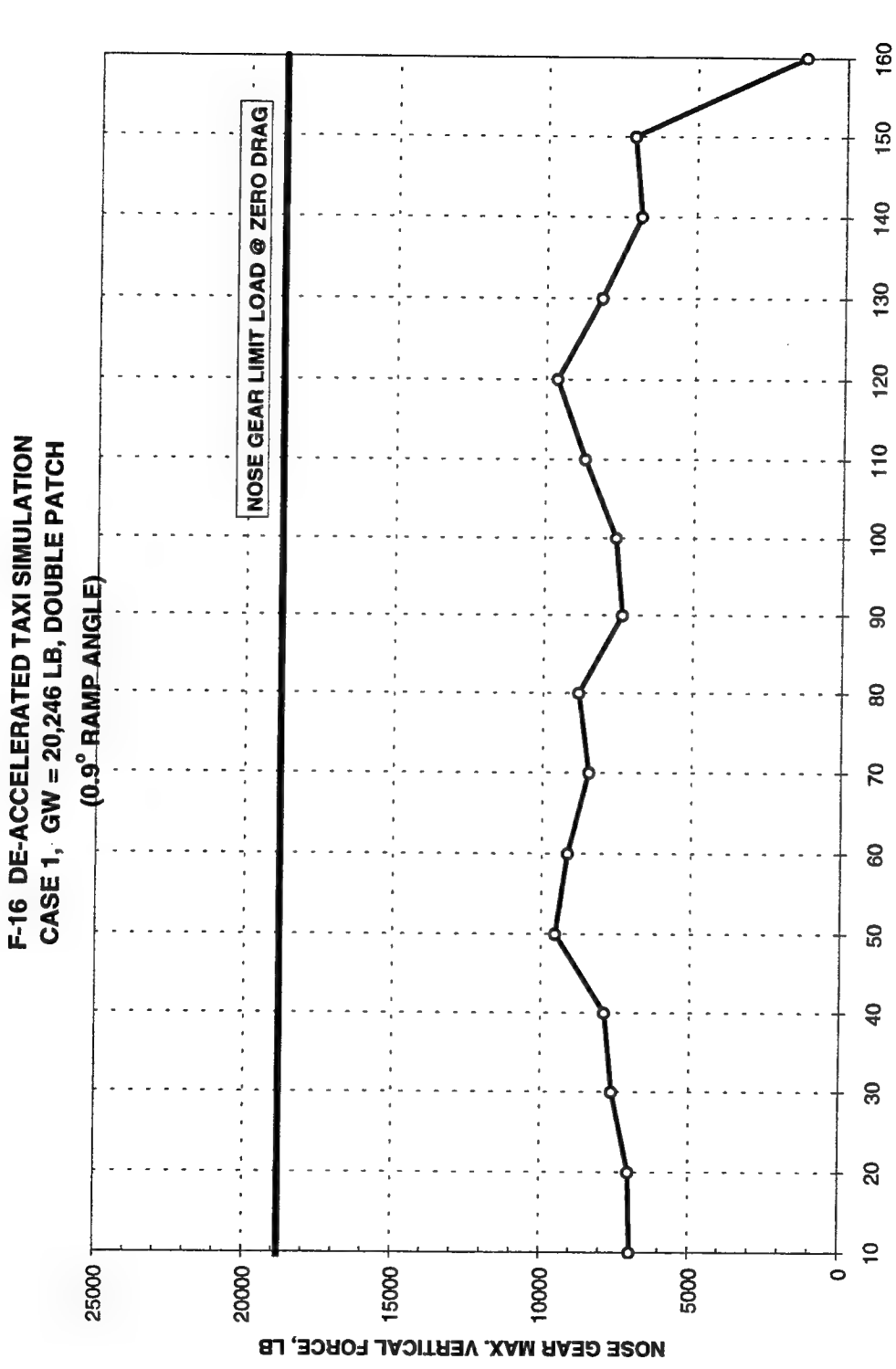

Figure B11. Nose gear forces for load case 1, deceleration (landing) mode, light gross weight, double mat, and 0.9-deg ramps

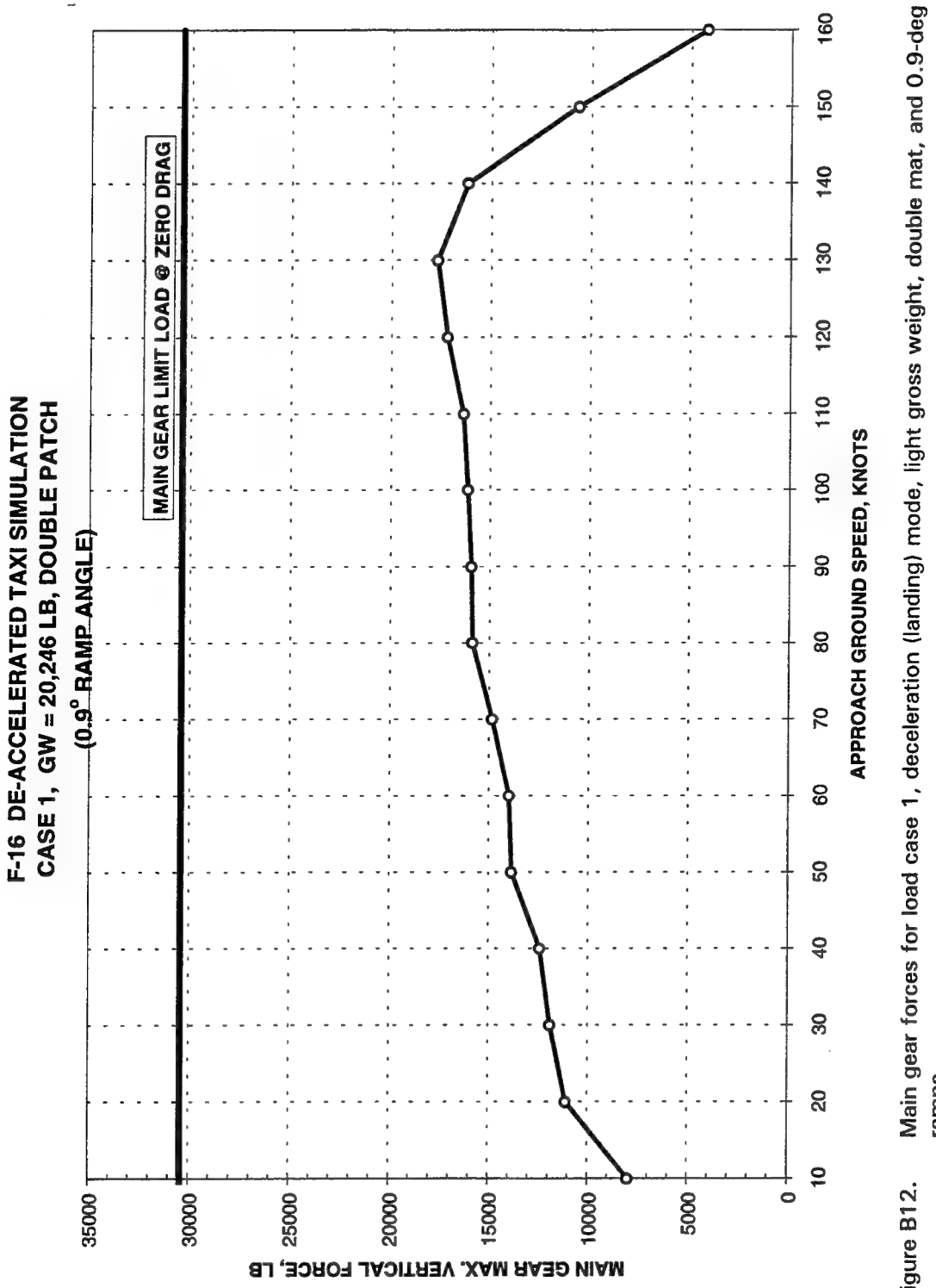

Figure B12. Main gear forces for load case 1, deceleration (landing) mode, light gross weight, double mat, and 0.9-deg ramps

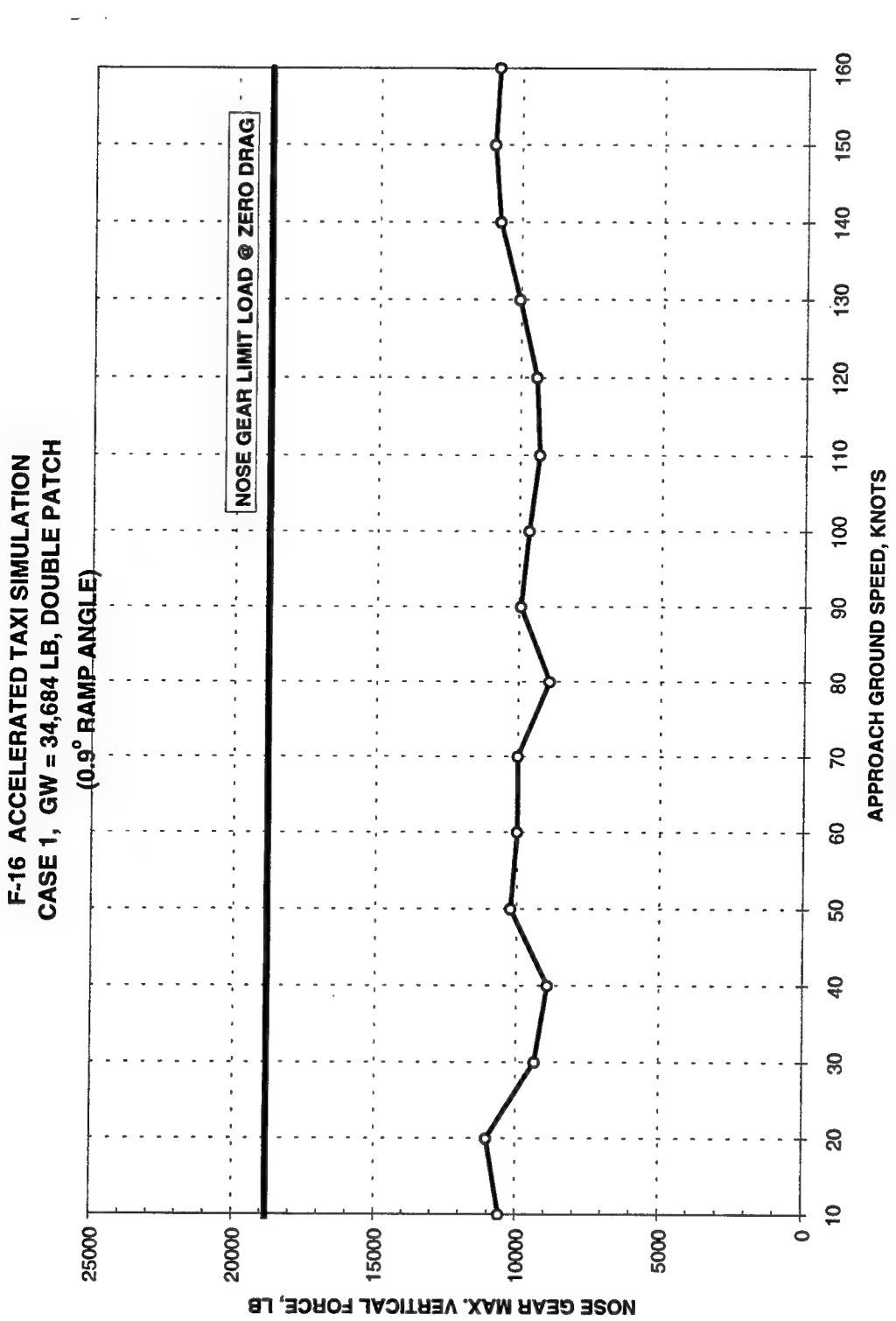

Figure B13. Nose gear forces for load case 1, acceleration (takeoff) mode, heavy gross weight, double mat, and 0.9-deg ramps

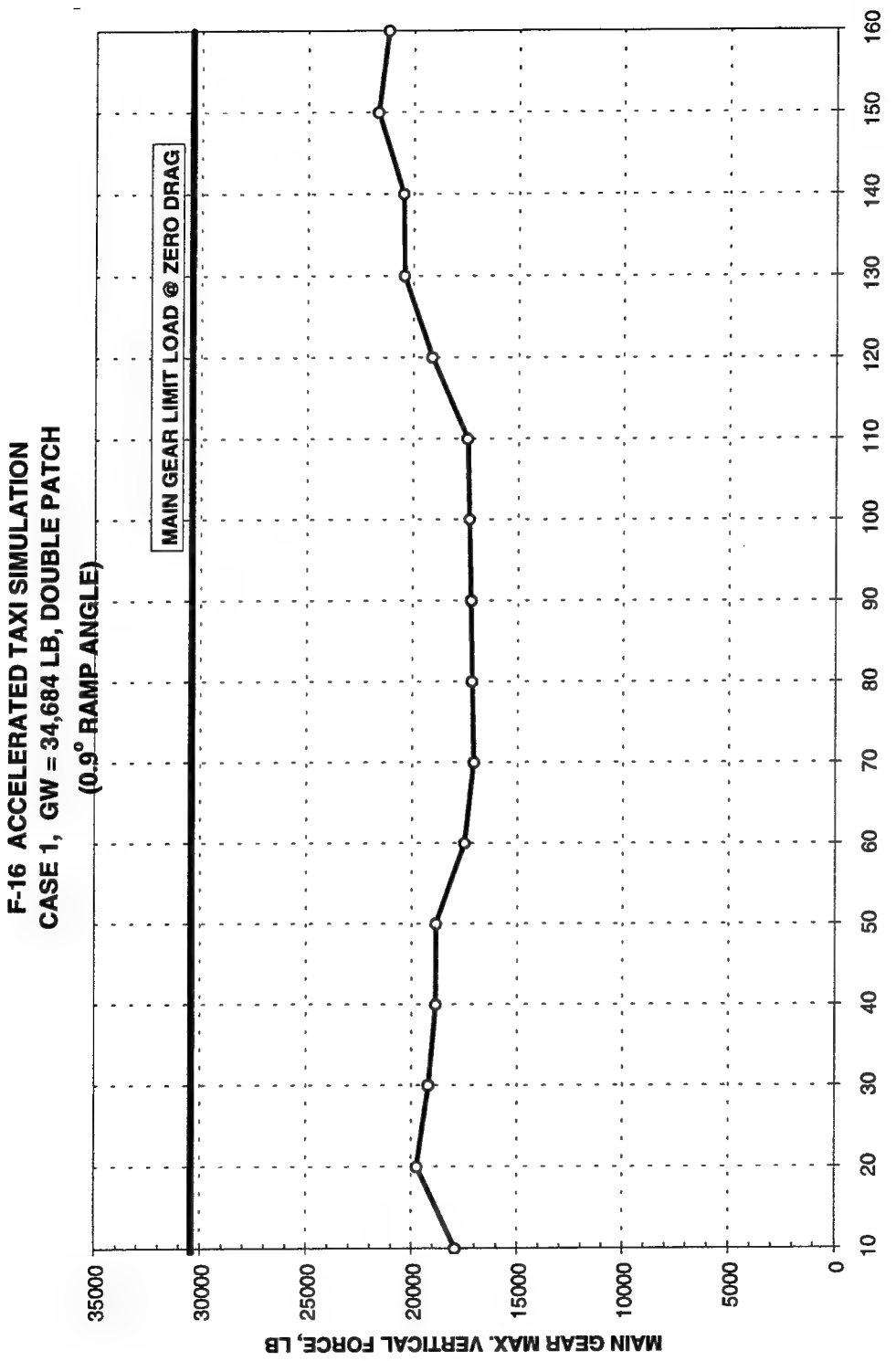

Figure B14. Main gear forces for load case 1, acceleration (takeoff) mode, heavy gross weight, double mat, and 0.9-deg ramps

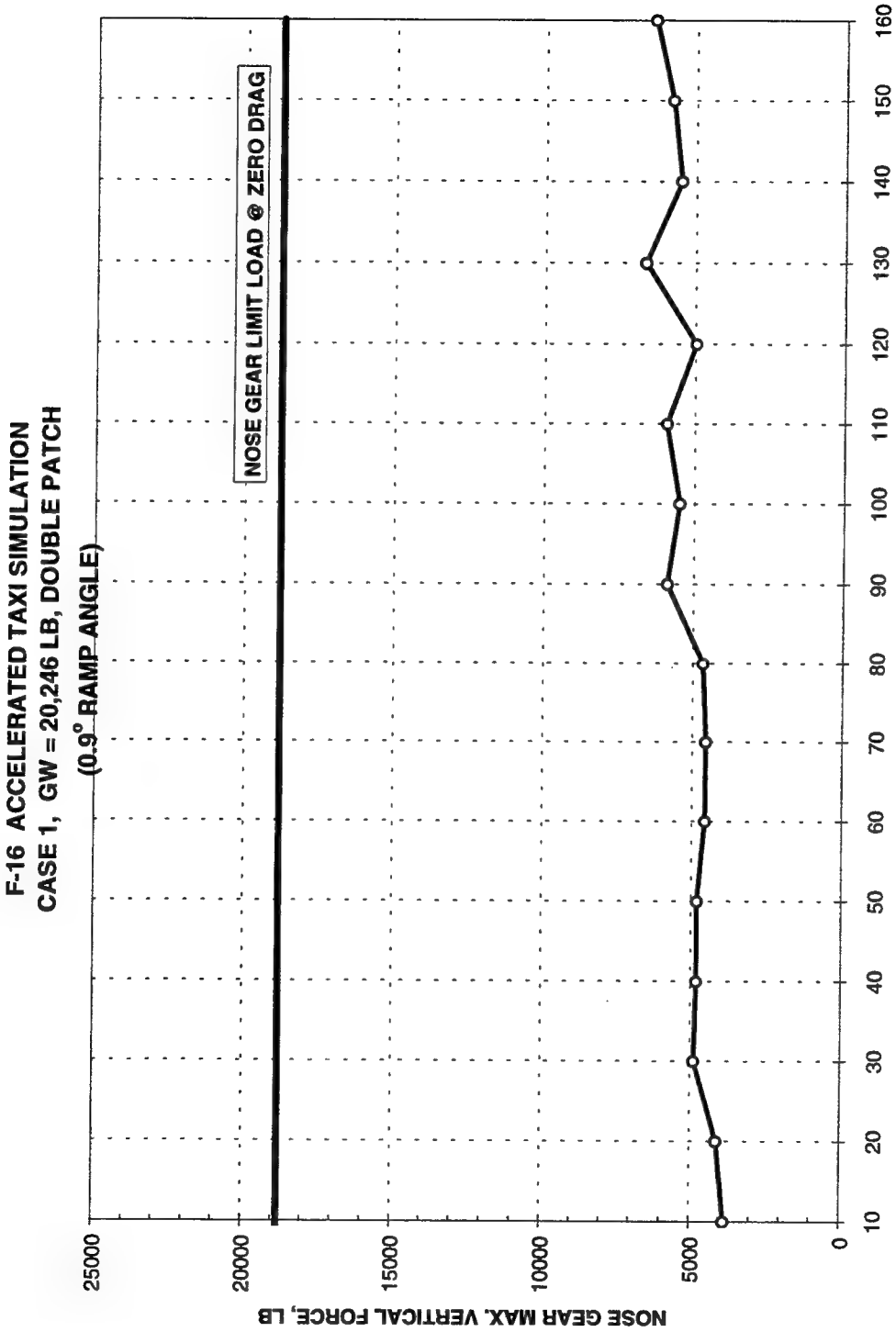

Figure B15. Nose gear forces for load case 1, acceleration (takeoff) mode, light gross weight, double mat, and 0.9-deg ramps

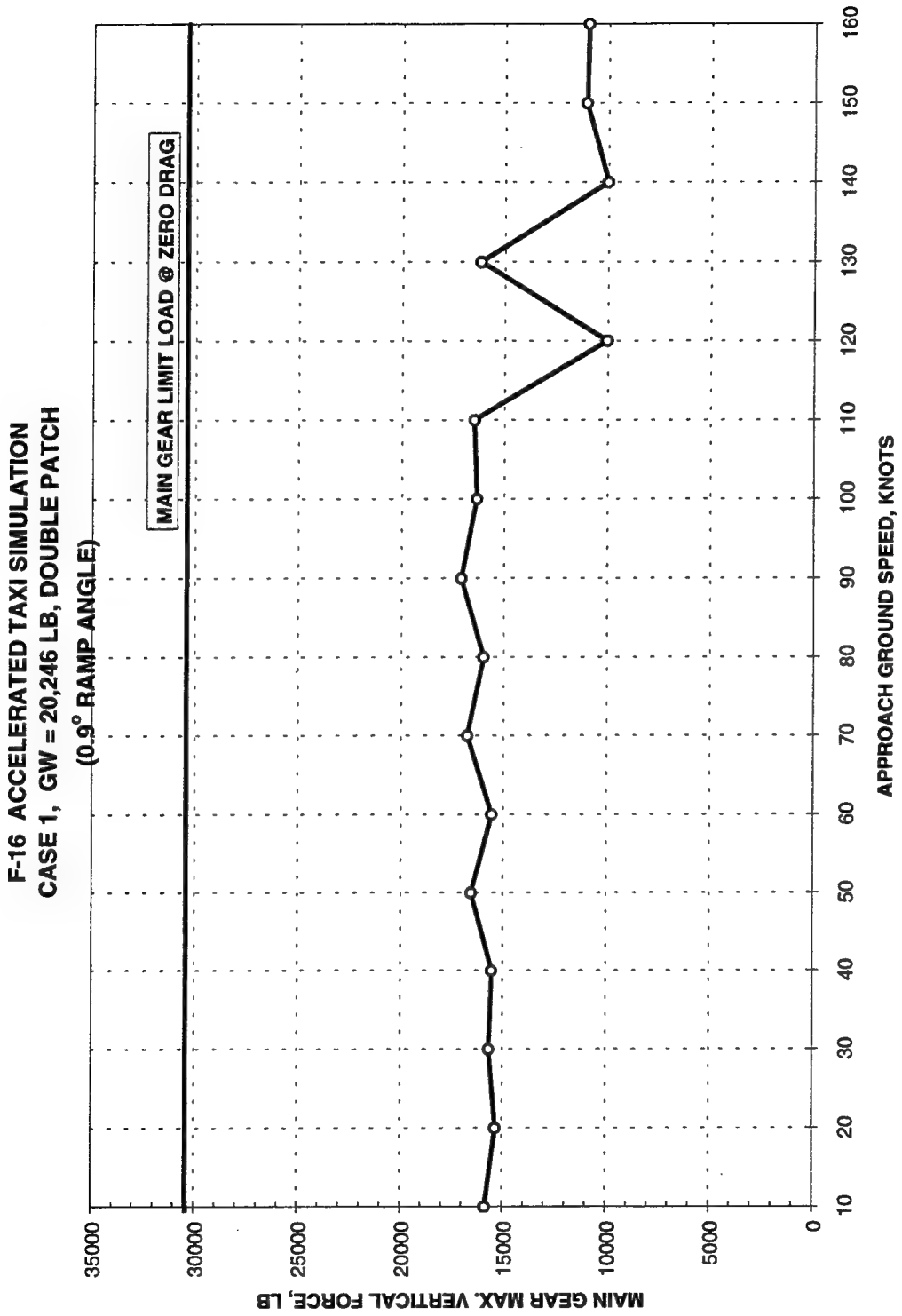

Figure B16. Main gear forces for load case 1, acceleration (takeoff) mode, light gross weight, double mat, and 0.9-deg ramps

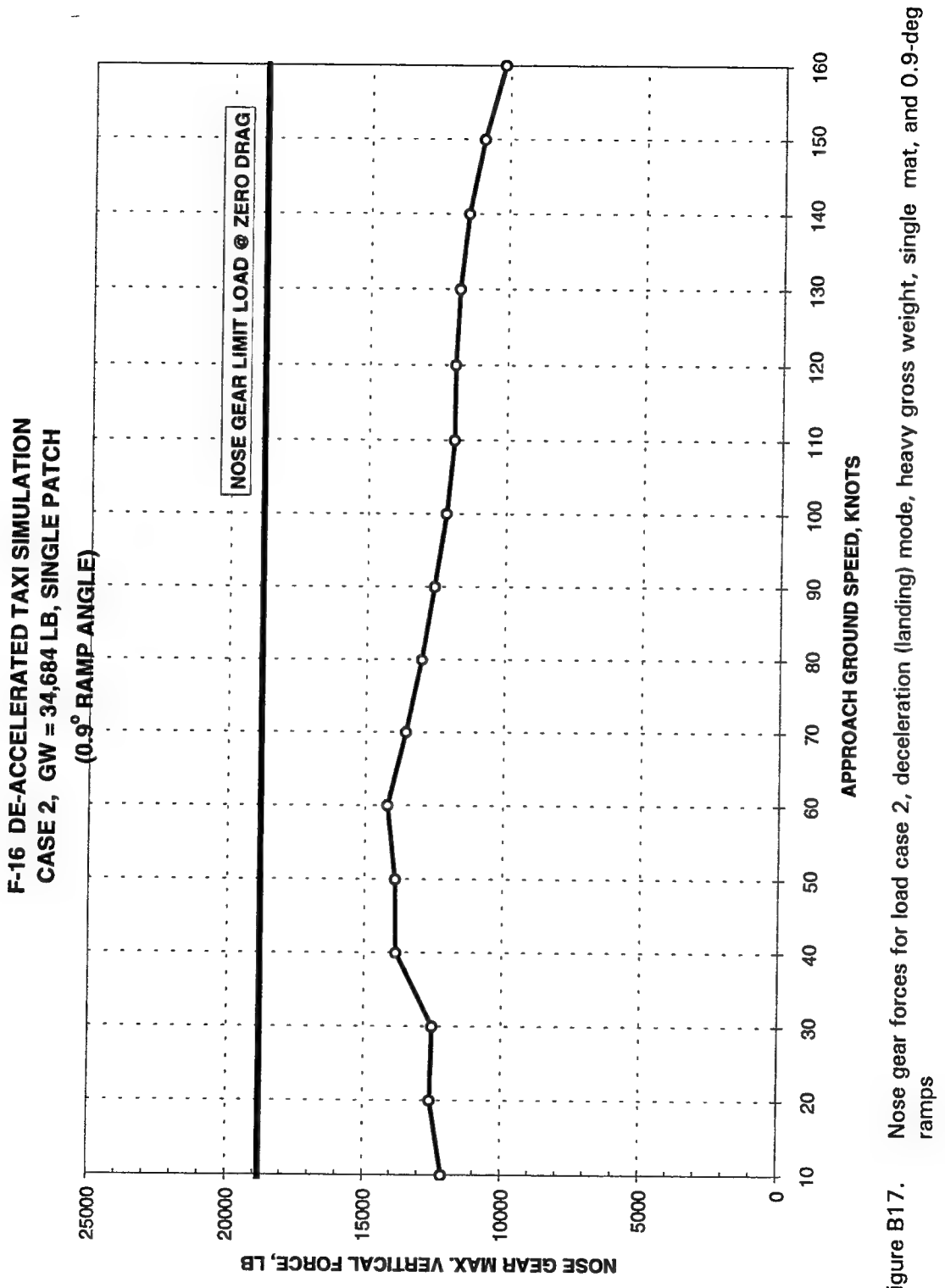

Figure B17. Nose gear forces for load case 2, deceleration (landing) mode, heavy gross weight, single mat, and 0.9-deg ramps

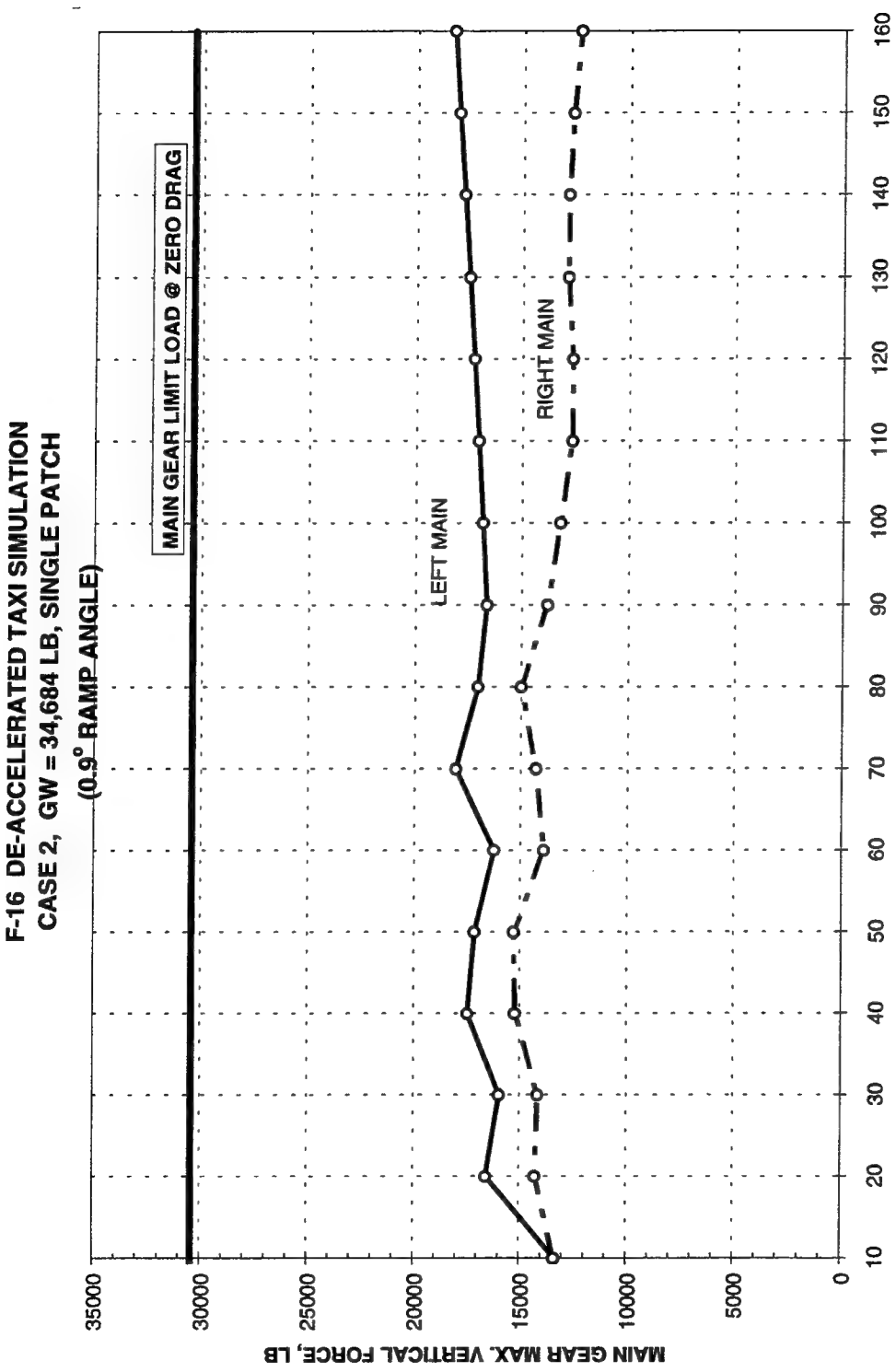

Figure B18. Main gear forces for load case 2, deceleration (landing) mode, heavy gross weight, single mat, and 0.9-deg ramps

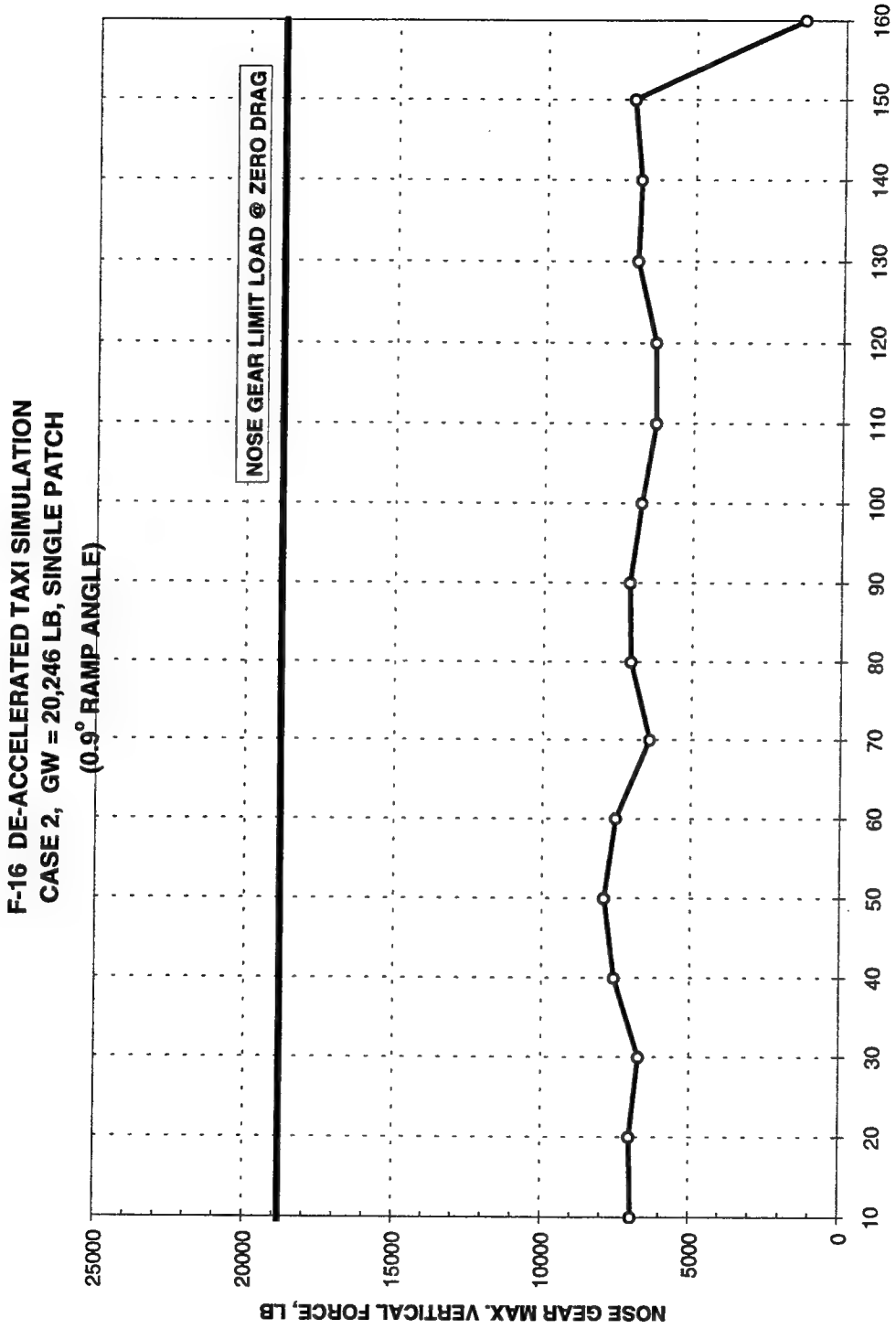

Figure B19. Nose gear forces for load case 2, deceleration (landing) mode, light gross weight, single mat, and 0.9-deg ramps

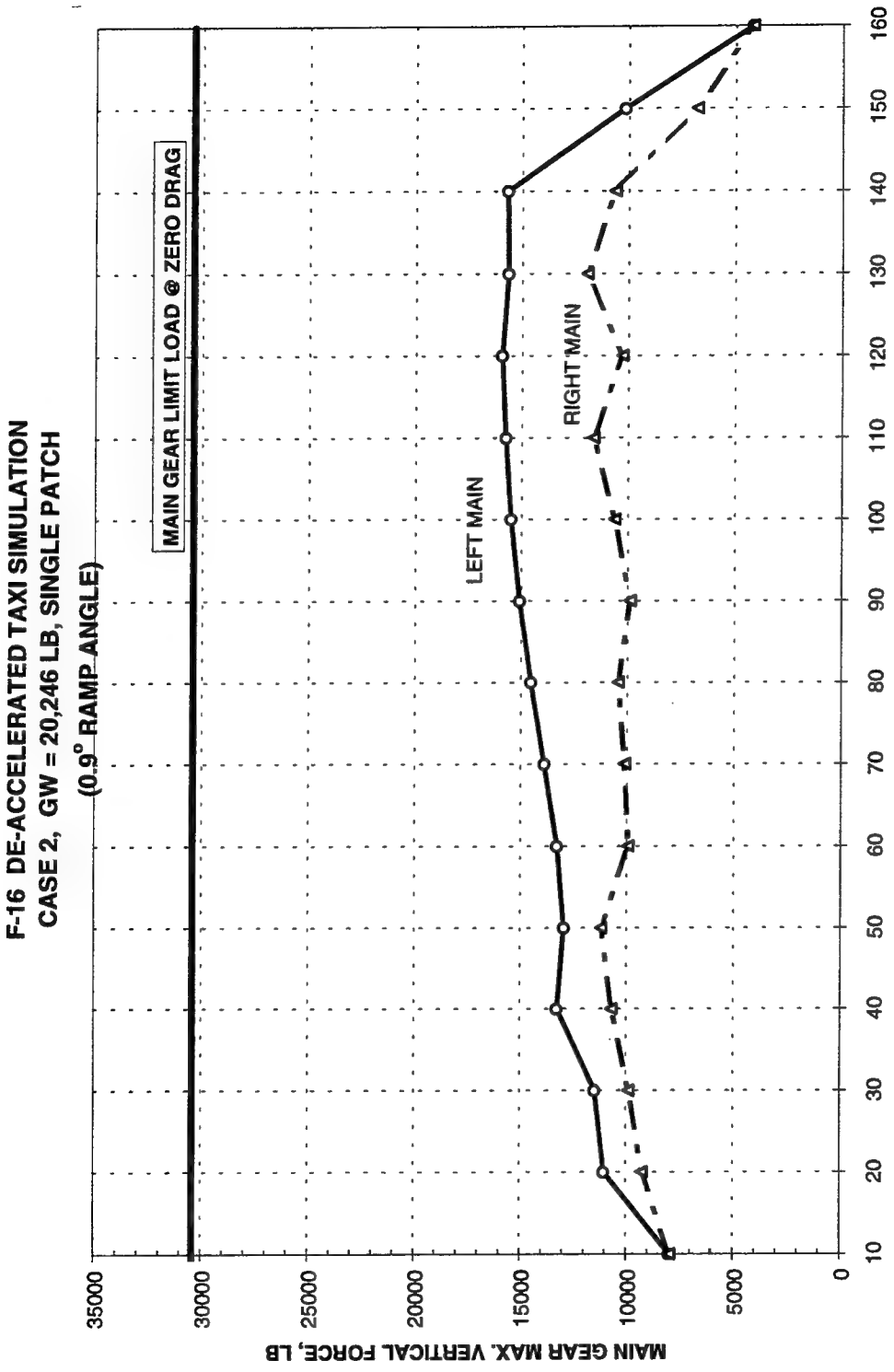

Figure B20. Main gear forces for load case 2, deceleration (landing) mode ,light gross weight, single mat, and 0.9-deg ramps

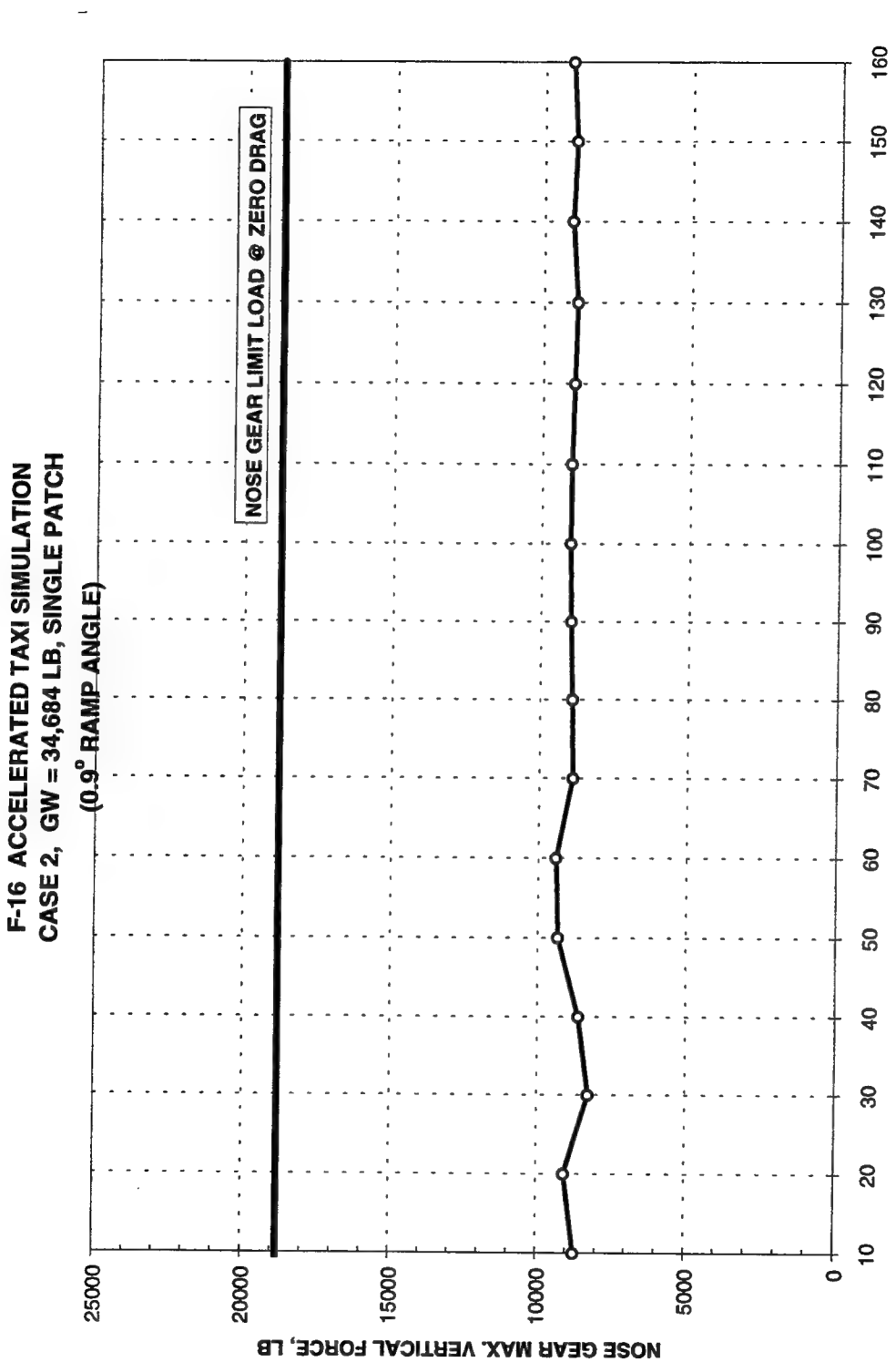

Figure B21. Nose gear forces for load case 2, acceleration (takeoff) mode, heavy gross weight, single mat, and 0.9-deg ramps

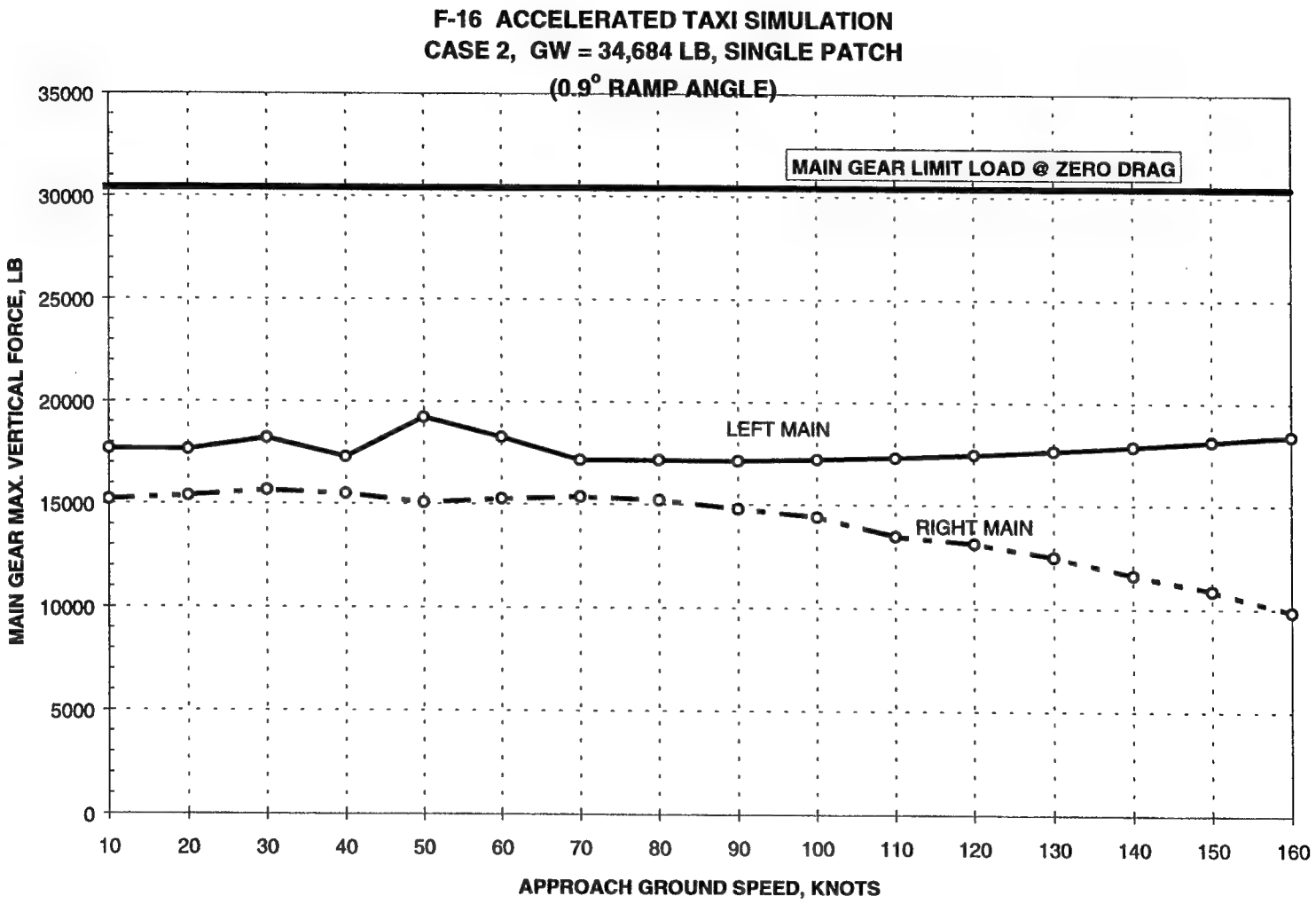

Figure B22. Main gear forces for load case 2, acceleration (takeoff) mode, heavy gross weight, single mat, and 0.9-deg ramps

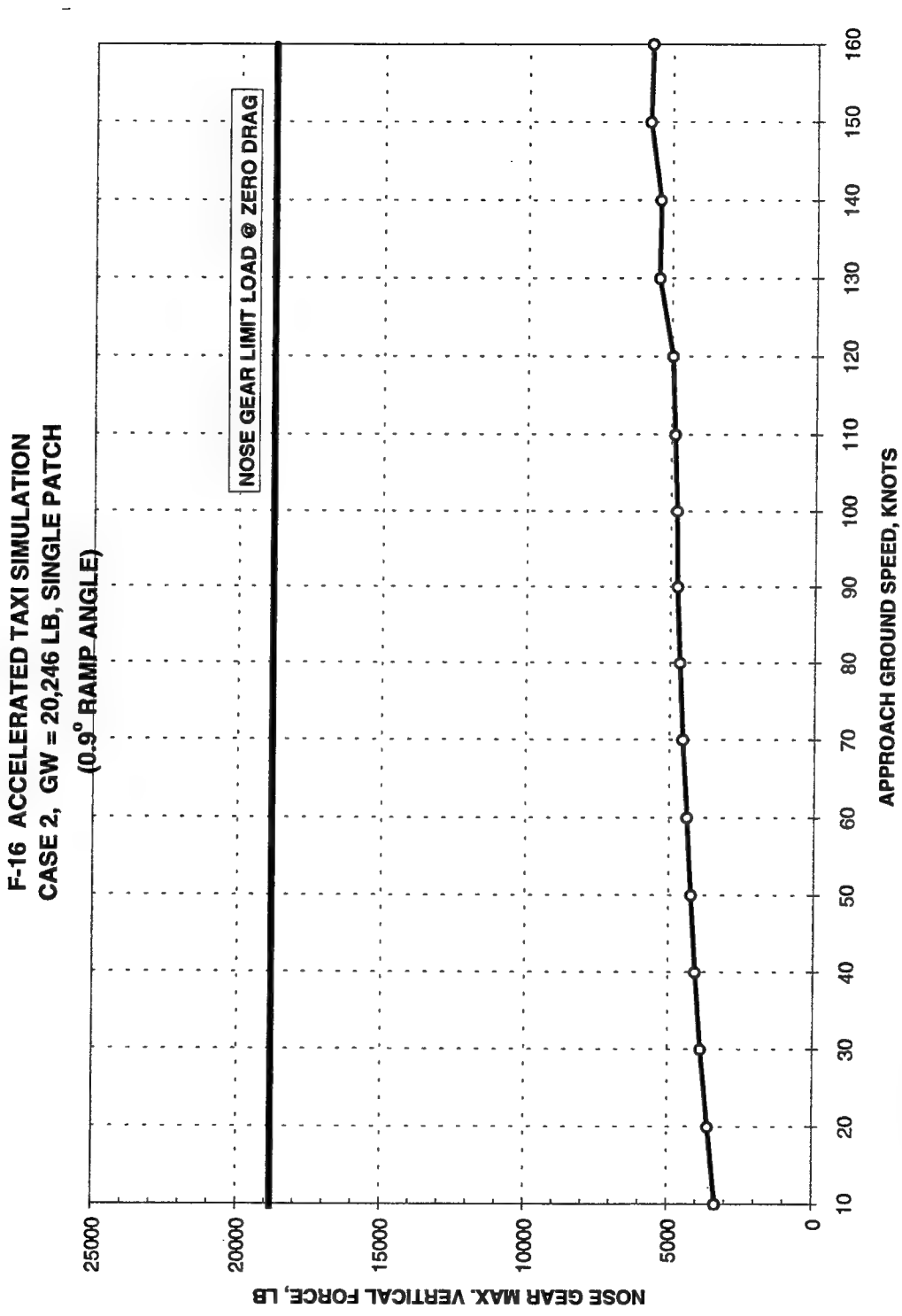

Figure B23. Nose gear forces for load case 2, acceleration (takeoff) mode, light gross weight, single mat, and 0.9-deg ramps

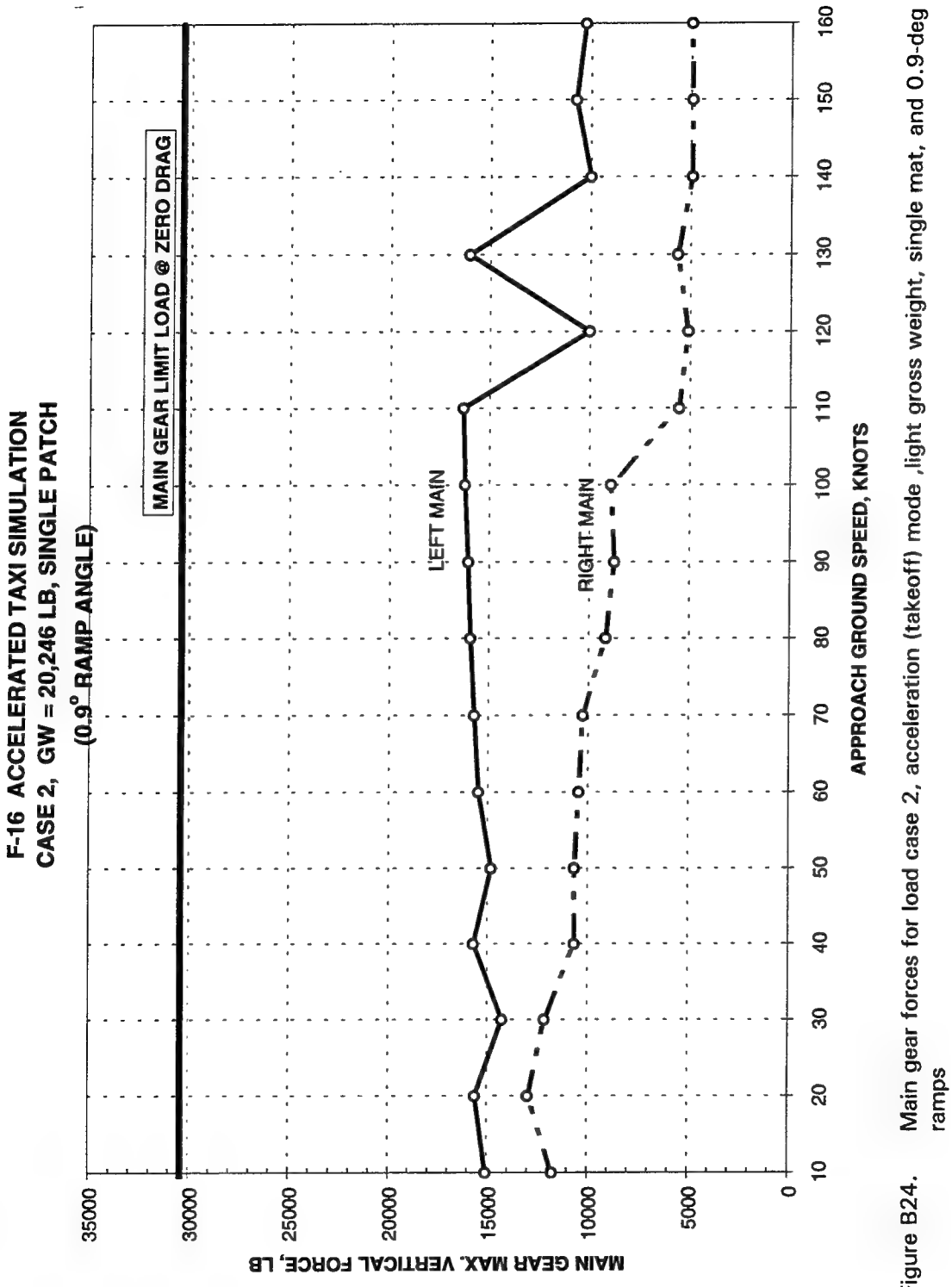

Figure B24. Main gear forces for load case 2, acceleration (takeoff) mode ,light gross weight, single mat, and 0.9-deg ramps

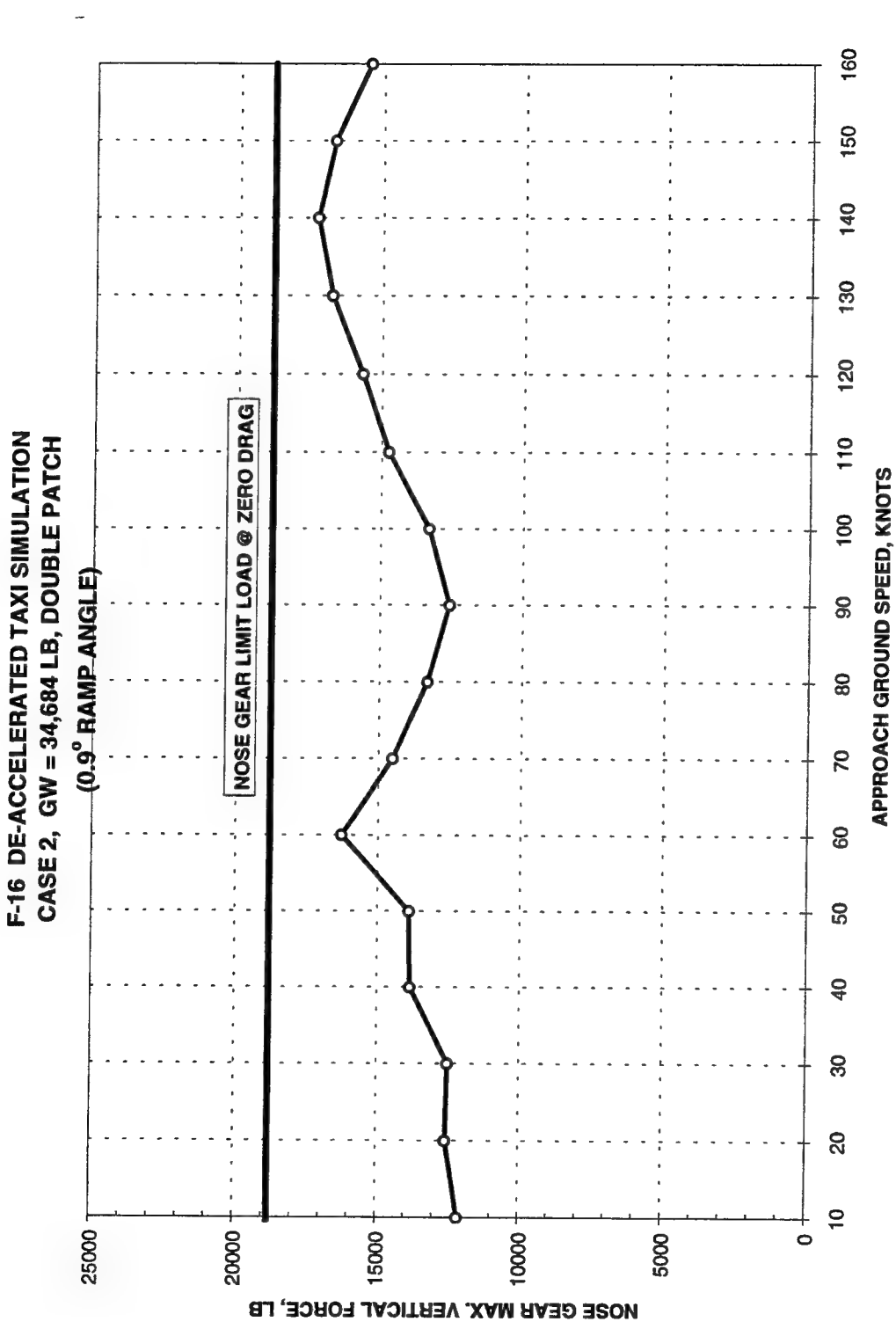

Figure B25. Nose gear forces for load case 2, deceleration (landing) mode, heavy gross weight, double mat, and 0.9-deg ramps

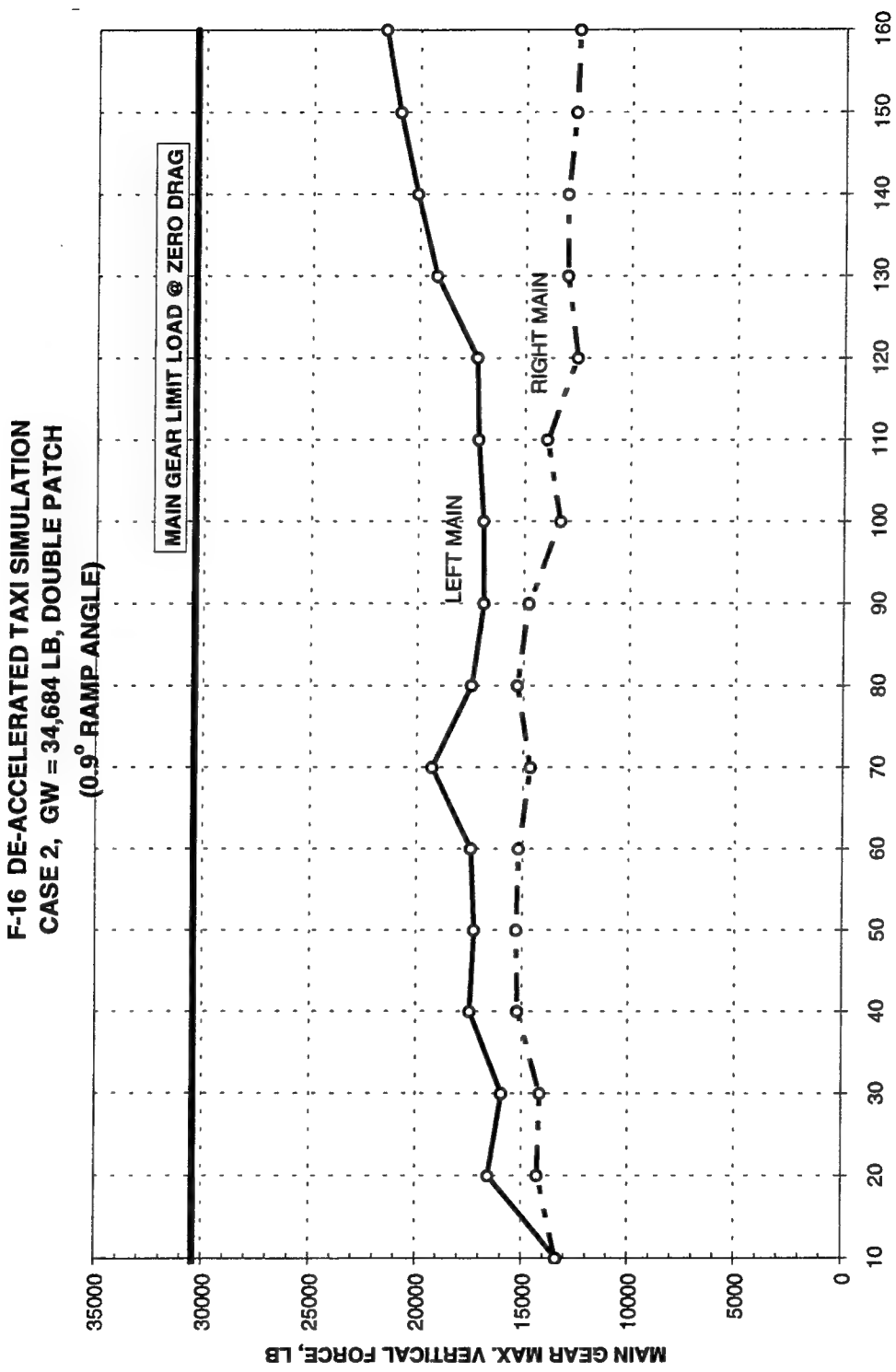

Figure B26. Main gear forces for load case 2, deceleration (landing) mode ,heavy gross weight, double mat, and 0.9-deg ramps

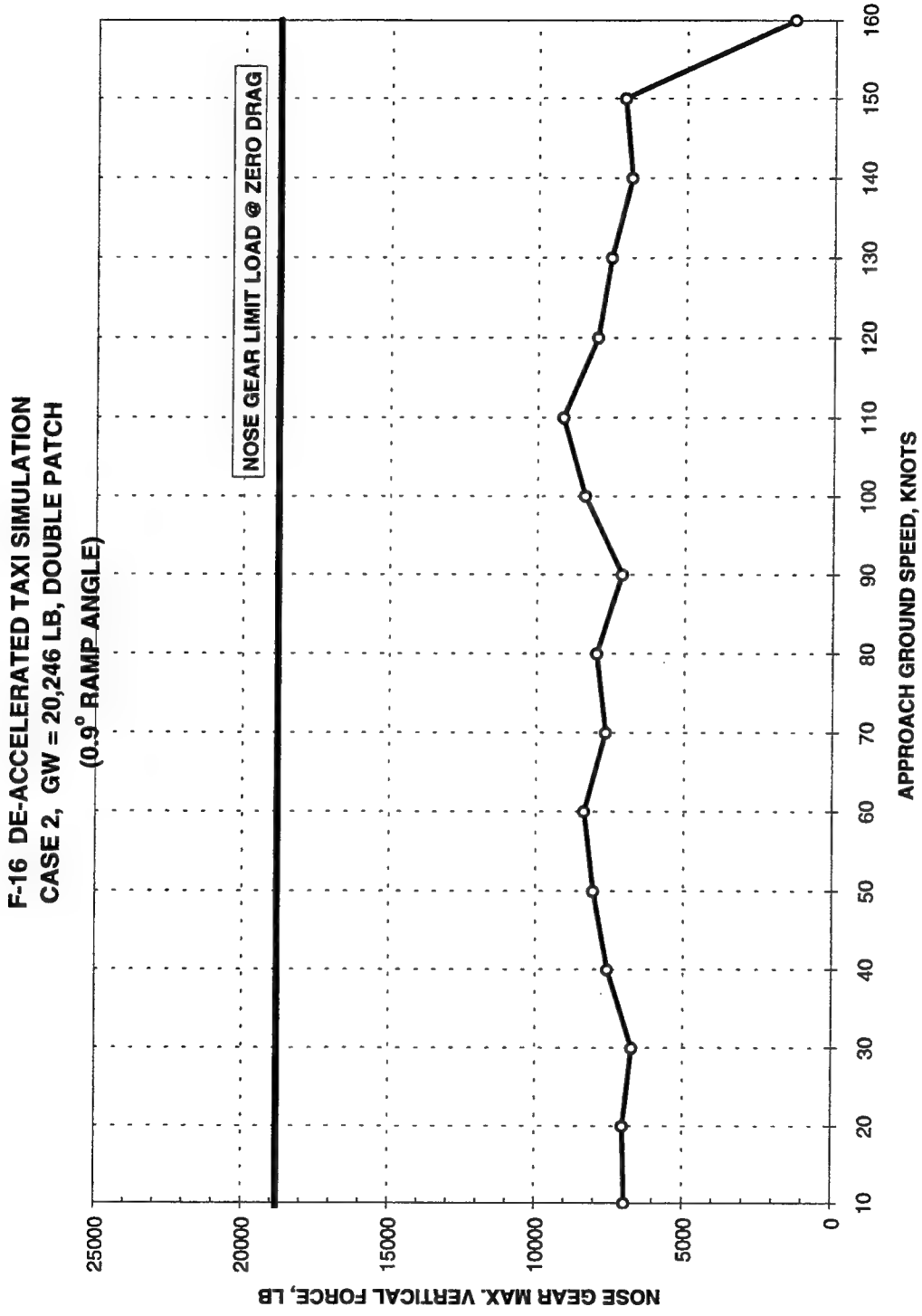

Figure B27. Nose gear forces for load case 2, deceleration (landing) mode, light gross weight, double mat, and 0.9-deg ramps

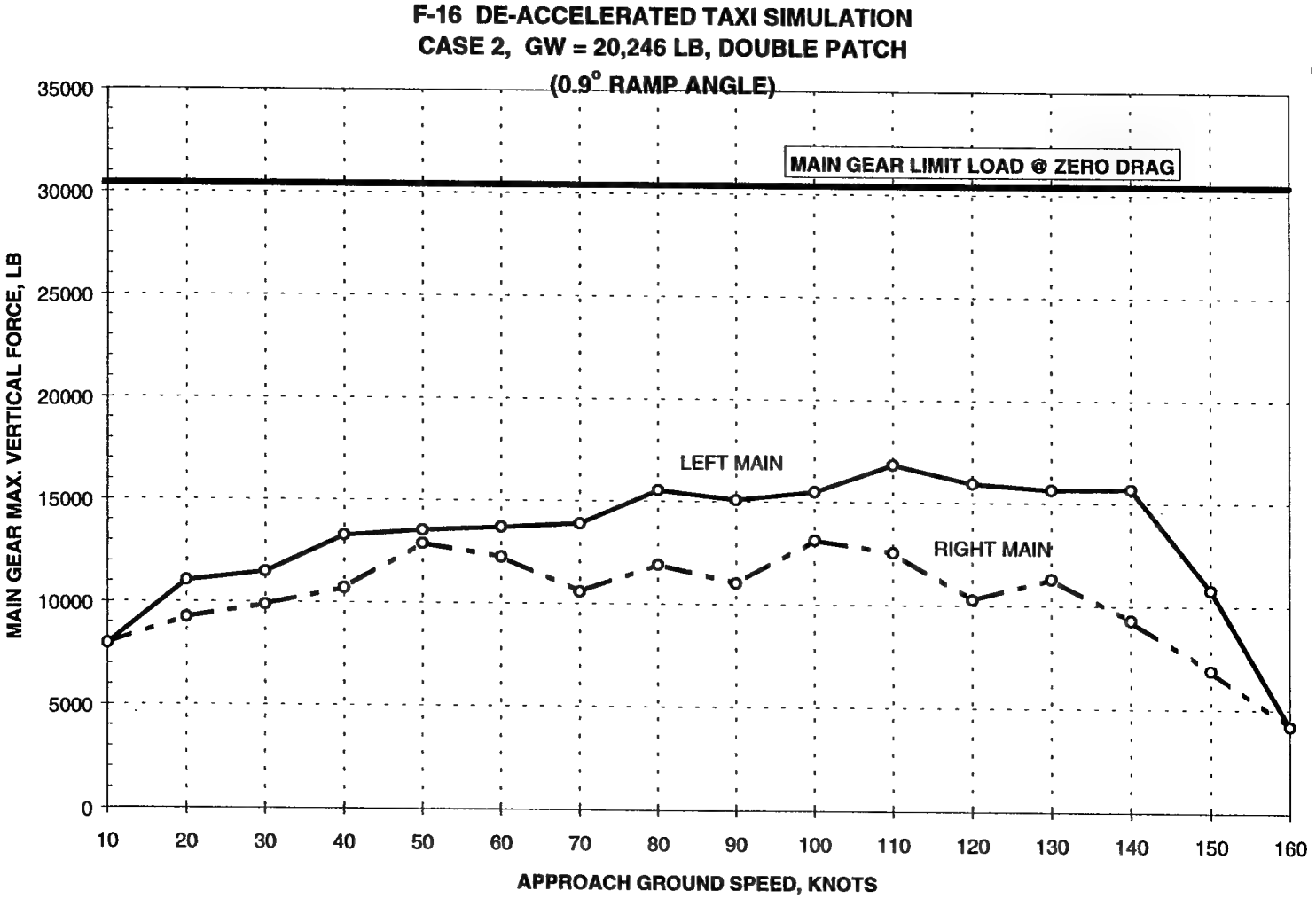

Figure B28. Main gear forces for load case 2, deceleration (landing) mode, light gross weight, double mat, and 0.9-deg ramps

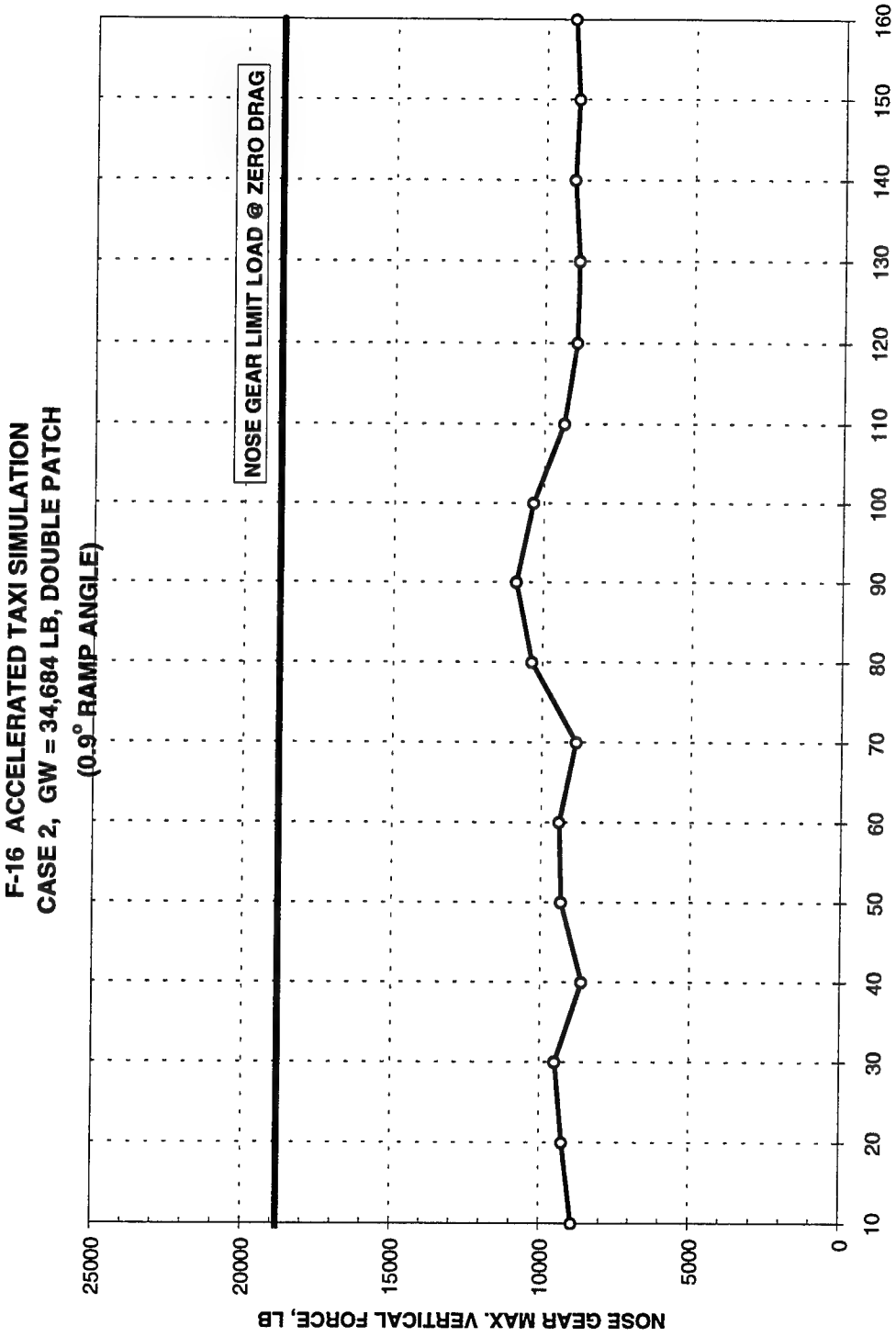

Figure B29. Nose gear forces for load case 2, acceleration (takeoff) mode, heavy gross weight, double mat, and 0.9-deg ramps

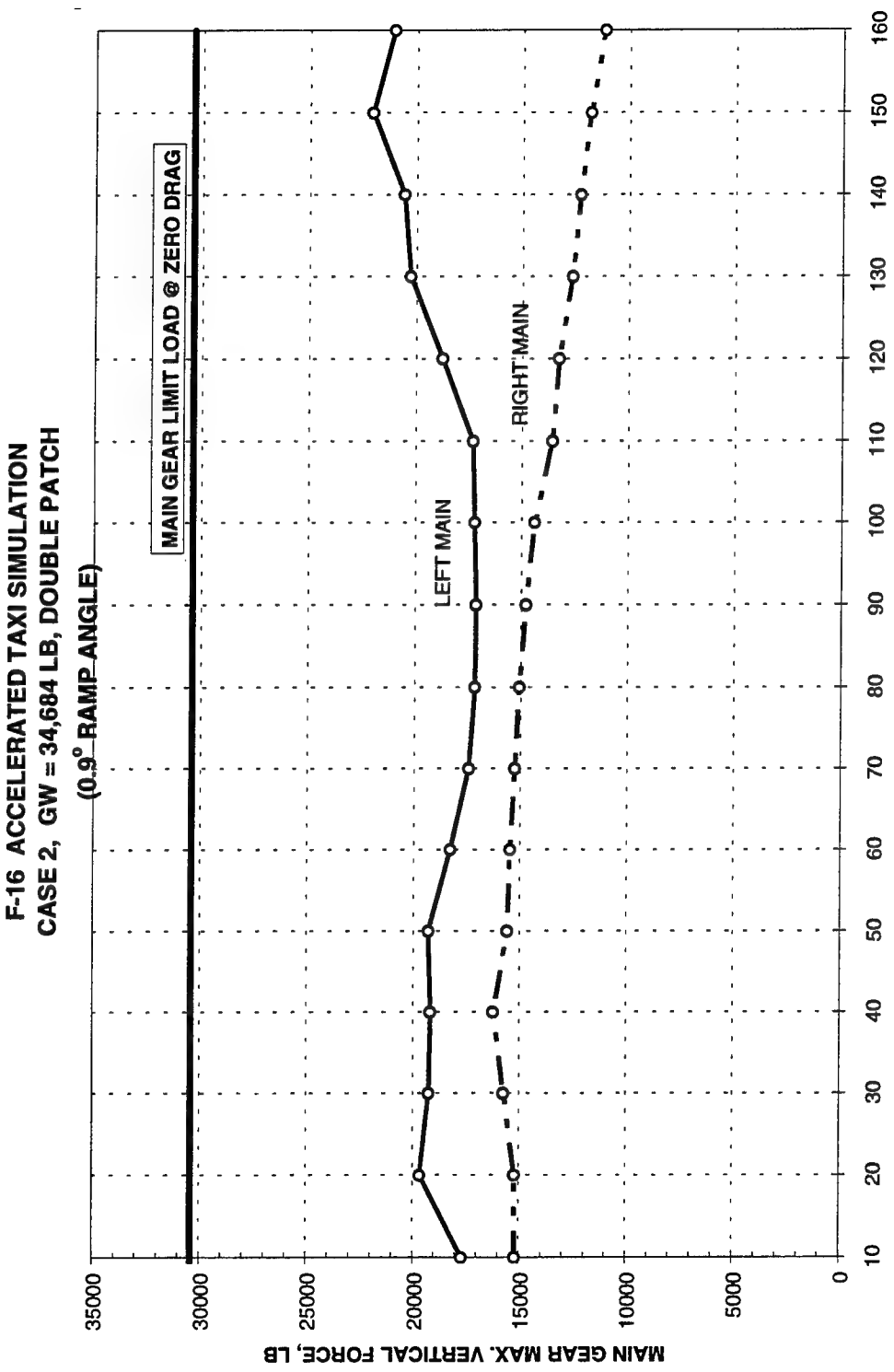

Figure B30. Main gear forces for load case 2, acceleration (takeoff) mode , heavy gross weight, double mat, and 0.9-deg ramps

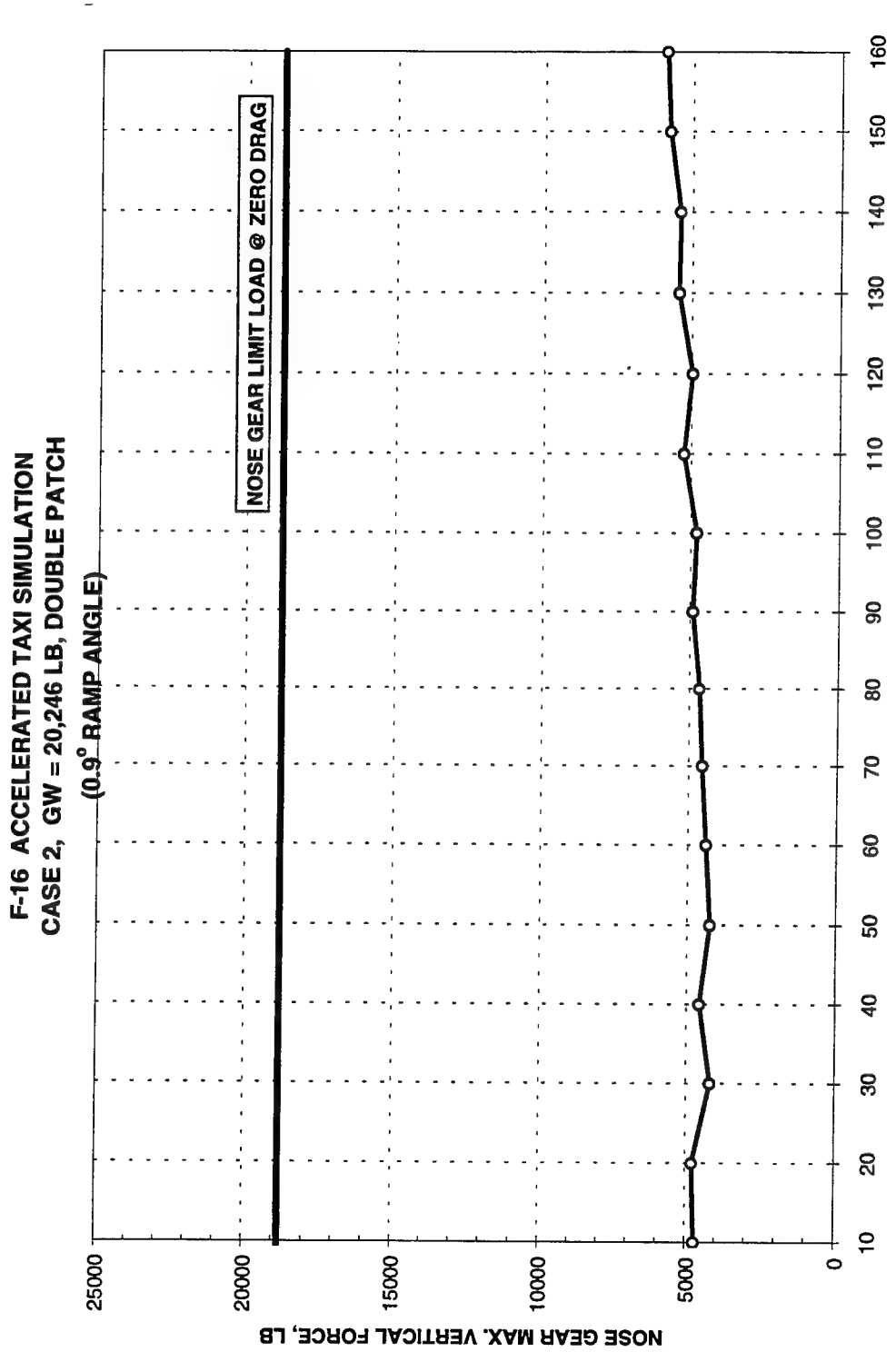

Figure B31. Nose gear forces for load case 2, acceleration (takeoff) mode, light gross weight, double mat, and 0.9-deg ramps

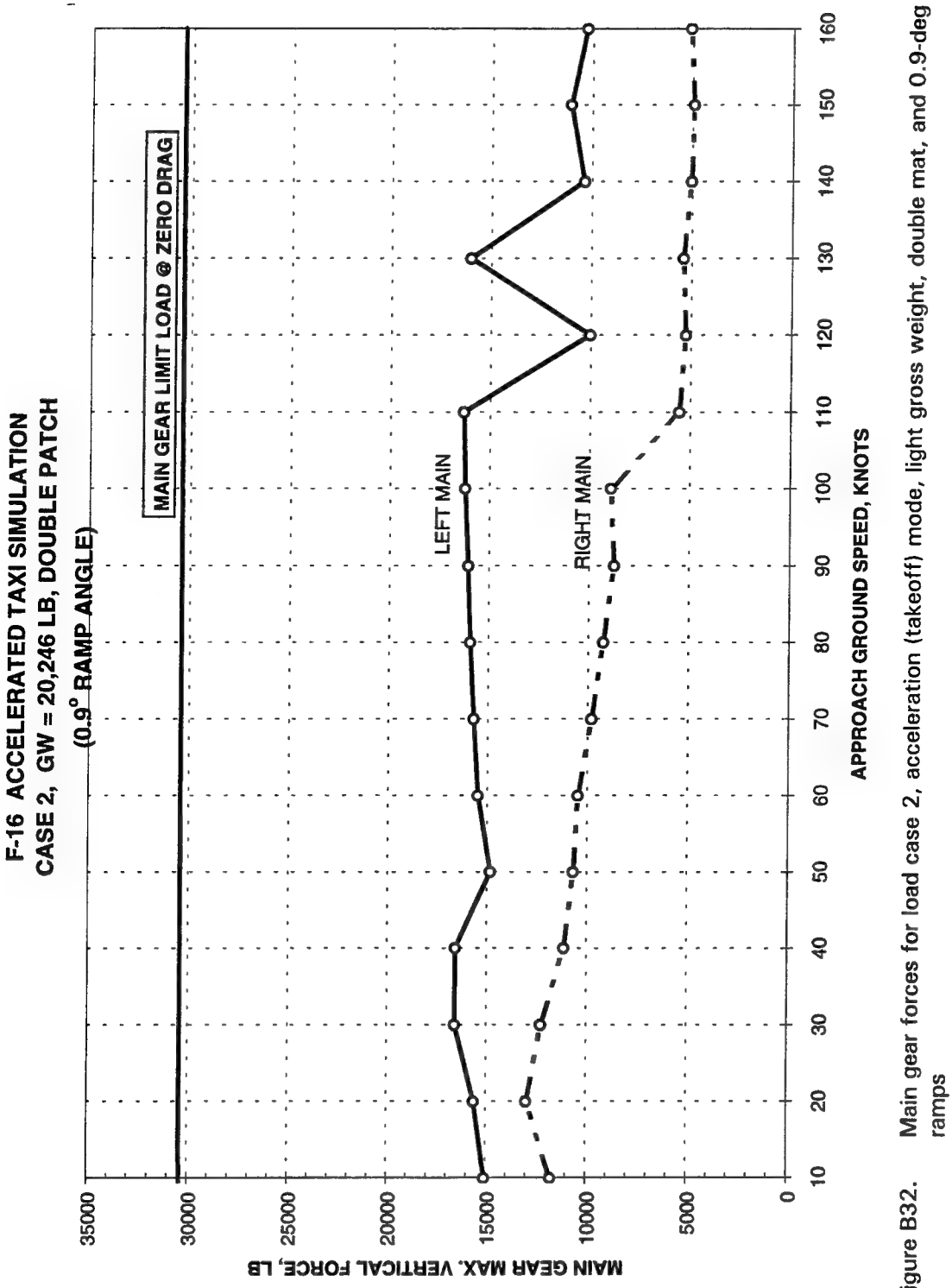

Figure B32. Main gear forces for load case 2, acceleration (takeoff) mode, light gross weight, double mat, and 0.9-deg ramps

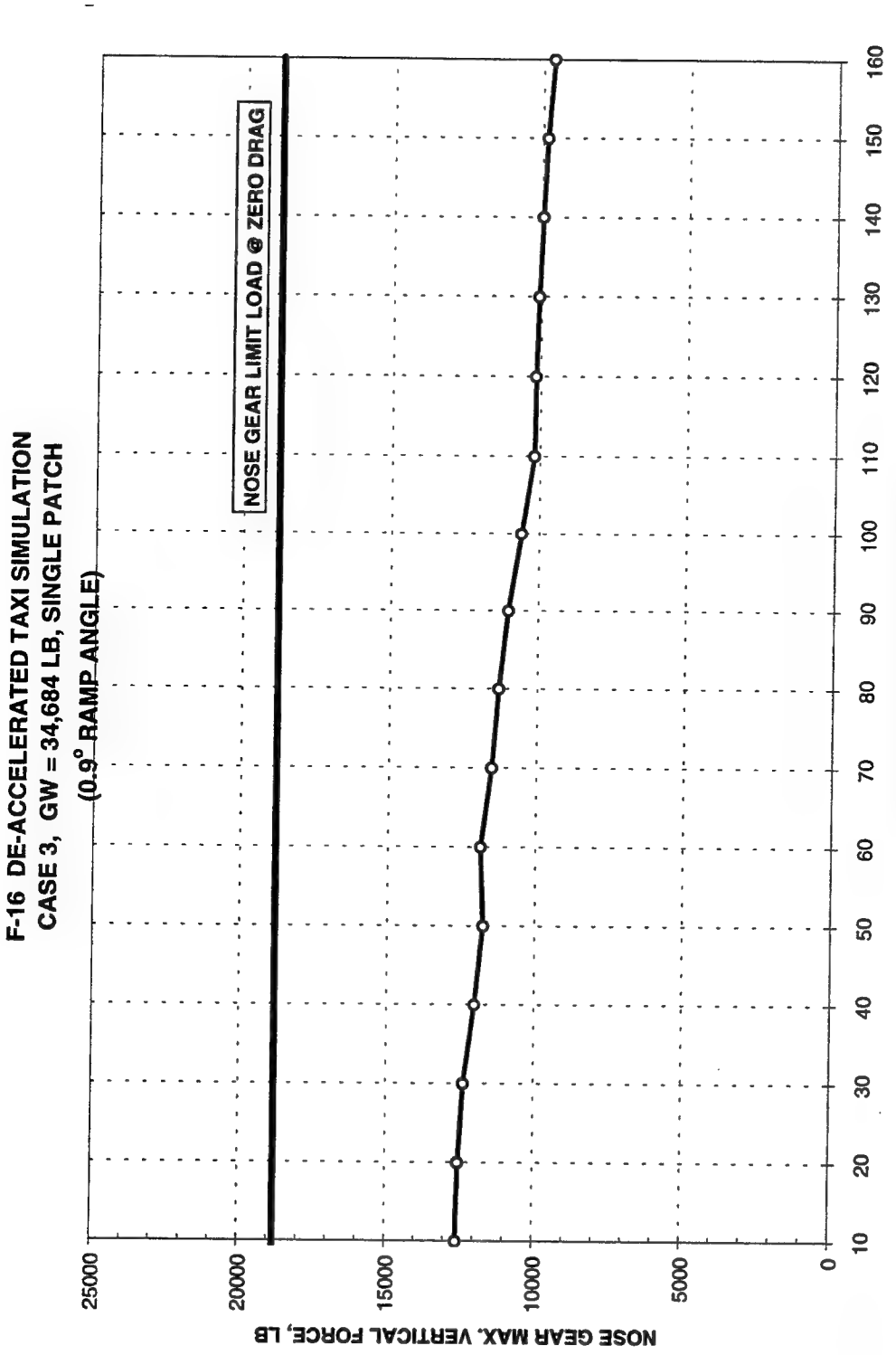

Figure B33. Nose gear forces for load case 3, deceleration (landing) mode, heavy gross weight, single mat, and 0.9-deg ramps

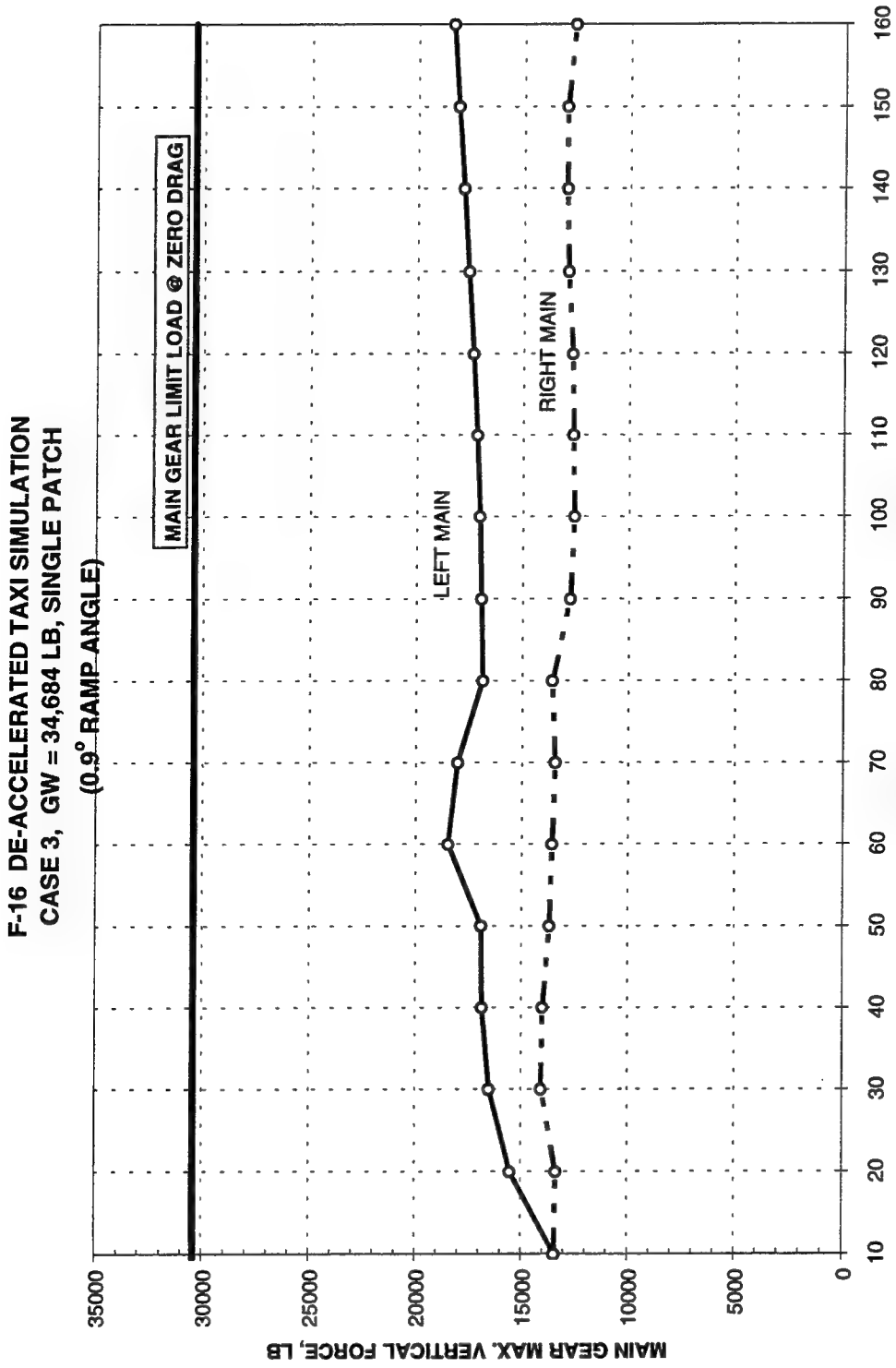

Figure B34. Main gear forces for load case 3, deceleration (landing) mode , heavy gross weight, single mat, and 0.9-deg ramps

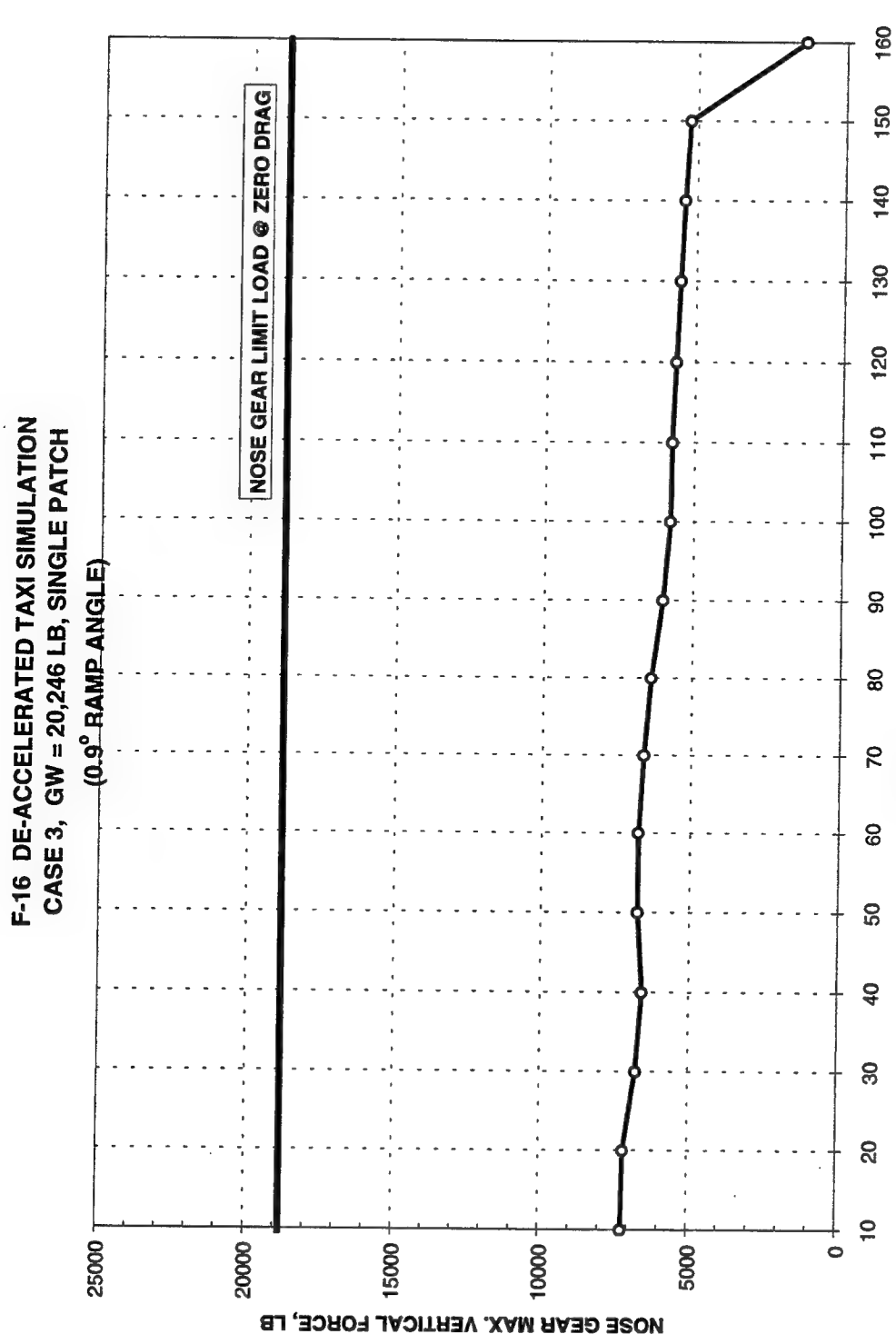

Figure B35. Nose gear forces for load case 3, deceleration (landing) mode, light gross weight, single mat, and 0.9-deg ramps

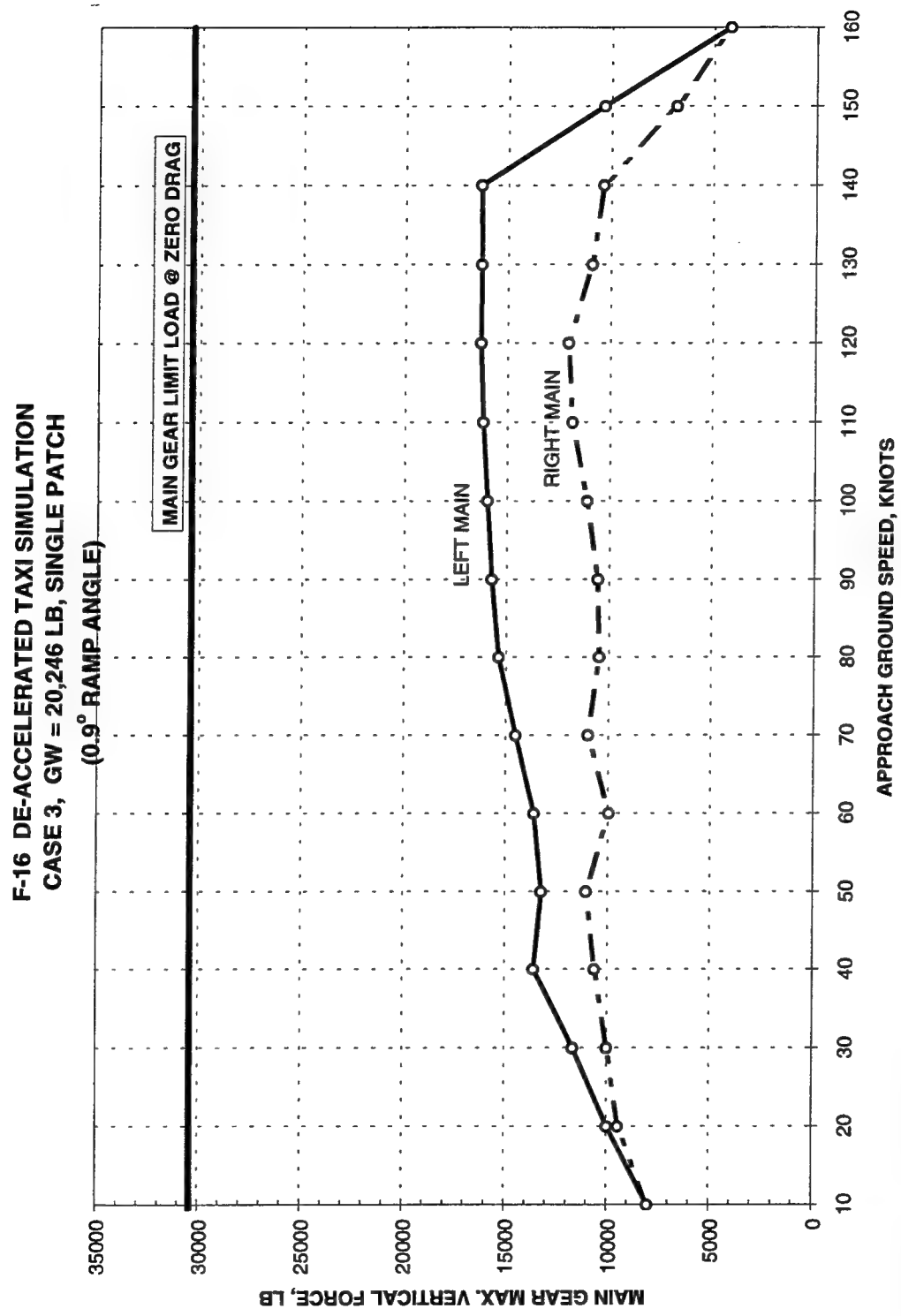

Figure B36. Main gear forces for load case 3, deceleration (landing) mode , light gross weight, single mat, and 0.9-deg ramps

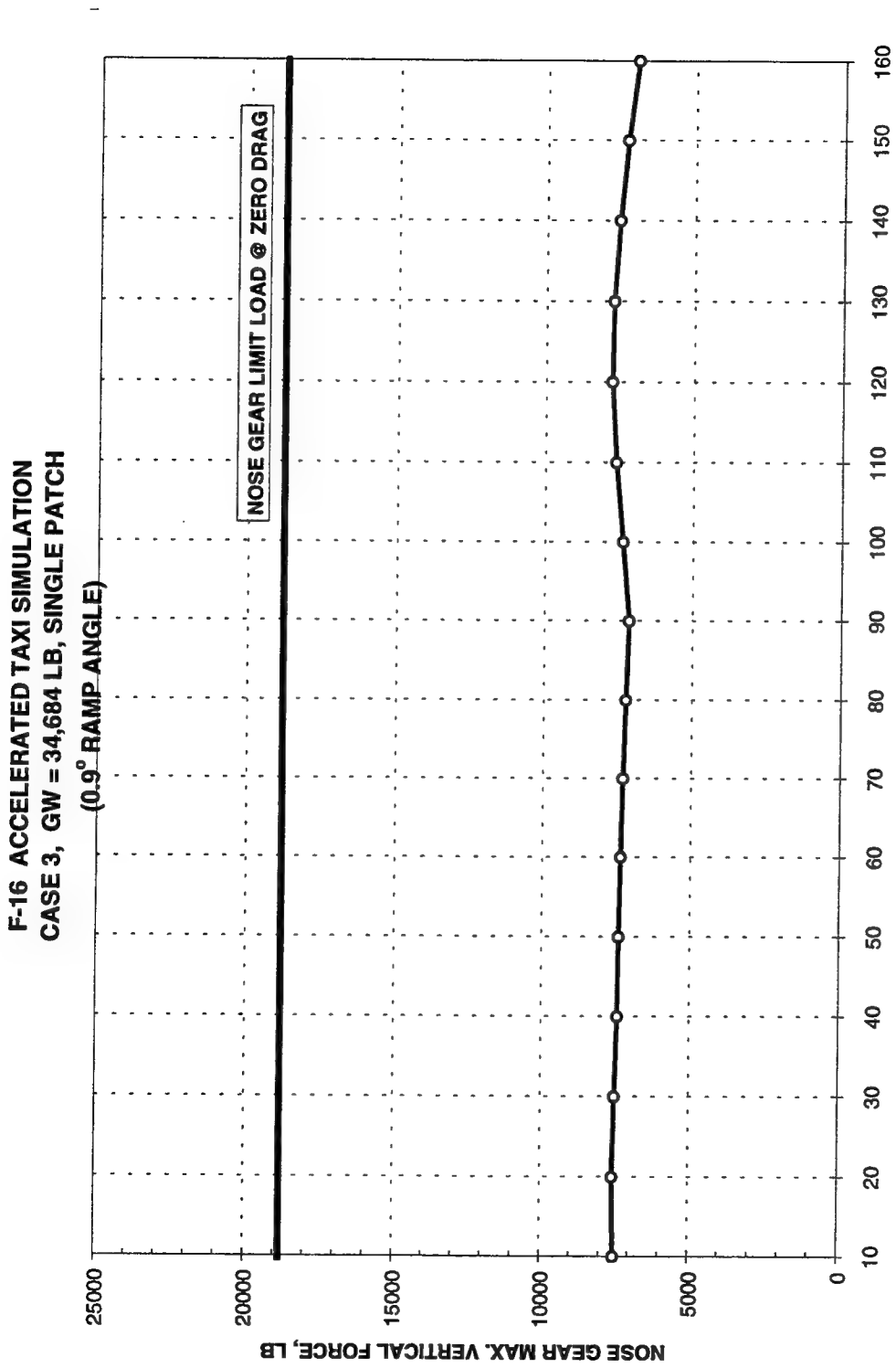

Figure B37. Nose gear forces for load case 3, acceleration (takeoff) mode, heavy gross weight, single mat, and 0.9-deg ramps

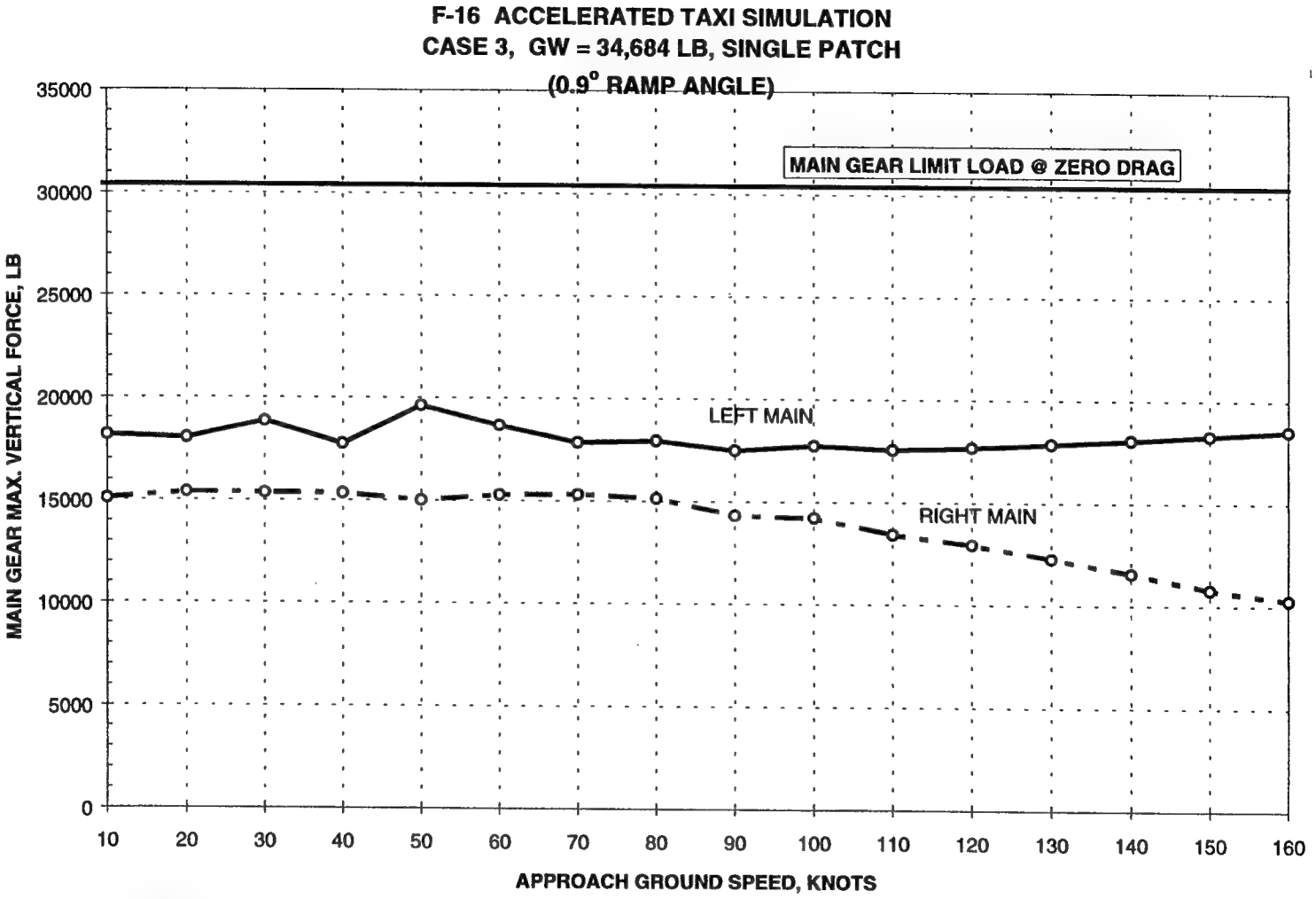

Figure B38. Main gear forces for load case 3, acceleration (takeoff) mode , heavy gross weight, single mat, and 0.9-deg ramps

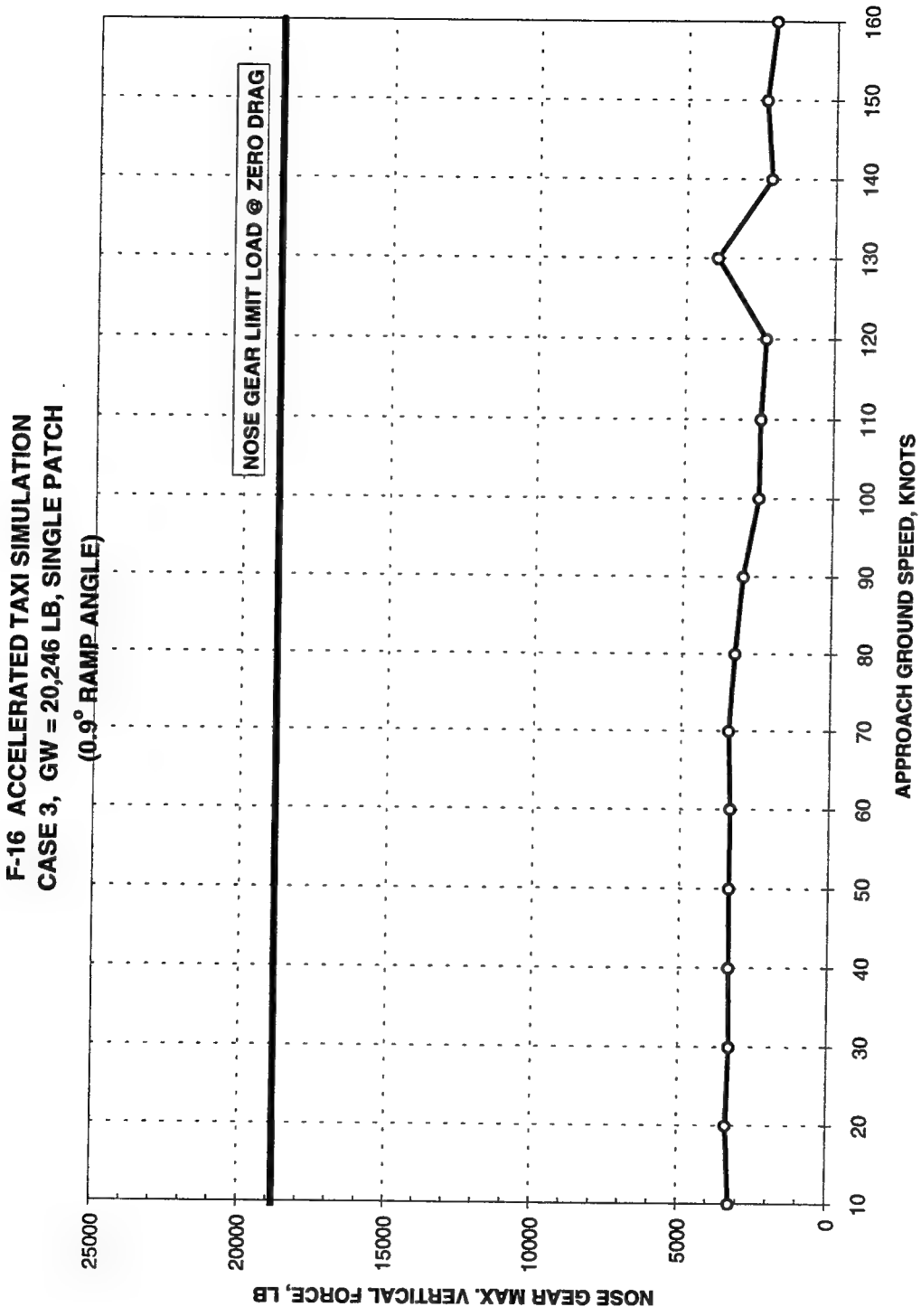

Figure B39. Nose gear forces for load case 3, acceleration (takeoff) mode, light gross weight, single mat, and 0.9-deg ramps

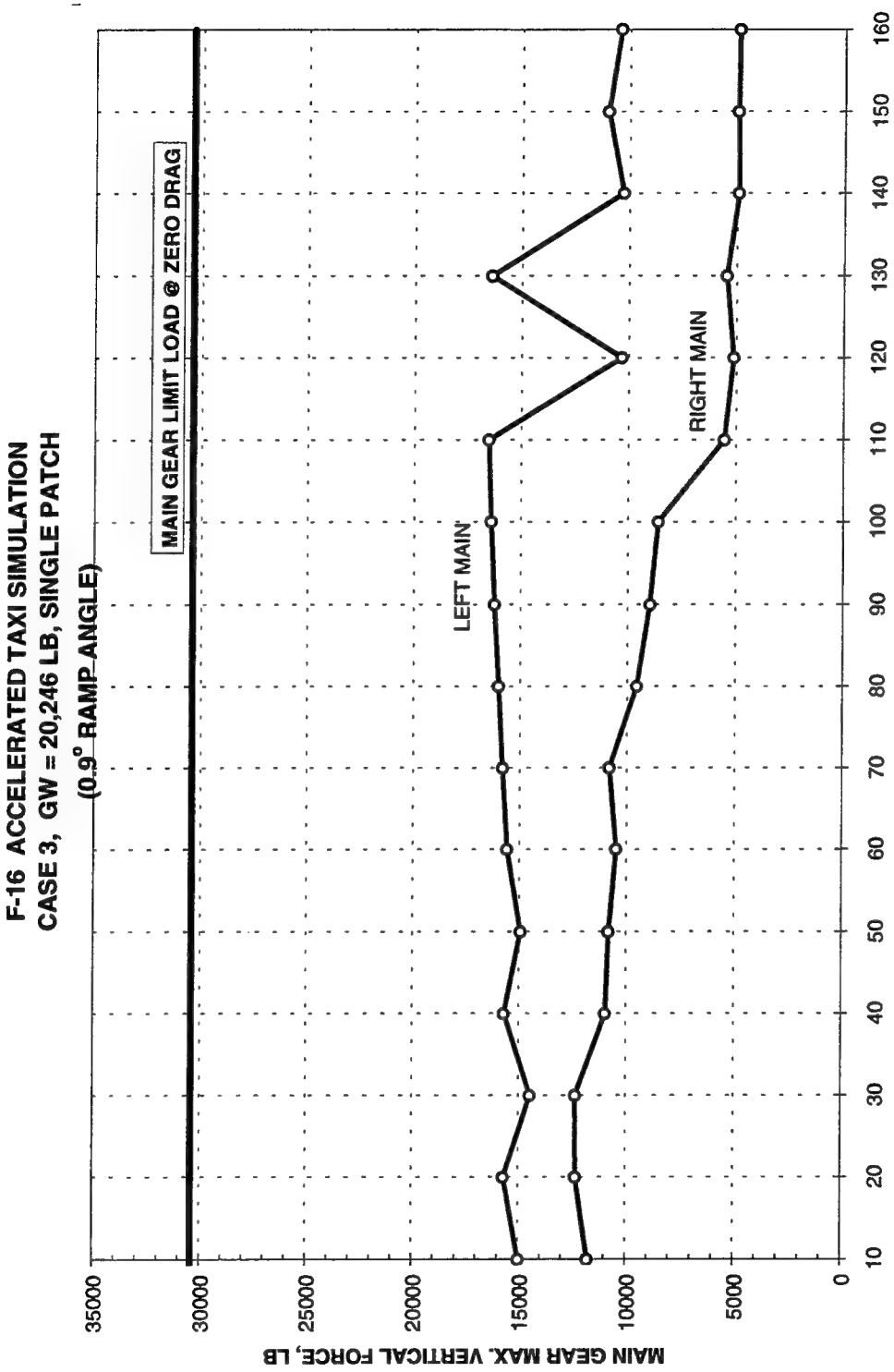

Figure B40. Main gear forces for load case 3, acceleration (takeoff) mode , light gross weight, single mat, and 0.9-deg ramps

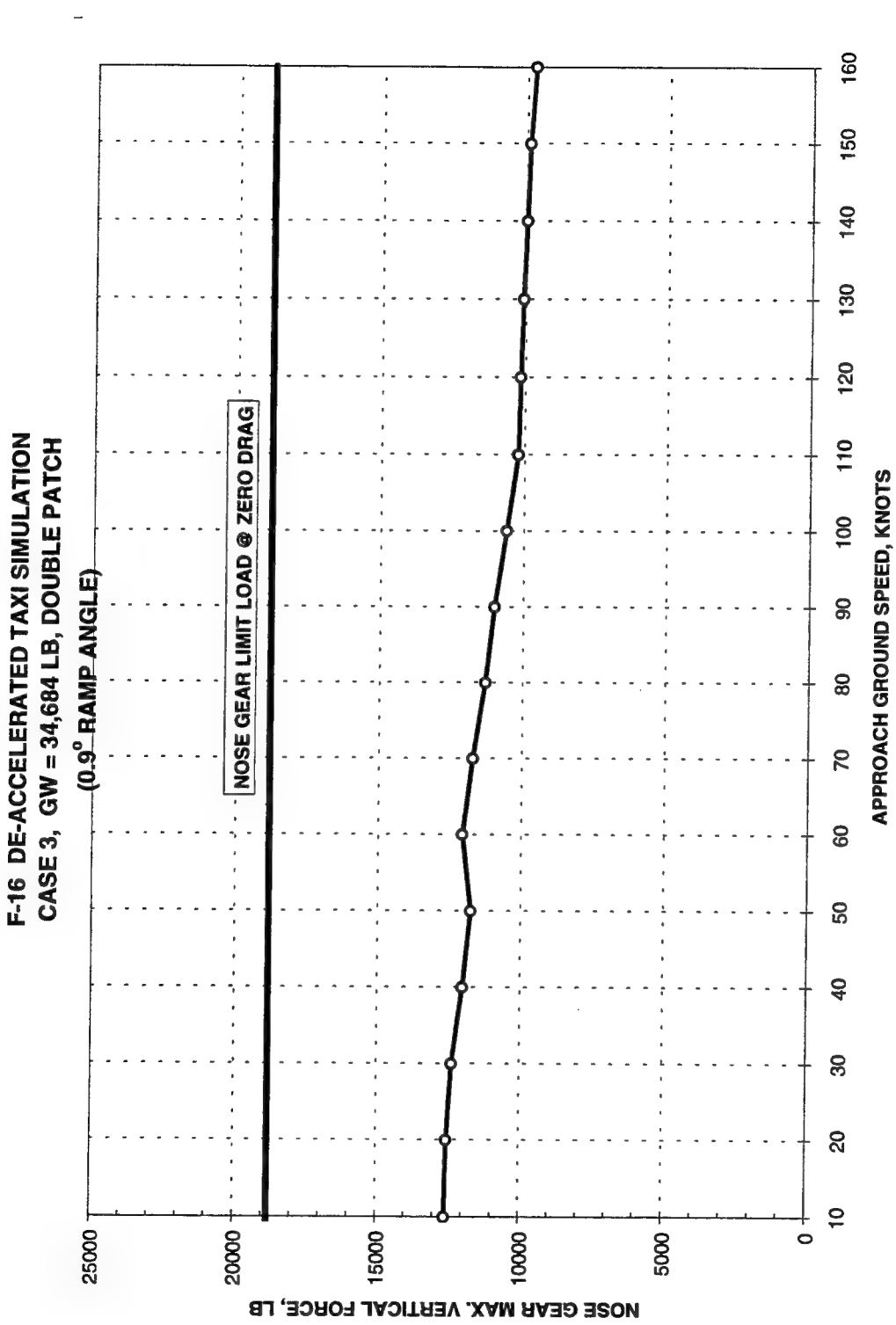

Figure B41. Nose gear forces for load case 3, deceleration (landing) mode, heavy gross weight, double mat, and 0.9-deg ramps

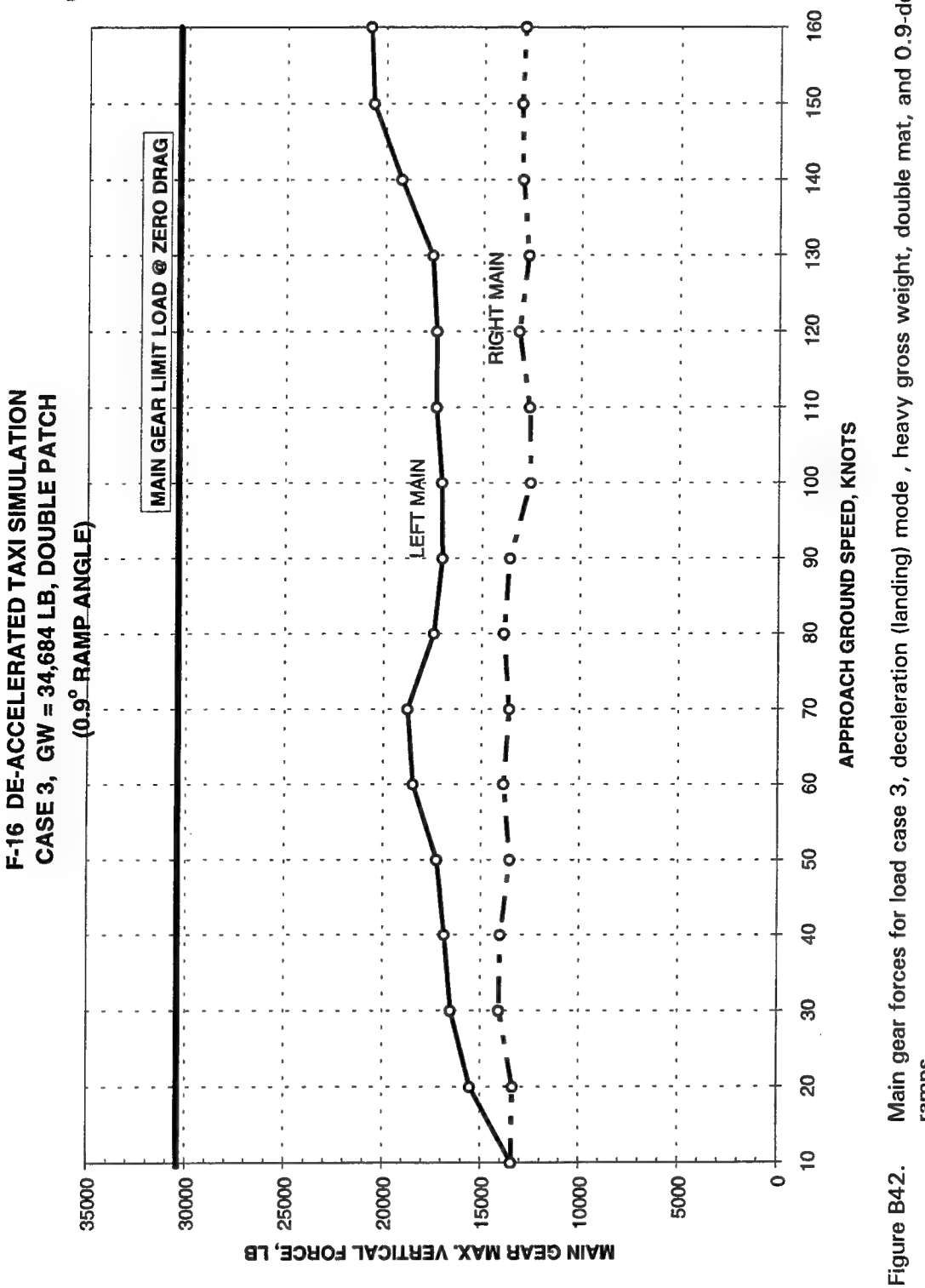

Figure B42. Main gear forces for load case 3, deceleration (landing) mode , heavy gross weight, double mat, and 0.9-deg ramps

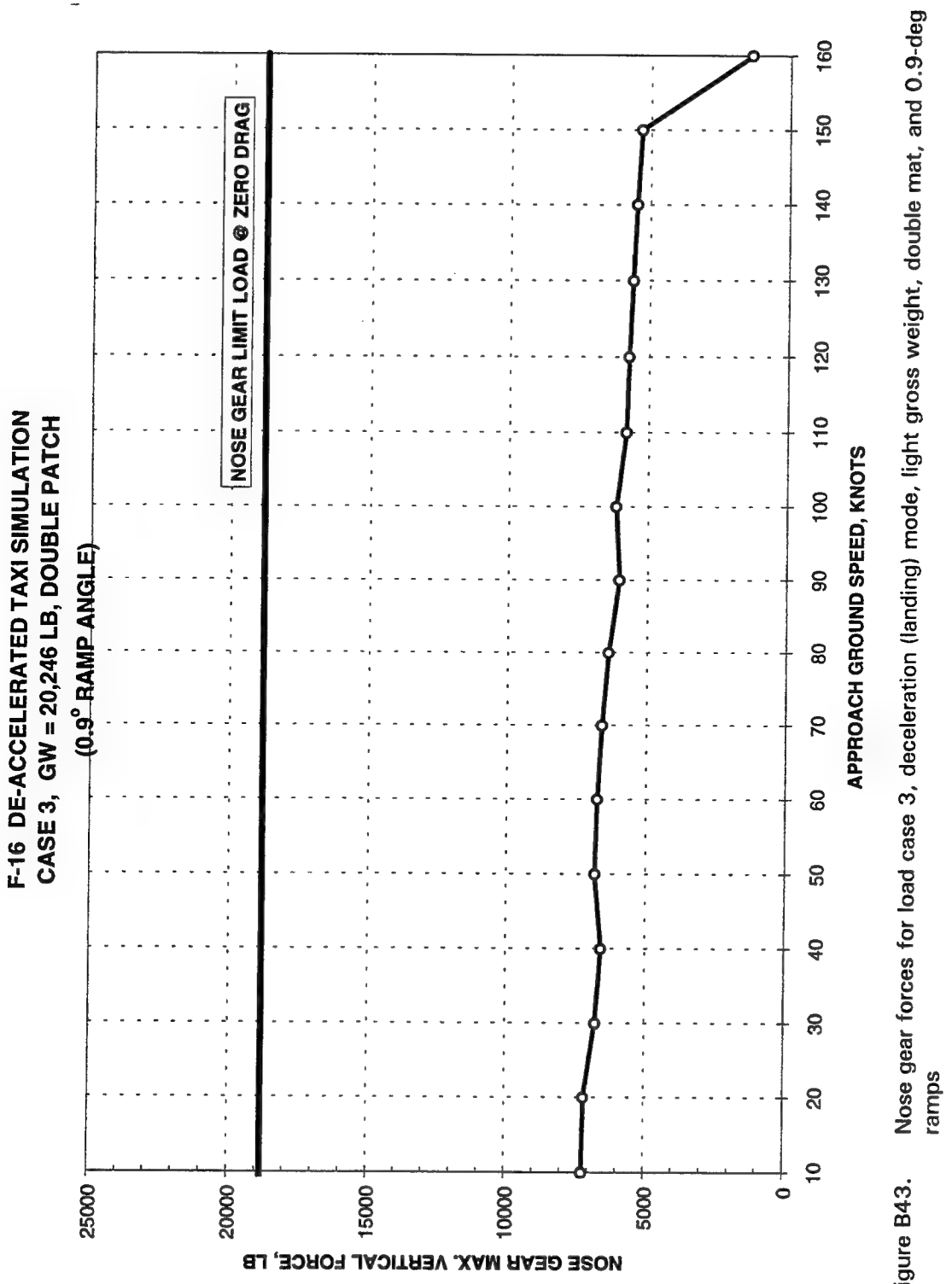

Figure B43. Nose gear forces for load case 3, deceleration (landing) mode, light gross weight, double mat, and 0.9-deg ramps

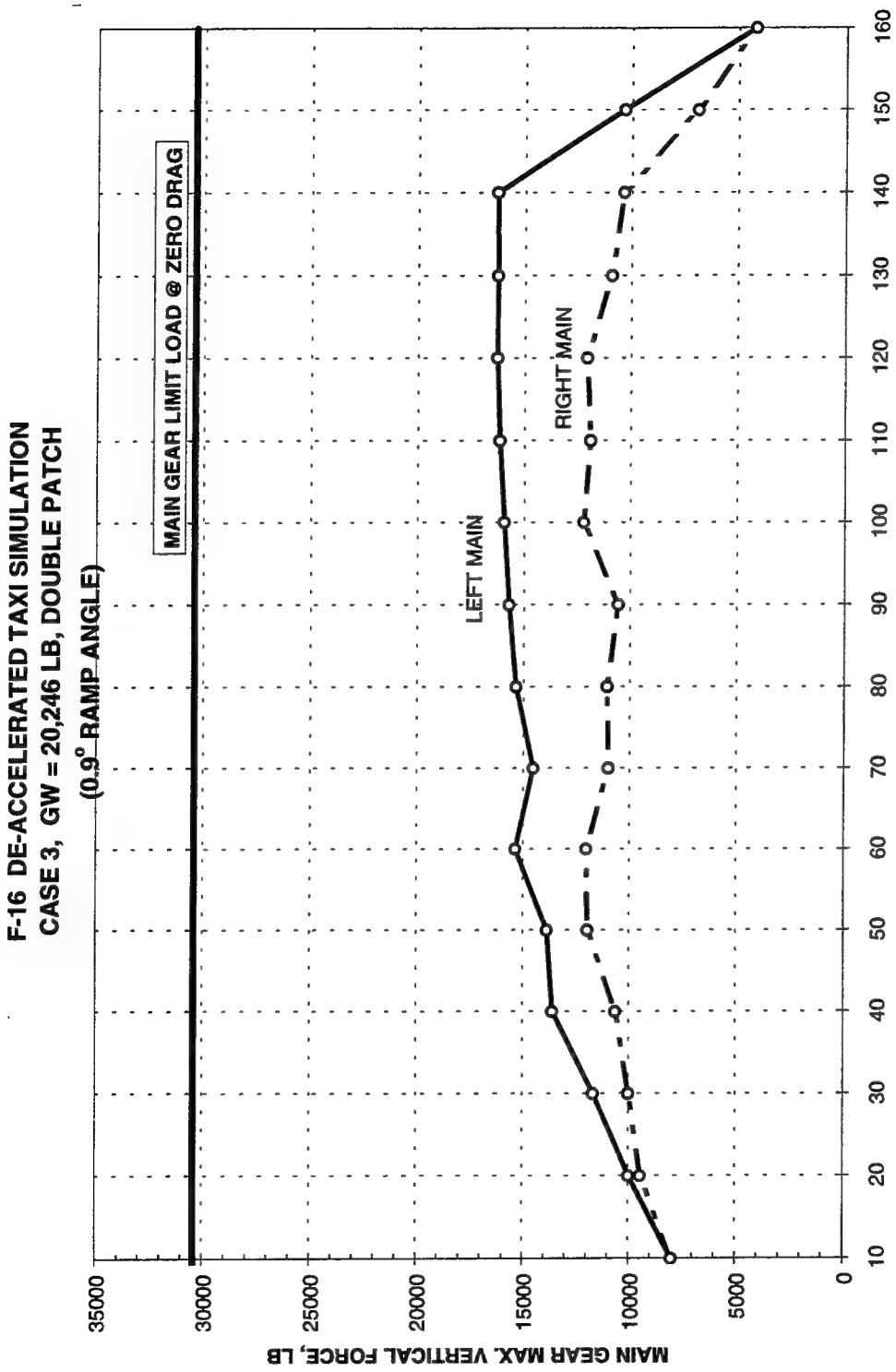

Figure B44. Main gear forces for load case 3, deceleration (landing) mode , light gross weight, double mat, and 0.9-deg ramps

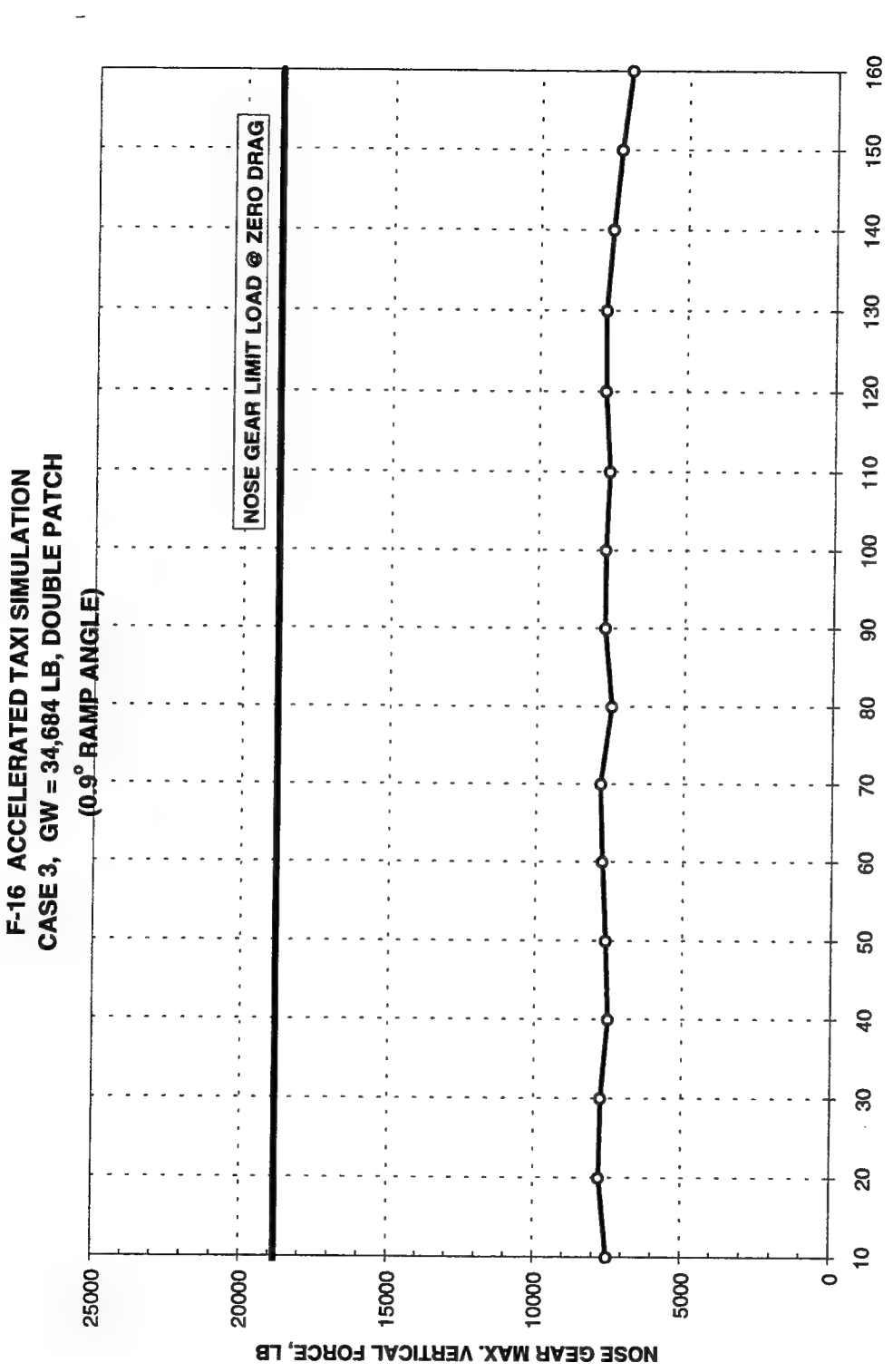

Figure B45. Nose gear forces for load case 3, acceleration (takeoff) mode, heavy gross weight, double mat, and 0.9-deg ramps

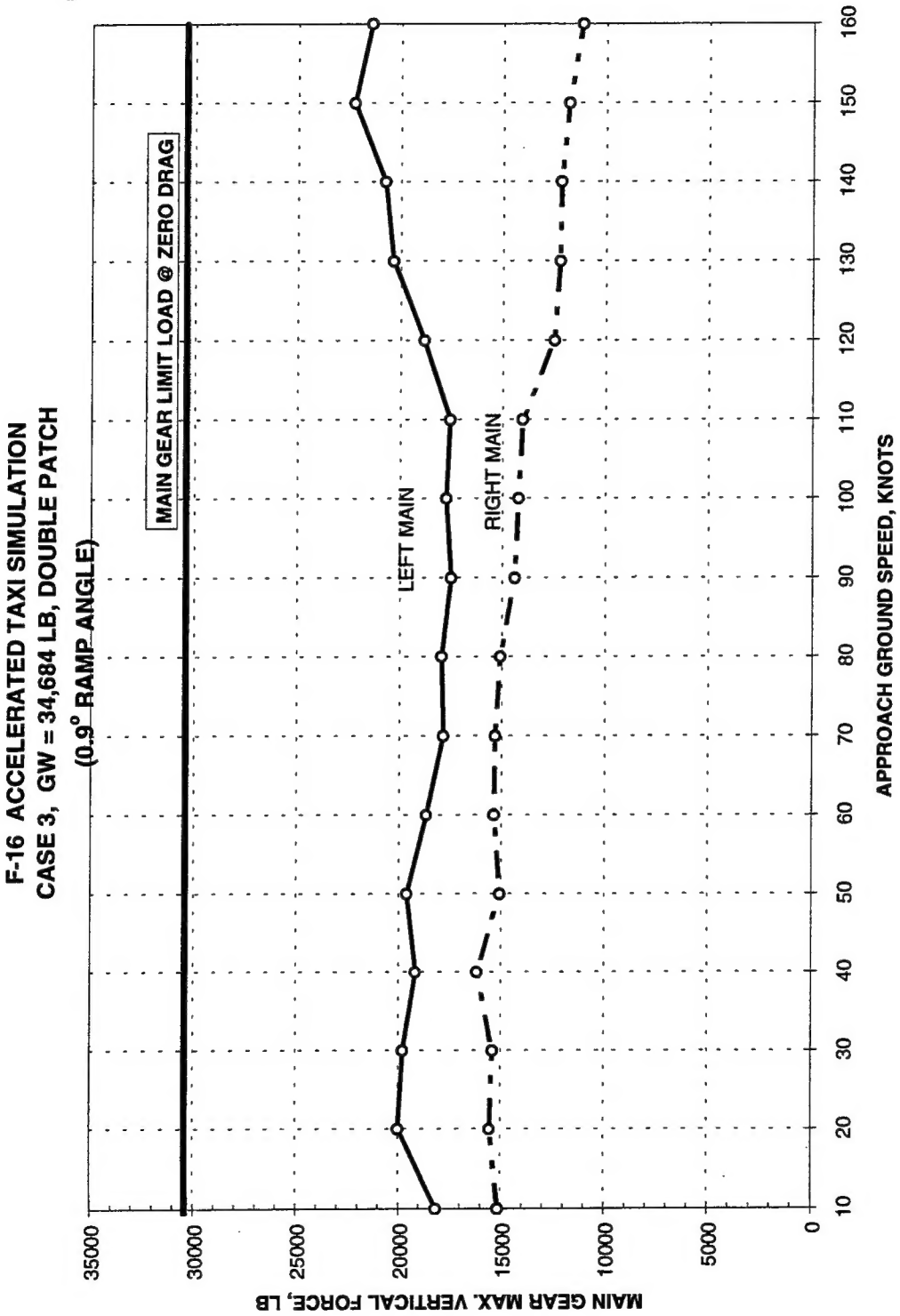

Figure B46. Main gear forces for load case 3, acceleration (takeoff) mode , heavy gross weight, double mat, and 0.9-deg ramps

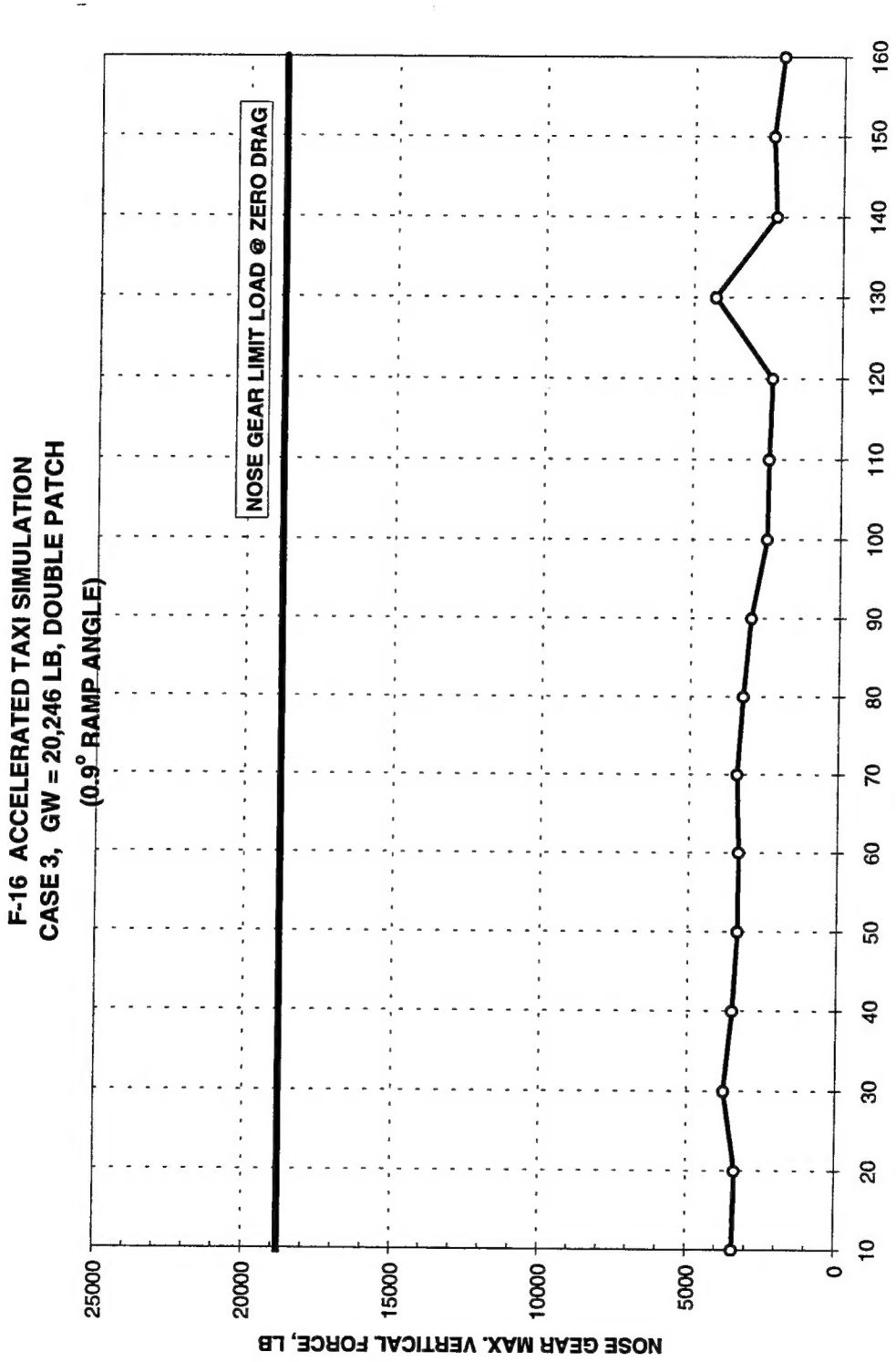

Figure B47. Nose gear forces for load case 3, acceleration (takeoff) mode, light gross weight, double mat, and 0.9-deg ramps

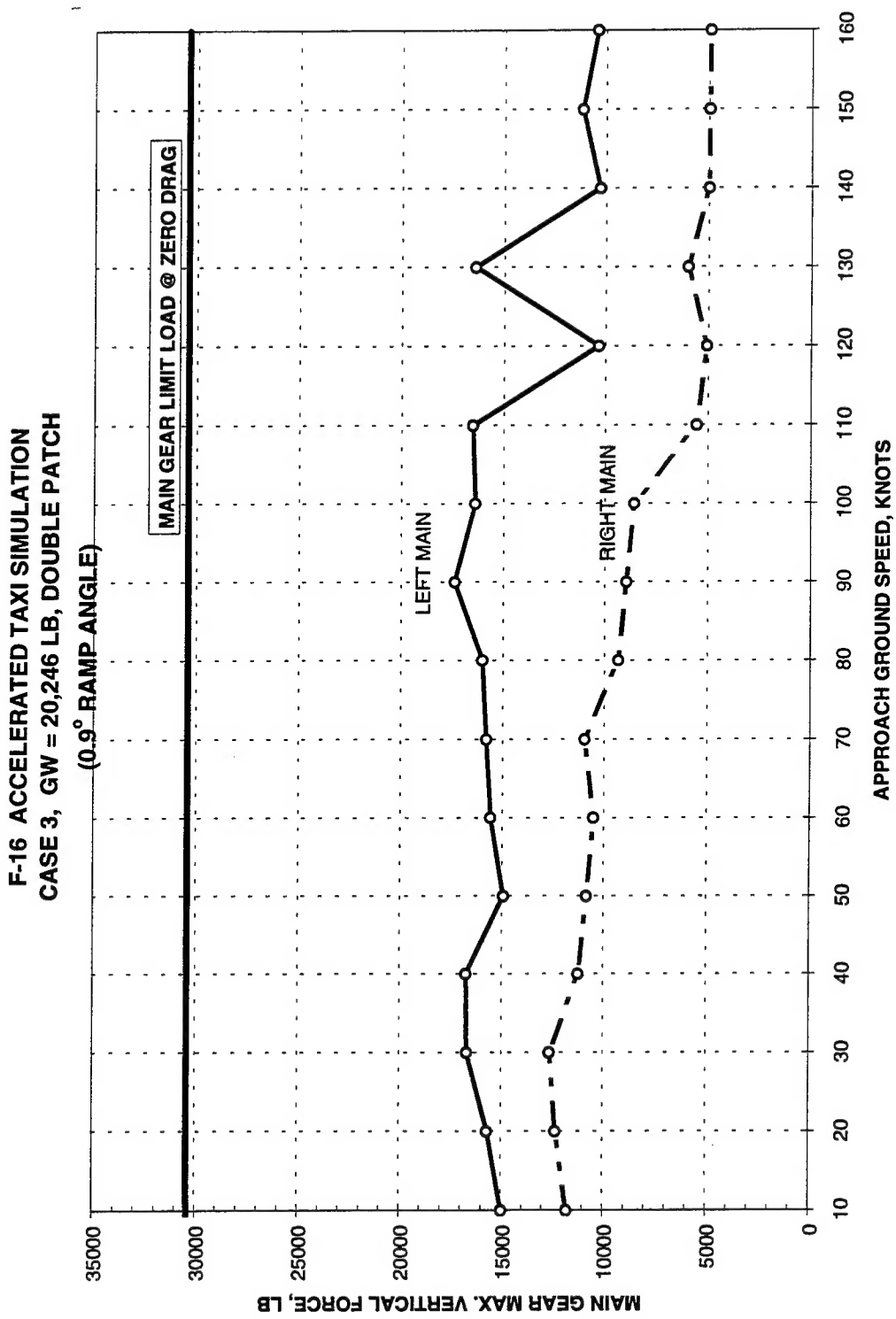

Figure B48. Main gear forces for load case 3, acceleration (takeoff) mode , light gross weight, double mat, and 0.9-deg ramps

REPORT DOCUMENTATION PAGE

Form Approved
OMB No. 0704-0188

1. AGENCY USE ONLY *(Leave blank)*	2. REPORT DATE	3. REPORT TYPE AND DATES COVERED
	November 1997	Final report

4. TITLE AND SUBTITLE
Analysis of Korean F-16 Aircraft Operating on AM-2 Landing Mat

5. FUNDING NUMBERS

6. AUTHOR(S)
Carroll J. Smith, Carlos R. Gonzalez, Donald M. Smith

7. PERFORMING ORGANIZATION NAME(S) AND ADDRESS(ES)
U.S. Army Engineer Waterways Experiment Station
3909 Halls Ferry Road
Vicksburg, MS 39180-6199

8. PERFORMING ORGANIZATION REPORT NUMBER
Technical Report GL-97-20

9. SPONSORING/MONITORING AGENCY NAME(S) AND ADDRESS(ES)
Samsun Industrial Company Ltd.
24 Youido-Dong, Youngdungpo-Ku
Seoul 150-010
KOREA

10. SPONSORING/MONITORING AGENCY REPORT NUMBER

11. SUPPLEMENTARY NOTES
Available from National Technical Information Service, 5285 Port Royal Road, Springfield, VA 22161.

12a. DISTRIBUTION/AVAILABILITY STATEMENT
Approved for public release; distribution is unlimited.

12b. DISTRIBUTION CODE

13. ABSTRACT ***(Maximum 200 words)***

An analysis was conducted to determine the aircraft-surface interaction and response of Korean F-16 aircraft traversing a 1.5-in. thick AM-2 landing mat pavement repair. Single and multiple patches of landing mat with ascending and descending ramps of 1.9- and 0.9-deg slopes were investigated. Operations of the F-16 aircraft were numerically simulated and the response calculations (gear loads and fuel tank ground clearances) were compared to aircraft design and operation criteria. Aircraft operations were modeled with various combinations of the three wheels or gears traversing along the repaired pavement profile. The three modeled load cases included: (1) nose gear and two main gears on landing mat patch(es), (2) nose gear and one main gear on landing mat patch(es), and (3) one main gear on landing mat patch(es).

14. SUBJECT TERMS
Aircraft-surface interaction
AM-2 landing mat
Korean F-16 aircraft
Numerical simulations
Pavement repair
Repair ramps (1.9 and 0.9 deg)

15. NUMBER OF PAGES
129

16. PRICE CODE

17. SECURITY CLASSIFICATION OF REPORT	18. SECURITY CLASSIFICATION OF THIS PAGE	19. SECURITY CLASSIFICATION OF ABSTRACT	20. LIMITATION OF ABSTRACT
UNCLASSIFIED	UNCLASSIFIED		